Tephra stratigraphy and geochemistry from three Icelandic lake cores: a new method for determining source volcano of tepra layers

Anna Jagan

School of Geosciences, The University of Edinburgh, Grant Institute, The Kings Buildings, West Mains Road, Edinburgh EH9 3JW.

Contents

Abstract

At present there is no consistent method for the identification of source volcanoes for a tephra layer found in a stratigraphy. This has led to several studies misidentifying source volcanoes. Geochemical analysis of the tephra layer can identify the source volcano. A methodology for identification of most Icelandic volcanoes is presented here following from the work of Jóhannsdóttir (2007). It has been constructed using an existing major element geochemical dataset from Icelandic tephra layers of known origin. In particular, it improves the difficult task of distinguishing between Hekla and Katla basalts. It is hoped it is simple and quick enough to use to encourage other workers to use it, but to still retain sufficient accuracy that a statistics based computer program could not produce. It was found that Cr, Ni, Sr, F, Cl and S are of no additional help in identifying the source volcano of the tephra layer.

In order to aid production of this method and to evaluate its success, three lacustrine cores from Iceland are analysed. 135 primary Holocene tephra layers were identified in the combined stratigraphy, which includes 42 layers from Hestvàtn, 49 layers from Vestra Gìsholtsvàtnand 69 layers from Hvítarvàtn. 106 of these tephra layers were analysed for major element geochemistry. Together with the work of Jóhannsdóttir (2007), this provides a unique tephrochronological record for Central South Iceland, because it constitutes a continuous chronology spanning the last 12kyrs at the resolution of decades to centuries.

These results enabled the examination of geochemistry, soil accumulation rate, identification of historic layers, frequency of tephra fall and associated hazard risks and preservation of tephra within lakes. 47.5% of the tephra layers from this study are basaltic, and another 41% contain a basaltic component, highlighting the importance of basaltic tephra layers in the tephrostratigraphy. Few tephra layers from the Western Volcanic Zone are present in the record despite its proximity to the study area. This emphasises the importance of ice caps on volcanoes for producing sufficiently explosive basaltic eruptions to generate widespread tephra fallout. Although not highly accurate the Sediment Accumulation Rate method gives a reasonable age for eruptions that have not been dated by another method. Frequency of tephra fall is highly variable in the area, it averages 8.4layers/500yrs. Katla is the most hazardous volcano for south-western Iceland, even though only 5% of its eruptions have produced tephra that reaches this location.

1. Introduction

Explosive basalt to rhyolite volcanism in Iceland has produced numerous widespread tephra layers during the Holocene, which provide instantaneous time marker horizons in Iceland as well across the North Atlantic (e.g. Thorarinsson, 1954, 1979, 1980; Dugmore et al. 1995a, Haflidason et al. 2000; Larsen et al., 2002). The combined influence of a divergent plate boundary and a mantle plume has made Iceland one of the most productive volcanic areas in the world. The high frequency of explosive eruptions is primarily due to the fact that most of the active volcanoes in Iceland are ice-covered thus turning basaltic eruptions, that which would otherwise be effusive, into explosive events. This high frequency of eruptions, combined with the rapid accumulation of Icelandic loess, has resulted in an exceptionally high resolution tephra[1] record for the last 8.5 ka (e.g. Larsen, 2000, Larsen et al., 2001; Óladóttir et al., 2005). Even tephra layers from eruptions closely spaced in time are clearly separated in the soil profiles. Tephra layers from soil sections have been examined since 1934 in work pioneered by Sigurdur Thorarinsson which has laid the foundation for present day research activity by touching on almost all facets of present tephra analysis work in the application of his tephrachronology. This work has been continued by Gudrun Larsen and co-workers at the University of Iceland, and more recently by researchers throughout Europe. The use of tephra from lake cores is a more recent event (Boygle 1994, Haflidason 2000, Jóhannsdóttir, 2007) and there is a great potential to acquire more information. The initiation of this work was driven primarily by the need for improved dating and correlation in lake and marine sediment sequences because results obtained by ^{14}C dating were of too low precision. As the studies mentioned above show, not only is there the potential to acquire more critical information on a finer time scale than ^{14}C would allow, such as erosion rate records, and climate and vegetation variability, but also to compare this variability to timings of volcanic eruptions.

Tephra layers are used as a dating tool for geological, paleoclimatic, geomorphological, glacial and archaeological events. Identification of tephra layers in ice cores, sediment and soil profiles also allows them to be used for correlation of paleoclimate proxy records throughout the North Atlantic region where traditional methods such as radiocarbon dating do not provide sufficient accuracy (e.g.

Geirsdóttir et al., 2009). In addition, radiocarbon dates can be cross-checked, thereby improving calibration of the ^{14}C record by accounting for temporal and spatial variation (Lowe et al., 2002, Jennings et al. 2002). Holocene tephrochronology provides a high resolution time sequence for a multitude of interdisciplinary studies including palaeoclimatic and palaeoenvironmental variations across the North Atlantic region (Bergman et al. 2004; Boygle, 2004; Grönvold et al. 1995; Hall et al. 1994, Hall and Pilcher, 2002; Holmes et al. 1999; Kristiansdóttir et al. 2007; Kvamme et al. 1989, Langdon and Barber, 2001; Pyne-O'Donnell, 2006; Ranner et al. 2005), dendrochronology and pollen studies (Hall and Pilcher, 2002), dating of Quaternary sedimentary sequences (Haflidason et al. 2000), studies of glacier fluctuations and cryoturbation features (e.g. Kirkbride and Dugmore, 2005). Tephrochronology is also used to study the spatial variation in sediment accumulation and soil erosion, and thus is used to assess both natural and human-related geomorphological changes (e.g. Dugmore et al. 2000, 2007). In order to apply these records accurately and effectively for correlation in distal regions, it is necessary to have robust chronologies for Holocene tephra layers in Iceland.

Tephra layers can be used for examining the past explosive eruption record (e.g. Thordarson and Höskuldson, 2008). It is possible to reconstruct eruption history, date individual events and to assess the eruption frequency. Mapping of tephra dispersal enables assessment of eruption intensity and magnitude as well as transport and depositional processes (Sparks et al. 1998). Studies of the physical properties of tephra such as grain morphology, grain size and vesicle size and density can be used to evaluate the eruption style and assessment of fragmentation and other conduit processes to improve understanding of eruption processes (e.g. Morrisey et al, 2000). All of these outcomes can be used to help hazard monitoring and mitigation.

Most previous tephra studies have focused their effort on identifying and documenting intermediate to silicic marker layers, primarily because it is easier to locate the light coloured felsic layers in the post-glacial sediment archives (Larsen et al. 2001). It has also been the more distal tephra layers that have received the greatest attention due to their usefulness in dating records. Consequently, tephra layers of basaltic composition have generally not been considred as potential marker layers, although notable exceptions exist within Iceland, for example the

tephra layers from the AD ~870 Vàtnaoldur, AD 1477 Veiðivötn and from several Katla eruptions (e.g. Larsen, 1984, 2000). However, 80% of explosive historical and post-glacial eruptions in Iceland are of mafic composition and have a periodicity of decades to centuries (Larsen et al. 1998, Thordarson and Larsen, 2007; Larsen and Eiríksson 2008a), in comparison to silicic eruptions which have recurrence intervals of thousands of years (Larsen et al. 2001; Larsen and Eiríksson, 2008b). The use of basaltic layers with regional and greater dispersal could be a valuable addition to the tephrochronological record because it has the potential to increase the time resolution significantly.

2. Aims and Objectives

At present there is no consistent method for the identification of source volcanoes for a tephra layer found in a stratigraphy. This has led to several studies misidentifying source volcanoes. A methodology for identification of most Icelandic volcanoes is presented here. It is hoped it is simple and quick enough to use to encourage other workers to use it, but to still retain sufficient accuracy that a statistics based computer program (e.g. Principal Component Analysis) could not produce.

In this study three lacustrine cores from Iceland are analysed. Tephra layers are identified and tephra stratigraphies are produced. Geochemical analysis of the tephra layer identifies the source volcano and aids correlation between cores. A method for identifying the source volcano of each tephra layer is constructed using the compositional dataset for known Icelandic tephra layers compiled and maintained by the Tephra Study Group at University of Edinburgh. An assessment of whether minor and trace elements measured by EPMA are useful for distinguishing Icelandic source volcanoes is made. An accurate record of the tephra stratigraphy including new geochemistry and tephra layer ages are presented from three lakes in Iceland. These results enable the examination of geochemistry, soil accumulation rate, identification of historic layers, frequency of tephra fall and associated hazard risks and preservation of tephra within lakes.

3. Background

3.1 Volcanic structure and magmatism in Iceland

Iceland's volcanism is controlled by the combined influence of a divergent plate boundary and a mantle plume. The plume is centered on East-Central Iceland and results in production of thicker than normal crust allowing Iceland to be subaerial despite its mid-Atlantic ridge setting (Wolfe et al. 1997). Figure 1 shows the general geology of Iceland, consisting of volcanic systems that are composed of either a fissure system, a central volcano or both (e.g. Gudmundsson, 2000). The post-glacial volcanism includes the axial volcanic zone that transects the island from the southwest to the northeast. This axial zone consists of the West (WVZ) and North (NVZ) volcanic zones, which are joined by the Mid Iceland Belt (MIB). The axial zone is linked to the Mid-Atlantic Ridge system by the Reykjanes Volcanic Zone (RVZ) in the south and the Tjörnes Fracture Zone (TFZ) in the north. The Eastern Volcanic Zone (EVZ) is the most volcanically active zone in Iceland and is evolving into an axial zone by southwest propagation through older crust. It is linked to the WVZ by the South Iceland Seismic Zone (SISZ). In addition, there are two intra plate volcanic belts Snæfellsjökull (SVB) and Öræfajökull (ÖVB) (Thordarson and Hoskuldson, 2008).

Thirty volcanic systems are considered active at present (Thordarson and Larsen, 2007). The Grímsvötn system on the EVZ has been the most active volcano in historical time, with 64 verified eruptions. Hekla, Veiðivötn-Bárðarbunga and Katla volcanic systems are the next most active, producing between 21-23 eruptions in historic time (Larsen et al., 1998). These four systems are responsible for 64% of historical eruptions in Iceland and are therefore the most important, both in terms of event frequency and also of volume of erupted material. They have produced ~80% of the total volume of magma erupted in Iceland in historical time and the proportions contributed by each system are as follows: Katla, 29%; Grímsvötn, 24%; Hekla, 15%; and Veiðivötn-Bárðarbunga, 12% (Larsen and Thordarson, 2007).

During historical time (AD870 onwards) eruption frequency has been calculated to be, on average, 20 eruptions (fissure and explosive) per century (Thorarinsson and

Figure 1. General geology of Iceland. The axial zone consists of the West (WVZ) and North (NVZ) volcanic zones, which are joined by the Mid Iceland Belt (MIB). The axial zone is linked to the Mid-Atlantic Ridge system by the Reykjanes Volcanic Zone (RVZ) in the south and the Tjörnes Fracture Zone (TFZ) in the north. The Eastern Volcanic Zone (EVZ) is evolving into an axial zone by southwest propagation through older crust. It is linked to the WVZ by the South Iceland Seismic Zone (SISZ). In addition, there are two intra plate volcanic belts Snæfellsjökull (SVB) and Öræfajökull (ÖVB). The most important individual volcanoes in terms of this study are shown, Hekla (H), Torajökull (T), Katla (K), Veiðivötn (V), Grimsvötn (G).

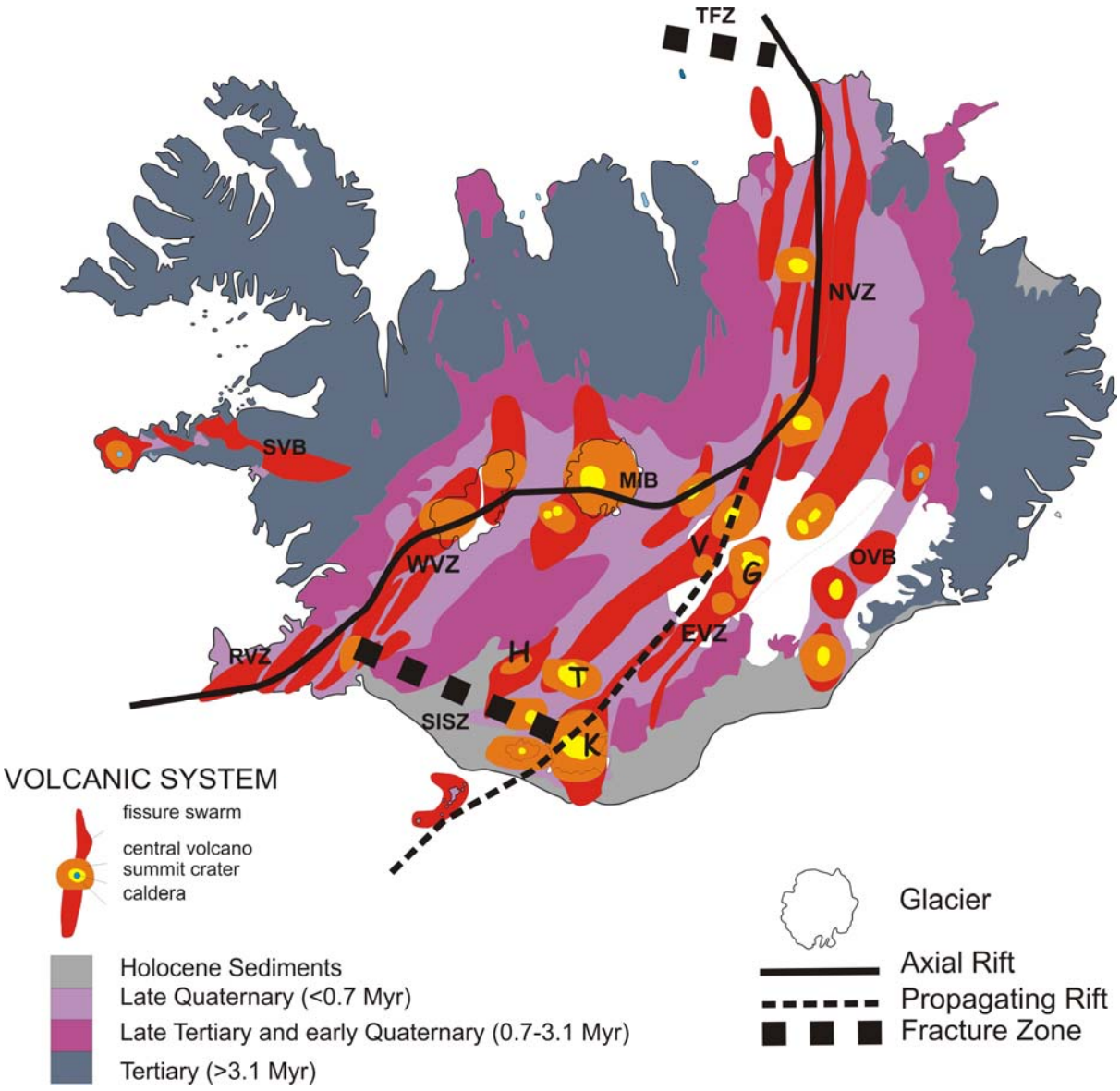

Saemundson 1979), usually characterised by small eruptions (<1 km^3) (Thordarson and Larsen, 2007). Deposition of approximately 800 basaltic tephra layers during the last 9000 ^{14}C years is estimated, but many of those erupted from volcanoes within ice caps have not been preserved (Larsen and Eiríksson, 2007). Volumes of uncompacted basaltic tephra layers range from <0.01 km^3 to >20 km^3, the majority of known tephra volumes lying between 0.1 and 1 km^3. Thordarson and Höskuldson (2008) estimate that basatic eruptions in postglacial time have produced 367 km^3 of uncompacted tephra, which is 82% of the total volume of tephra produced.

3.2 Chemical Composition of Icelandic Volcanism

Products from Icelandic volcanoes are grouped into three magma suites (Figure 2), characterized by alkaline, transitional-alkaline and tholeiitic compositions (Sigmarsson and Steinþórsson 2007, Jakobsson et al. 2008). The composition of basalt to rhyolite magmas erupted within the axial rift zone, i.e. in the Northern Volcanic Zone (NVZ) and the Western Volcanic Zone (WVZ), are of the tholeiitic suite. The EVZ has more complex spatial patterns in composition. The northern part of the zone, including the volcanic systems Grímsvötn and Veiðivötn-Bárðarbunga, is characterized by tholeiitic magmatism. The southern part of the EVZ generally produces products that follow the transitional-alkaline suite with the exception of the Vestmannæyjar volcanic system, that produces mildly alkalic magmas (Jakobsson 1979b). Katla and Hekla both produce high FeO*-TiO_2 transitional alkali basalts (Larsen et al. 2001). Intraplate volcanism occurs on the Snæfellsjökull (SVB) and Öræfajökull (ÖVB) Volcanic Zones, which are characterized mostly by mildly alkalic magmatism although the basalts of the ÖVB are tholeiitic to transitional alkaline (e.g. Jakobsson 1979a, Sigurdsson & Sparks 1981, Hardarson 1993, Jónasson 1994, Slater et al. 1998, Larsen et al. 1999, Larsen et al. 2002, Sinton et al. 2005).

As a consequence of magma suite variability, the identification of source volcano or volcanic zone for a tephra layer can be acheived through the use of major element geochemistry. However, the method is not straightforward. For instance, chemical composition between individual volcanoes of the NVZ, WVZ and RVZ (Jóhannsdóttir, 2006) is often too similar to be able to link their products to specific volcanic systems solely on the basis of chemical composition. For the EVZ, the commonly used FeO-TiO_2 plots discriminate well between a few of the main tephra

Figure 2. Alkali versus silica diagram showing the evolution trends of characteristic magmatic suites in Iceland. From Jóhannsdóttir (2007).

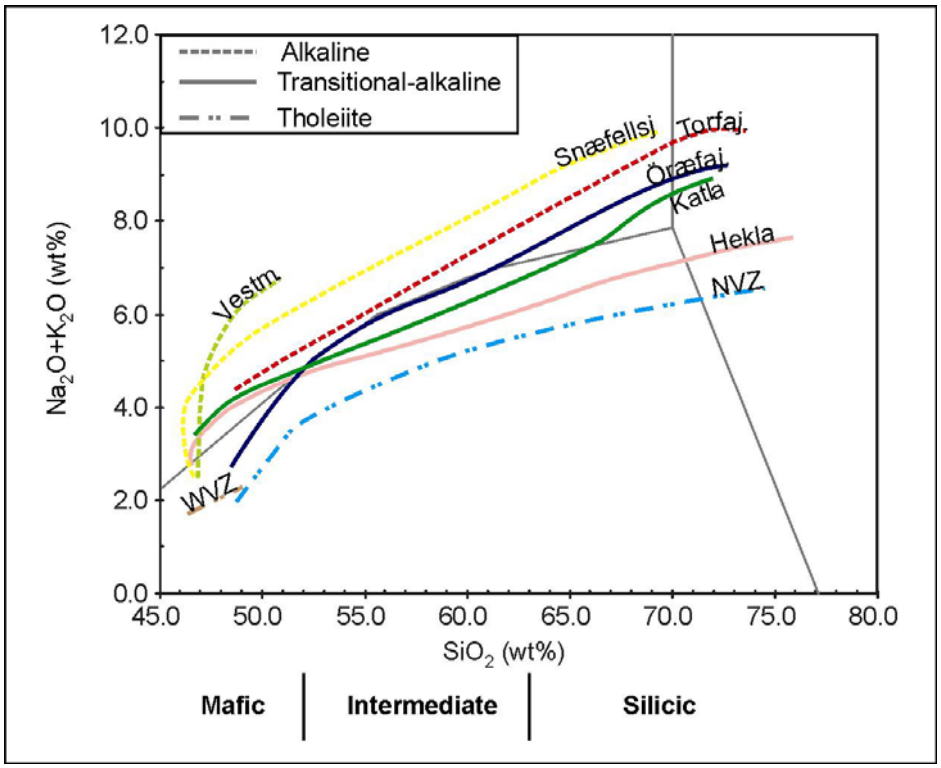

producing volcanoes, i.e. Katla, Veiðivötn and Grímsvötn (Larsen 1981). However, they are not capable of distinguishing between all of the potential volcanoes, in particular Hekla, which can therefore possibly lead to mis-identification. Two of the most prolific tephra layer producers, Katla and Hekla, have basaltic compositions that are very similar and therefore very difficult to distinguish (Jóhannsdóttir, 2007). In these instances sometimes other criteria, such as sampling location, thickness, and grain size of the tephra layers can be useful for identification of the source volcanic zone and system.

There are also difficulties in discriminating between different eruptions from the same volcano solely on basis of major element composition. There are often slight differences in composition but also considerable overlap (Figure 3). All tephra layers in figure 3 are Hekla tephra layers with an icelandite composition but they show subtle differences in composition and clustering. For example H1300 and H1845 have higher MgO than the rest, and the data from H1300 is much more spread out than that for H1845. It is however, very difficult to tell other samples apart, such as

H1510 and H1947 (Larsen et al. 1999). This is where the stratigraphic position of the tephra layers becomes important.

Figure 3. Plot of 5 different Hekla layers: H1510, H1947, H1845, H1300, H1206 of TiO_2 and K_2O. All have an icelandite composition but show slight differences in composition and clustering.

This plot illustrates both the benefits and potential problems of this approach of using a distinctive chemistry to identify a tephra layer. Whether it is necessary to establish which volcanic zone or volcanic system or particular eruption from a volcano, the same applies. Some can always be identified as they have extremely different chemistry; H1206 has much lower TiO_2 than H1300, whereas it would be difficult to discriminate H1947 and H1845 using these two oxides.

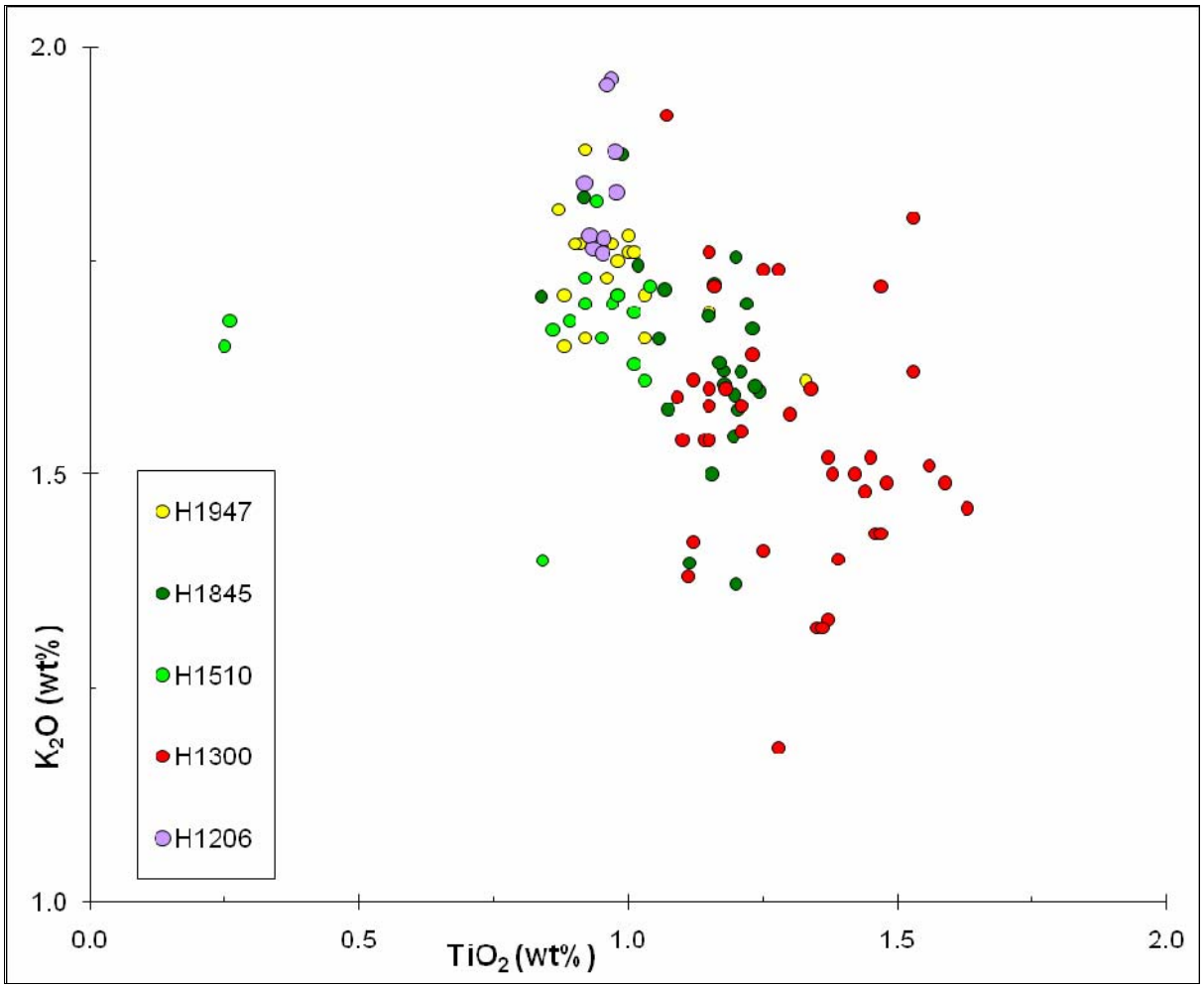

3.3 Holocene Tephrostratigraphy in Iceland

Work by Thorarinsson (Thorarinsson, 1944, 1958, 1967, 1974, 1979, 1981) on historical tephra layers in Iceland and the widespread rhyolitic Holocene tephra layers, has produced the basis for tephrochronological studies in Iceland. Subsequently, studies by Jakobsson *et al*. (1978) and Jakobsson (1979a,b) defining the petrological and the geochemical character of the active volcanic systems in Iceland, have contributed to a more accurate use and better understanding of the tephrochronological sequences.

Over the last 40 years or so there has been considerable effort in recording Holocene eruptive events, mapping tephra dispersion and recording the tephra stratigraphy (eg. Jakobsson, 1968, 1979a,b; Johannesson, 1982,1998; Jóhannsdóttir, 2006; Jonsson, 1978a,b, 1983; Larsen 1982, 1984a, 2000; Larsen and Thorarinsson, 1977, Larsen et al. 1998, 2000, 2002; Mattson and Höskuldson, 2003; Óladóttir et al. 2005; Saemundsson, 1991, 1992, 1995, 2001; Sigvaldson et al. 1992; Sinton et al. 2005; Thorarinsson, 1951, 1965, 1968, 1974, 1975; Thordarson and Self, 1993; Thordarson et al., 1998; Vilmundardóttir et al. 1983, 1988, 1990, 1999a,b). Despite this effort, the history of Holocene eruptions in Iceland is far from complete. Records of fundamental parameters, such as number and age distribution of eruptions and volume of erupted magma (lava and tephra) are incomplete for many volcanic systems: less than 10% of the known tephra layers have been mapped and records from different parts of the country have not been synchronised (Thordarson and Höskuldson, 2008). In particular, little work has been published so far in terms of detailed stratigraphy of individual layers and examination of geochemical analyses and identification of source volcano, with the exception of Jóhannsdóttir (2006), who examined lake cores from 4260-12400BP in South-central Iceland, Óladóttir et al. (2005), who studied an 8.5 ka long tephra record from the Katla system and Óladóttir (2009) whose PhD centres on the Holocene tephra record around the Vàtnajökull glacier. These gaps result in limitations on the assessment of Holocene volcanism in Iceland.

The record of explosive eruptions is most comprehensive in historical times (i.e. since1200AD). Thordarson and Larsen (2007) identify 205 eruption events in historical time. Of these events, 172 (~84%) have been verified by field identification of their products and of those, 150 (~87%) featured tephra-producing (i.e. explosive

or mixed) eruptions. The remaining 13% were purely effusive events (Larsen, 2006). Products from 164 eruption events have been correlated to their respective sources and out of those, ~85% produced basaltic magmas, while ~15% are intermediate to silicic. The composite record for this time period has been put together from three types of archives:

- Soil profiles (37%)
- Ice cores within the Vàtnajökull Glacier (38%)
- Information on eruptions contained in written records (24%), (eg. Thordarson and Larsen 2007, Larsen and Eiríksson, 2007)

However, written records and ice core records from Vàtnajökull only exist since ~1200AD, leaving the sediment/soil record as the only record for earlier periods. Consequently the preservation is likely to be lower than one third of the actual eruption frequency prior to AD1200. During historical time, Grímsvötn has been most active with 47% of the volcanic events followed by Veiðivötn-Bárðarbunga (15%), Katla (12%) and Hekla (11%).There is a bias towards the preservation of Katla and Hekla layers in soil profiles presumably due to the remoteness of Grímsvötn and Veiðivötn-Bárðarbunga from good soil trap sites. Without the presence of the ice core and historical records during historical time we would not know that Grímsvötn and Veiðivötn had been more active than Katla and Hekla so this must be taken into account when prehistoric records are examined. The tephra capture at any one site near the active volcanic zones is approximately 20-35% of the composite record (Thordarson and Höskuldson, 2008) emphasising the importance of recording tephra at multiple sites and comparing and correlating records.

The prehistoric record consists of thousands of measured soil profiles and has been steadily improved (see reviews by Haflidason, 2000 and Larsen and Eiríksson, 2007and 2008). Most published terrestrial records only extend back to ~4Ka and some to ~7Ka (Boygle 1999; Hardardóttir et al. 2001, Jóhannesson et al. 1981, Larsen, 1979, 1984b; Larsen et al., 2001, 2002; Robertsdóttir et al. 1992,). Only a few measured sections exist beyond 8Ka (Sigurgeirsson and Leosson, 1993; Ingolfsson *et al*., 1995, Saemundsson 1991; Óladóttir et al 2005, 2008; Óladóttir 2009) due to Iceland being almost completely ice-covered until ~10Ka except for some peninsulas and elevated coastal mountains. Therefore soil cover was not well

established in general until 8.5Ka (Ingolfsson, 1988, 1991; Norddahl, 1991) and consequently, tephra fall-out has rarely been preserved as distinctive tephra horizons on land. Studies of lacustrine sediments (Björck et al, 1992, Jóhannsdóttir, 2006) and offshore marine and Greenland ice cores extend the record further back in time although the numbers of events that are preserved are reduced significantly with distance from the volcanic source (eg. Grönvold et al., 1995, Haflidason et al., 2000, Jennings et al., 2002, Larsen et al., 2002, Kristjánsdóttir et al., 2007).

In general, basaltic tephra layers have not been considered as good potential marker horizons. Historically, this is due to the big silicic eruptions (particularly those from Hekla) produce very widespread light coloured tephra layers, which stand out and make good distinctive marker horizons against the multitude of thin black layers (eg. Larsen et al., 1999, 2001). It is also partly due to the fact that basaltic eruptions do not tend to be as explosive as rhyolitic events. Therefore, their dispersal areas are generally smaller and thus of less interest to those working outside Iceland. The exceptions are the basaltic Eldgja 934-40AD, Veiðivötn 1477AD and Vàtnaoldur 870AD and Saksunarvàtn (~10Kyr BP). However it is mostly due to preferential sampling of rhyolitic tephras from cryptotephras using heavy liquid separation which is the current accepted technique for lacustrine records. The basaltic tephras may be present in distal deposits but are not being detected. Basaltic tephras are noticeably absent from European peat sequences (Andy Dugmore, pers comm. 2010). Óladóttir et al. (2005; 2008) have improved the basaltic proximal record immensely in just one study of the tephra layers to the east of Katla in a composite section. This is the only detailed published work on a basaltic tephra sequence in a proximal location to a major tephra producing volcano.

One of the main advantages of lake cores is their potential to extend the tephra record back in time as the soil records rarely reach beyond ~8.5Ka due to scouring by the glaciers and the covering of land with ice. Lake cores also have the, as yet not fully developed, potential for the linking of tephra records with paleoclimate. Primarily this has been used to improve the dating of the paleoclimate records to give higher resolution eg. Axford et al, (2005), Geirsdóttir et al. (2009). It can also be used to assess the influence of the volcanoes on climate, or of tephra fall in the lake environment. The main disadvantage is the large catchment area for each lake in

comparison to a soil profile which increases the chances of reworking (e.g. Boygle, 1994).

3.4 Tephra layers outside Iceland

The identification of Icelandic tephra layers outside of Iceland enables a better understanding of the dynamics of explosive volcanism in Iceland through the knowledge of dispersal directions and thicknesses of deposits found at varying distances from the volcanoes. This, in turn, can be used to enhance our understanding of atmospheric transport processes as the tephra layers provide a record of transport directions and volumes of materials transported. Tephrochronological dating at sites outside of Iceland is a very important tool, in particular in archaeological and paleoclimate studies. Tephra layers of Icelandic volcanic affinity have been found in sediments on land in Scandinavia, the British Isles, Ireland, the Faeroe Islands, Denmark and Germany. (e.g. Birks et al., 1996; Björck and Wastegård, 1999; Björck et al. 1992, Bogaard et al., 1994; Boygle, 1998; Davies et al. 2003, Dugmore, 1989, Dugmore and Newton, 1998; Dugmore et al., 1992, 1995a; Eiríksson et al. 2000a, Grönvold et al. 1995, Haflidason, 1983; Haflidason et al., 1998a,b, 2000; Hall and Pilcher 2002, Ingolfsson et al., 1995; Jennings et al. 2002, Koc Karpuz et al., 1992; Kristjánsdóttir et al., 2007, Kvamme et al., 1989; Lacasse et al., 1995; Larsen et al. 2002, Lowe and Turney, 1997; Mangerud et al., 1984, 1986; Merkt et al., 1993; Norddahl & Haflidason 1992, Persson, 1966a,b; Pilcher and Hall, 1996; Pilcher et al., 1995; Rasmussen et al. 2006, Sjøholm et al., 1991; Thorarinsson, 1954, 1979, 1980; Thordarson and Self, 1993; Turney 1998, Turney et al., 1997; Waagstein and Johansen, 1968; Wohlfarth et al., 1993; Wastegård 2005, Wastegård et al., 1998, 2000b).

The more widespread analysis of samples for cryptotephra (tephra grains that are not visible to the naked eye) has contributed to the identification of a number of widespread tephra layers outwith Iceland (Haflidason et al, 2000). Tephras have been found that are known in cryptotephra form only outside Iceland with equivalents having not yet been reported in Iceland. Examples are the Borrobol Tephra (Davies et al., 2003, Eiríksson et al., 2000, Turney et al., 1997) and the rhyolitic Hovsdalur Tephra (Wastegård, 2002).

It therefore seems necessary to have a rigorous and detailed record of tephra layers in Iceland so that layers found elsewhere can be correlated into the tephra succession in Iceland. In cases when geochemical data is required for positive identification of particular tephra horizons, a good geochemical reference base is essential. Such a reference dataset is most rigorous when established via the analysis of tephra from proximal sections, where the layers can be positively identified by other means such as on basis of stratigraphic position and physical properties. The increasing use of cryptotephra makes such a reference data base of particular importance as small sample size increases the difficulties of geochemical analysis since a very small beam is required.Detailed tephra studies in Iceland will help establish which layers are likely to extend beyond the shores of the island.

3.5 Stratigraphy

Stratigraphic sections are important for establishing complete records of eruptions over a particular time span and for obtaining information about volcanic processes and eruption frequency, and to enable good correlation. Lake cores are particularly useful as they can contain a continuous record extending beyond 10 000yrs, which is not possible in soil sections because the soil cover in Iceland is younger than 8.5 ka. The resulting tephrostratigraphy can increase the time resolution of paleoclimate and environmental records from the lakes without introducing the errors associated with radiocarbon dating. The effect of volcanic eruptions on lake environments and paleoclimate can be assessed directly. A discussion of the issues concerning the deposition of tephra in the stratigraphy and in particular lacustrine deposition follows.

Lake location and bathymetry

The location of the lake chosen is important; close to a volcano the tephra is often deposited on barren ground increasing the likelihood of erosion and reworking of the primary fallout tephra. Too far from the volcano and the section will not include tephra from low intensity eruptions. Choice of lake is also important, as suspension deposition needs to be the dominant method of deposition, which usually means a lake with shallow gentle slopes and minimal drainage into and minimal drainage out of the lake. Even when the core is taken from the centre of a basin, Boygle (1994) found that reworked layers were still present due to the input of reworked tephra. It is also necessary to check the lake has been a depositional area for the required

time period. Bathymetry of the lake-bed and currents within the lake may affect settling of tephra which will be different within each lake.

Dispersal mechanisms

Even deposition of tephra layers does not necessarily occur due to uneven topography (or bathymetry) and dispersal. Deposition patterns are also dependent on the weather conditions at the time of eruption. Calm, dry conditions produce blanket-like deposition of tephra while precipitation-bearing systems produce sporadic and discontinuous patterns. The nature of the eruption can also cause differences in deposition. A wet eruption is relatively cold and moist and so results in flocculation and the premature deposition of fine to medium ash (Parfitt and Wilson, 2008).This will result in less deposition in the distal archives of tephra stratigraphy. It is thought that this is the factor in the limited dispersal of tephra from Grimsvötn as opposed to eruption size and intensity (T. Jude-Eton pers comm. 2009). Thick layers in proximal areas do not necessarily indicate wide dispersal of tephra. Any transport mechanism will result in fractionation of material leading to a possible gradual change in composition with distance from source if composition changes with density of the tephra grains. For example the highly vesicular rhyolitic grains of a Hekla eruption will be able to travel further before they are deposited than less vesicular grains. Wind can blow floating tephra along the surface as a thin film as seen in the Hekla 1970 eruption (Thorarinsson, 1979). Wind can also create waves and currents which disturb the water column and therefore the settling of tephra. This is not usually a problem as although the tephra grains are deposited later than the eruption the timescale is negligible. However, it will cause grains with low vesicularity settling prior to those with a high vesicularity.

Erosion and reworking

Erosion of stratigraphy leaves gaps in the record; often an erosional surface will be present in the stratigraphy but not necessarily. This would usually take the form of slumps within or on the slopes of a lake or from river entrance and exit. Reworking either within the stratigraphic section or deposition of tephra eroded from elsewhere causes addition of ‘extra’ tephra layers of the same origin. It is important to recognise the difference between primary tephra and reworked horizons and to create records of primary tephra only. Detailed examination of sections can give indications of whether the deposit is primary or secondary. Reworked tephra within

lake sediments is usually connected to slope stability of the surrounding catchment and not to slumps within the lake although earthquake impact can be significant here (Boygle, 1994; Hardardóttir et al., 2001).

Ideally, if tephra has settled from primary fallout it should be stratified with the densest tephra at the bottom and a decrease in grain density upwards. If this was not the case then it could be an indication that the deposition mechanism was not primary fallout. However changes in density and or size throughout a deposit can be due to fluctuations in the eruption intensity and amount of magma fragmentation. Internal stratification and or size grading in pyroclastic deposits can be due to episodic eruptions, such as the AD 1783 Laki eruption, and not necessarily due to the influx of reworked tephra (e.g. Thordarson and Self, 1993). Therefore, it can be challenging to differentiate between primary tephra fallout and immediately reworked tephra from the stratigraphy, although as with terrestrial tephrostratigraphy, a wide dispersal throughout the lake is indicative of primary fallout. Experience of studying tephra has shown that reworked grains show evidence of abrasion via rounding of corners and edges, delicate grains are usually absent and there is usually a mixture of tephra and sediment or soil in the sample (T. Thordarson pers comm. 2010).

Transport mechanisms

Tephra grains are very susceptible to abrasion. Even on a 5-10m scale they show abraded morphology from rain induced surface run-off (T. Thordarson pers comm. 2010). Therefore it is possible to identify deposits containing grains that have been reworked by water from their rounded edges. Hardardóttir et al. (2001) found that washing in of tephra continued for 60 years into VGHV after the H4 eruption. Boygle (1994) found that discrete layers of H4 and H3 were found deposited 3150yrs and 1950yrs later, respectively, implying that the tephra has remained stored in the catchment for a long period. As long as it is a constant washing in of material, there should be a gradual tailing off in concentration of shards. However if there are pulses of wash-in, this could present as multiple discrete layers. Presence of weathered grains or of grains from several different source volcanoes is often a good indicator of reworking, but it is not universally seen. Boygle (1994) and Jóhannsdóttir (2007) found that a mixed geochemistry is a more reliable indicator. Gudmundsdóttir (2008) found that secondary layers on average had a smaller grain size than primary layers.

There are several transport mechanisms where it is not easy to identify whether tephra has been reworked. For tephra that has been caught in ice on top of the lake during winter and then melted out, no noticeable difference in morphology is likely. However this will result in an age error of <6 months unless there are periods when the lake remains frozen throughout the year. Fall of tephra onto ice may also result in the non-preservation of the tephra in the record, as it may blow away completely or get mixed into snow drifts. Effects of wind are exacerbated when they act in conjunction with deep, loose snow cover as drifting and non-uniform melting creates complex distribution patterns of tephra around a catchment as seen during the January 1991 eruption of Hekla (Hunt and Hill, 1993). It can also be difficult to identify wind re-deposited tephra as opposed to primary fallout tephra.Tephra falling onto a glacier and being preserved there and then calved into the lake could produce a deposit which looks very similar to primary fallout tephra as the tephra would not necessarily have experienced any erosion (Anthony Newton pers comm. 2008). Presence of ice-rafted debris may indicate this as would non-uniform dispersal. As with terrestrial tephrostratigraphy, a wide dispersal throughout the lake is indicative of primary fallout.

3.6 Dating in Iceland

Accurate age determinations are critical for studies aimed at establishing high-resolution records of climatic and geological events. Tephra layers can be used to increase accuracy of the dating of the lake core. Additionally identification of prehistoric tephra layers in a lake sediment core can help with further constraining the age of the prehistoric tephra layer through the use of other dating methods on the lake core such as varve counting or sediment accumulation rate models.

Tephra layers deposited in Iceland in historical time have often been identified and dated with relative accuracy using written records, in many cases even to the exact day of the tephra fall (e.g. Thorarinsson, 1958, 1967, 1975). In Iceland, from AD1500 onwards accurate records have been kept. Data is less detailed from 1000-1500AD and incomplete for 870-1000AD (Dugmore et al. 1995b; Thordarson and Larsen, 2007). Tephra layers not mentioned in written records can be dated either directly (e.g. by fission track dating of the shards) or indirectly (e.g. by radiocarbon

dating organic sediments adjacent to the tephra layers, or by their position relative to tephra layers of known age.

Radiocarbon is the traditional method for dating late Quaternary sedimentary sequences, in particular lacustrine cores. However the method has some inherited complications and has been shown to be inconsistent when dating Icelandic lake sediments (Bard et al., 1994, Bradley et al. 1994, Sveinbjornsdóttir et al. 1998). Generally radiocarbon determinations of lake sediments in Iceland give ages that appear to be too high due to influx of old carbon into the lacustrine environment or contamination of lake waters by geothermal water (Sveinbjörnsdóttir et al. 1998). This upward shift, however, is not consistent from one record to another, thus making correlation between radiocarbon dated records more complicated (Jóhannsdóttir, 2007). A major problem when using these to help interpret climatic records is that periods of climate change are often accompanied by major perturbations in atmospheric radiocarbon content. Other problems include the lack of a precise radiocarbon calibration model for the last glacial termination as well as for marine and atmospheric reservoir uncertainties, the magnitude of which appear to have varied both spatially and temporally (Björck et al., 2003, Bondevik et al., 2001; Eiríksson et al., 2004, Lowe and Walker, 2000; Siani et al., 2001; Turney et al., 2000; Waelbroeck et al., 2001).

Single radiocarbon dates usually give a range of 350yrs. In comparison historic written records give accuracy to the month of eruption. Dugmore et al (1995b) attempted to decrease the range and lack of precision for radiocarbon dates. They found that although effective dates can be found with a single profile; precision can be considerably increased (to ±12 yrs) by combining analyses from several sites. High precision multisample ^{14}C dating techniques (wiggle-matching) can produce particularly accurate and precise determinations, but this requires rapidly accumulating peats and so not many Icelandic tephras can be dated in this manner. Tephra layers can be dated when found in ice cores through the counting of the annual ice layers. This can give age determinations accurate to ±2years (Rasmussen et al. 2005, Zielinski, 2000). Obviously if a known tephra layer is being used to check the dating of the ice core it can not then be given a date by this method. The additional problem being that the tephra layer must have dispersed far enough to reach the Greenland Ice Sheet.

Archaeology, pollen analysis, sediment/soil accumulation rates and varve counting can be used to give an age for undated tephra layers relative to accurately dated tephra layers by the methods described above (Thorarinsson, 1979, 1981). Therefore there is considerable potential to increase the accuracy in dating tephra layers through the use of lake cores

4. Study area

This study covers the three lakes of Vestra Gíslholtsvàtn, Hestvàtn and Hvítarvàtn in the South Eastern part of Iceland.

Lakes Hestvàtn and Vestra Gìsholtsvàtnare located approximately 10km apart in the southern lowlands of Iceland (Figure 4). They are situated on a 0.7-2.5Ma basalt crust wedged between the WVZ and EVZ (Hardardóttir, 2001).

Lake Vestra Gìsholtsvàtnis at 61 m a.s.l. and is the western of two lakes (Eystra (East) and Vestra (West) Gíslholtsvàtn) situated in glacially eroded bedrock basin located just east (<3km) of the Thjorsa river into which it drains (Hardardóttir, 2001; Jóhannsdóttir, 2007). The main inflow is through Dallaekur in the north, although small streams enter the lake at Hrutalindir and Lindir at the southern and south-eastern end of the lake. The lake has an area of 1.57km^2, with mean depth of 6.8m and deepest part of the lake at 15m. Gísholtsfjall is a small fell to the north-east at 168m a.s.l.

Lake Hestvàtn is at 49.5m a.s.l and situated in a glacially eroded bedrock basin on the northwest side of Mt. Hestfjall, which rises to 317m a.s.l. (Hardardóttir, 2001; Jóhannsdóttir, 2007). The lake has an area of 6.8 km^2 and average depth of 23.7 m. It comprises two basins, a 60 m deep one in the northern part of the lake and another in the southern part that is 61.5 m deep and extends 12 m below extant sea level. At present, no major rivers drain into Lake Hestvàtn. The glacial river Hvítá, which originates at Lake Hvítárvàtn, approaches the lake from the north but is diverted along the eastern side of Mt. Hestfjall by a 5-15 m high ridge trending north from the mountain. The river Slauka discharges from the northeast corner of Lake Hestvàtn and drains into Hvítá. Ice dams form from time to time in the Hvítá River during spring thaw and often raises the water level such that the river overflows its banks and temporarily drains into Lake Hestvàtn from the northeast (Kjartansson 1943, Tómasson 1961).

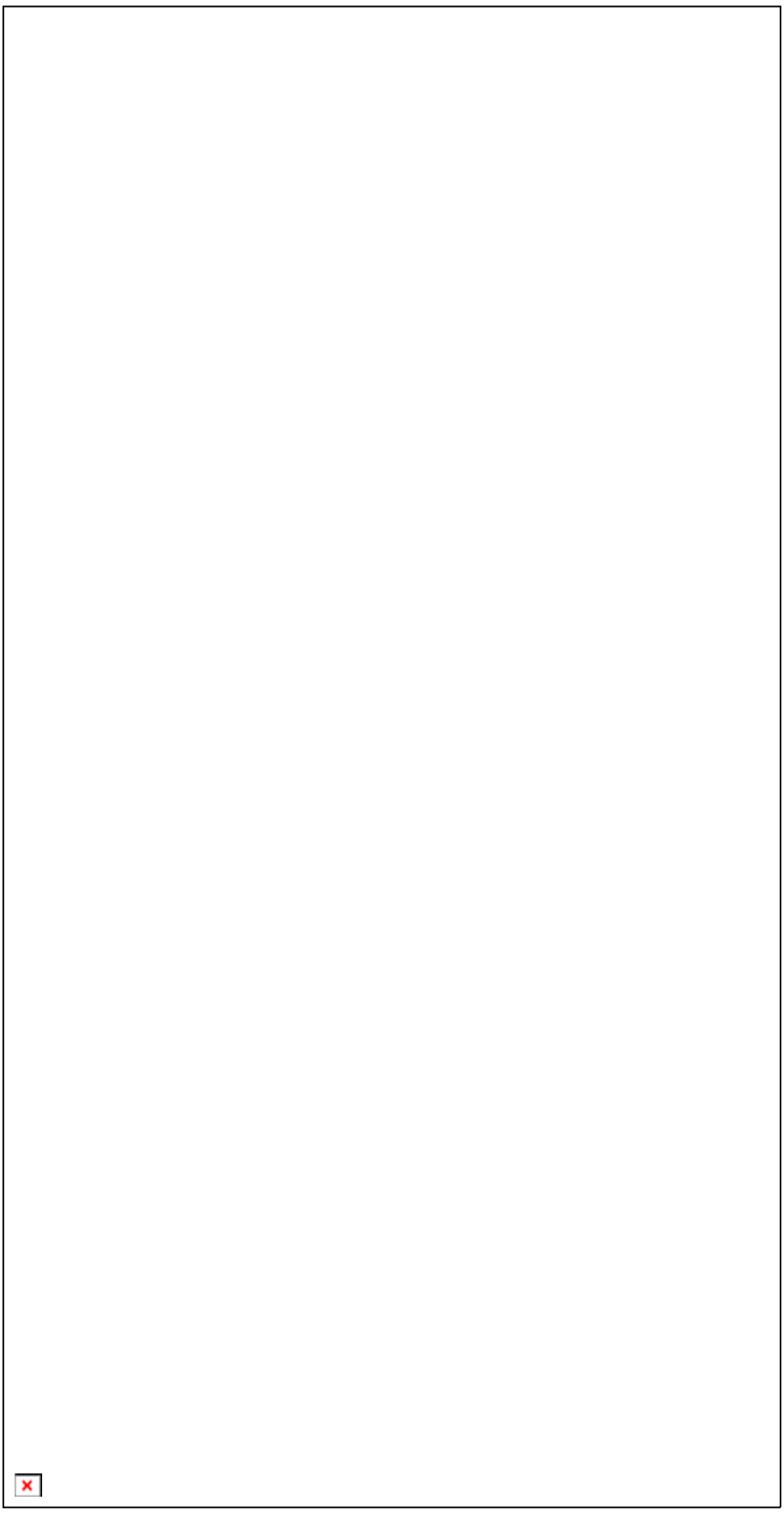

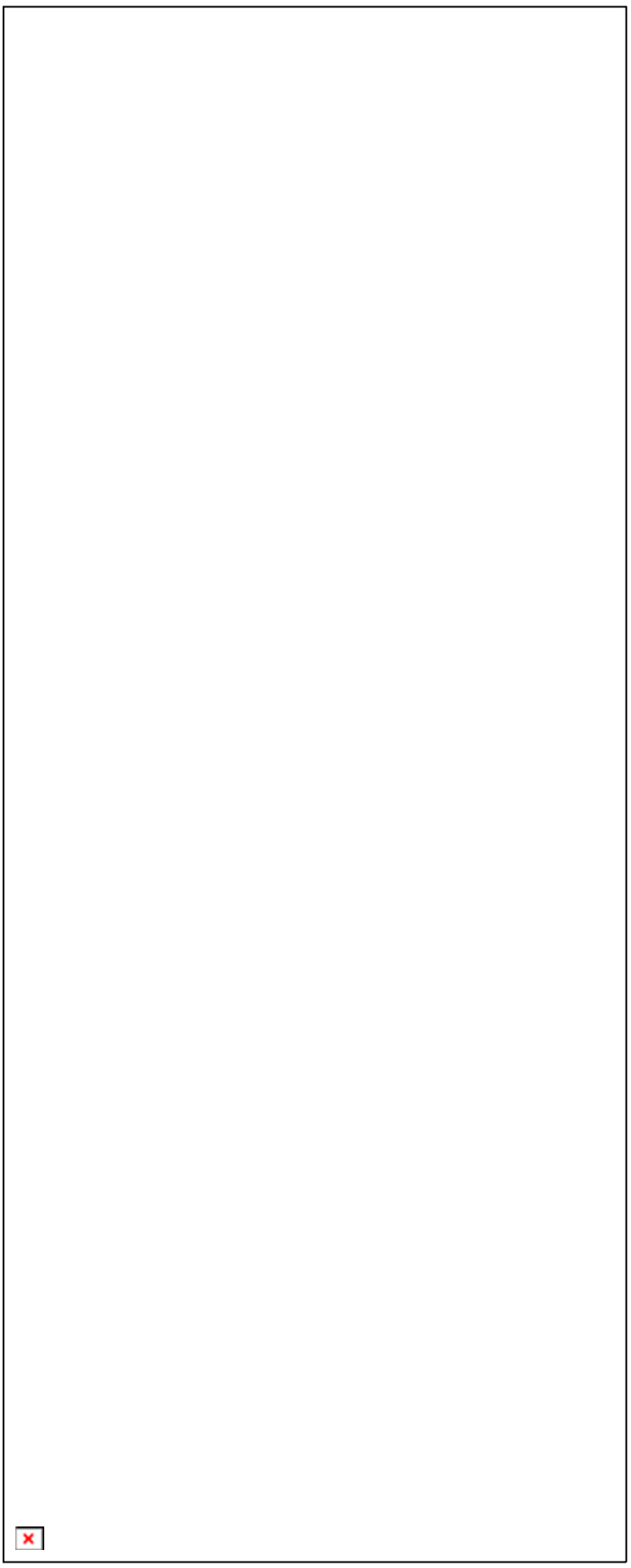

Figure 4a) page 24; a) Map of Iceland showing general geology and main volcanoes and volcanic zones, and location of lakes studied; b) Photo of Vestra Gìsholtsvàtn; c) Photo of Hvítarvàtn looking north from the south end of the lake, the glaciers are visible; d) Photo of Hvítarvàtn looking south from the north end of the lake.

Figure 4b) previous page; a) Topographical and bathymetric map of Vestra Gìsholtsvàtn and surrounding area; b) Topographical and bathymetric map of Hestvàtn and surrounding area; c) Topographical and bathymetric map of Hvítarvàtn and surrounding area;

Figure 5 (below), Hvítarvàtn core 2B-2H-1 from 60cm to the bottom of the core. Each black or yellow band is 10cm. The varves show that deposition is dominated by particles in suspension.

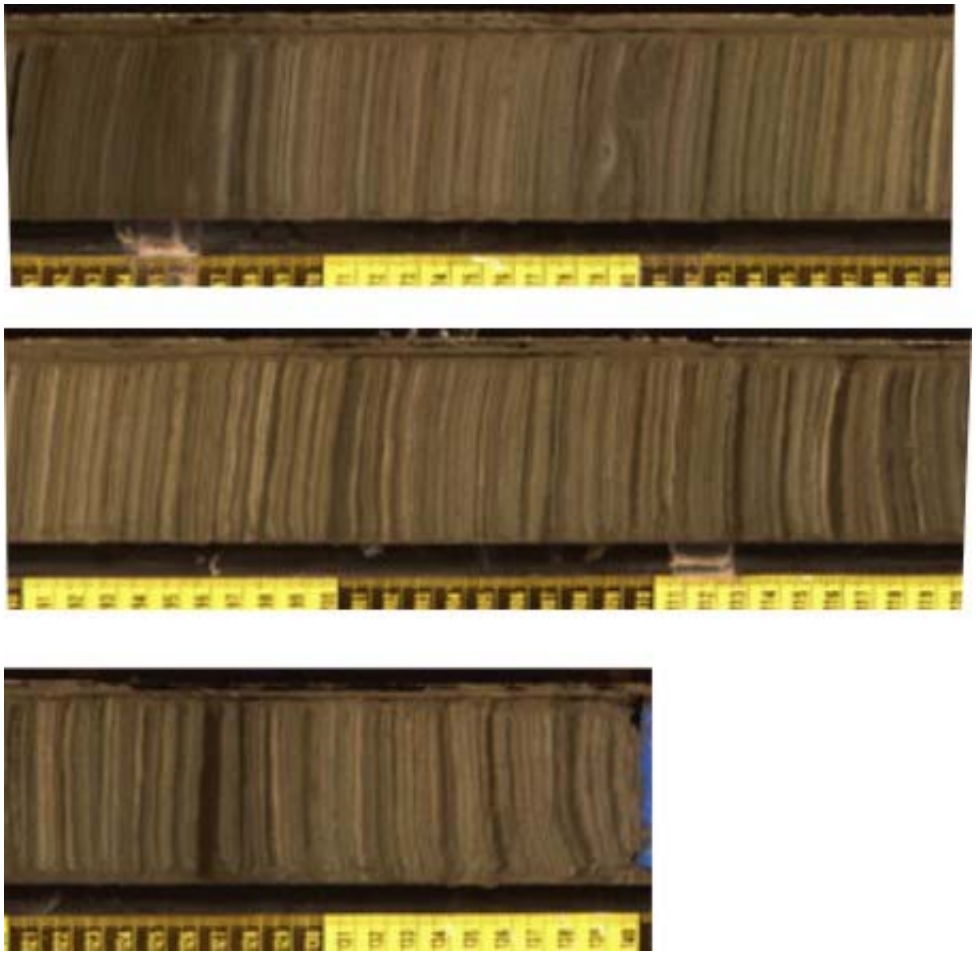

Hvítárvàtn is a glacier fed lake located at the eastern side of Langjökull, the second largest glacier in Iceland (Figure 4). The lake is at 420 m.a.s.l. and covers 29.6 km^2. The northern part of the lake features a ~84 m deep basin whereas the southern part is shallow (<20 m) and sloping gently towards the north (Jóhannsdóttir, 2007). The main discharge from the lake is the Hvítá River. At present, two outlet glaciers, Suðurjökull and Norðurjökull, drain into Lake Hvítárvàtn. Suðurjökull extended into the lake up until the mid 20th century (Black et al. 2004) but now its snout is located approximately 1 km from the western shores while Norðurjökull still calves into the lake.The river Fródá drains from Kirkjujökull glacier into the northeast of the lake, the river Fúlakvísl drains from Hrútfjellsjökull glacier into the east of the lake and the river Svartá drains down the valley to the northeast. During the Little Ice Age (i.e. from about 1600-1900 AD) both of these glaciers terminated in the lake. Although there is a large amount of input and output from the lake, the presence of varves (Figure 5) shows that deposition is dominated by particles in suspension (Darren Larsen, pers comm. 2009).

5. Methodology

5.1 Core collection

Several sediment cores were collected through lake ice from Lake Hestvàtn (cores 94-HV01, 94-HV02 and 94-HV03) in 1994 and Lake Vestra Gìsholtsvàtn(cores 94-VGHV01, 94-VGHV02, 94-VGHV03 and 94-VGHV04) with a Nesje gravity coring system (Nesje et al. 1987; Nesje, 1992). Overlapping twin cores were collected at each coring site to ensure complete sediment sequence retrieval.

The lake sediment cores used from Lake Hvítarvàtn were collected in summer 2003 by a joint University of Iceland and INSTAAR, University of Colorado, Boulder expedition. The DOSECC´s GLAD200 core-rig (www.dosecc.com), equipped with ODP-style coring tools, was used to recover over 20 m long cores. There are 3 main core sites, with 2 cores at site 1, 3 cores at site 2 and 2 cores at site 3 (Figure 4). Twin cores, overlapping, were collected at each coring site to ensure complete sediment sequence retrieval. The cores are 6 cm in diameter and retrieved in 3 m-long sections.

The cores are stored with The Limnological Research Center (LacCore) at the University of Minnesota and examination took place at their facilities. Storage takes place at 4◦C. The polycarbonate liners of the cores are grooved using a pair of adjustable medical cast saws. To avoid introducing polycarbonate shreds into the sediment and losing sediment prematurely, the saws are set to stop short of cutting through the liner. The remainder of the cut is made with utility knives. Endcaps are cut through as well, and the core is split with fishing line, if sediments are consolidated and firm, or a pair of guillotines placed back to back.

When a core is newly cut open or unwrapped after storage, it is often necessary to lightly scrape the cut surface to expose fine sedimentary structures in preparation for imaging or core description. The core is cleaned by scraping parallel to the bedding planes with the flat of the slide. A minimal amount of sediment is removed, wiping the slide on a damp sponge between scrapings.

The Geotek XYZ core logger automates the measurement of high-resolution magnetic susceptibility by point-sensor, color analysis by spectrophotometry, and detection of natural gamma emissions. This gives information for limnological studies and the magnetic information helps identify where crytotephra layers might be as increased magnetic can be an indication of tephra due to high Fe contents. Cores were scanned in the DMT CoreScan Colour to produce high quality digital images for core description and cataloguing. (See Appendix 1 and 2 for core photos and logs).

5.2 Sampling of cores

The tephra layers were visually identified within each core. Very thin layers were detected by running a knife through the core to detect changes in texture.The thickness of individual layers was measured and their colour, grainsize, fabric and depositional structure were recorded. Samples were collected from each layer for analyses of clastic components, grain morphology and chemical composition.

Precaution was taken to avoid unnecessary contamination from the sediment above and below. Multiple samples were collected from exceptionally thick layers or layers that showed marked variations in depositional structures or fabric in order to capture potential changes in grain morphology, clastic components or chemical composition. For this project tephra layers are only of interest if they are primary tephra layers; those directly deposited from the air after an eruption. The addition of reworked tephras into the record presented here would give erroneous results of tephra fall frequency and cause confusion over the identification of tephra layers. Redeposited tephra layers are distinguished from pristine tephra fall layers based on their grains' mottled appearance, chipped edges, sediment lining crevasses and grain alteration when examined using a binocular microscope. Smear slides were made of all tephra layers identified in the stratigraphy to establish whether the layer was primary airfall tephra or reworked tephra (Figure 6). Tephra layers which upon microscope examination were definitely redeposited were not sampled for geochemical analysis. Layers which were ambiguous were taken for geochemical analysis as a mixed set of geochemical data is indicative of reworked tephra whereas a single geochemical population is indicative of primary tephra.

Figure 6. Binocular microscope images of four smear slides. Slides a and b look to be pristine tephras, c and d are reworked tephras. a) Image is from HAK03-6H-2, 2.3cm and shows pristine tephra. The grains are nicely shaped and have sharp pointed ends which would be abraded if they had undergone any erosion. There is a reasonable amount of non glass material but this can enter through the sampling of very thin layers. b) Image is from HAK-6H-2,5-9.3cm and is pristine tephra. Glass grains have sharp corners in particular the grain in the middle of the slide. The grain just above this has a pipe shaped structure which is very fragile. There is little other material in the slide. c) Image is from HAK-6H-2,18.1cm and is reworked tephra. The majority of the slide is not made up of glass grains but of lithics, oxides, diatoms and other sedimentary material. Grains are rounded and display broken edges. Grain size is small which is not indicative of reworked tephra but when taken into account with other indicators can be helpful. d) Image is from HAK-6H-2,44cm and is reworked tephra. The glass grains display broken edges and rounded corners. There is little non-glass material, indicating that the catchment which provided the material was completely covered in tephra at the time or lacked other potentially mobile material.

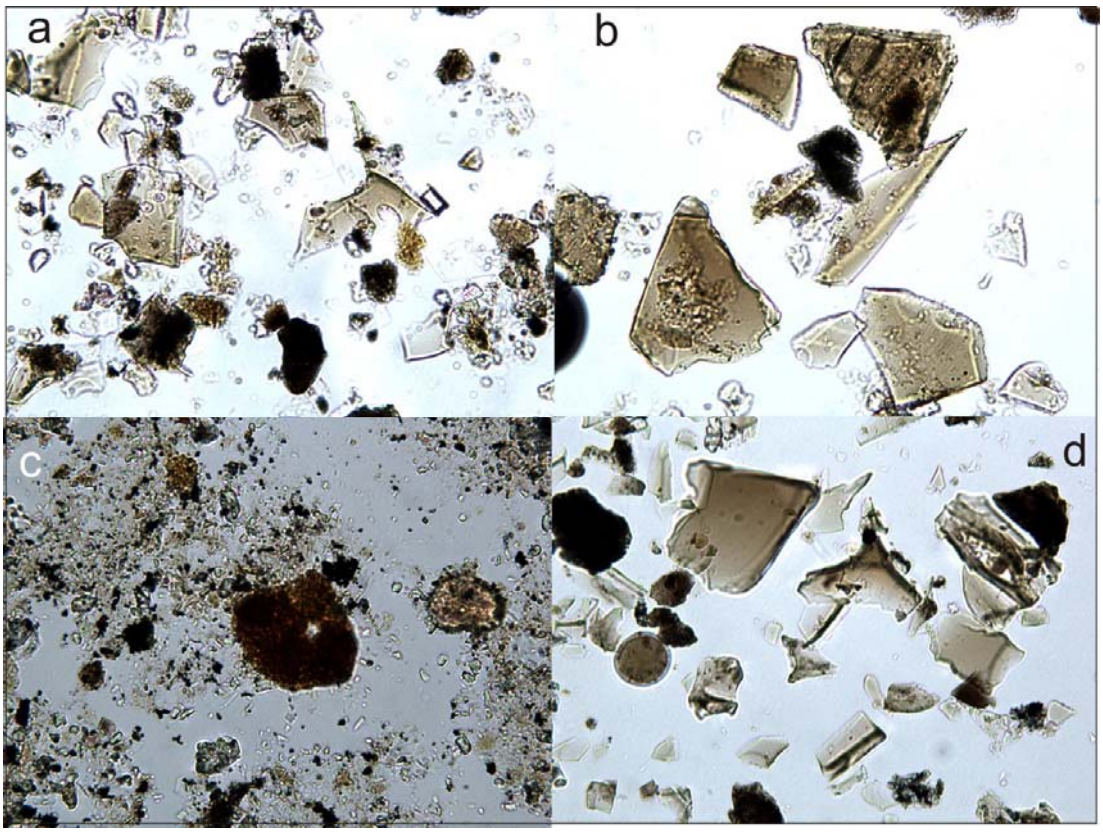

5.3 Sample preparation

Samples are washed in tapwater to remove organic material and then dried. This process is sometimes repeated 10 times to obtain a clean sample. Each tephra sample is sieved to obtain the coarsest size fraction possible to use for the technique (typically retaining the 100-250µmm fraction). The choice of method of separation is important as glass is vesicular and with a large surface area can absorb fluids. Therefore physical separation means are preferable to chemical means to avoid contamination from chemicals. The efficiency of separation is monitored by examining a small amount of sample under a binocular microscope.

The samples were prepared for EPMA analysis as follows. 7 holes were drilled in probe plugs. One sample was poured into each hole which was then filled with epoxy resin. This was left in a vacuum to remove bubbles. Once dry the bottom side was polished with 6 μm and 1 μm diamond paste to expose fresh glass surfaces. Plugs were cleaned in an ultrasonic bath for 15 minutes with washing up liquid and deionised water, then 15 minutes with deionised water and then 10 minutes with petroleum ether.

Cleanliness was checked under the microscope and plugs were then C-coated. Digital maps were made of each sample (prior to cleaning and C-coating) (Figure 7). Examination of the grains under a microscope recorded vesicularity, grain size, and other characteristics (Figure 6). This enabled planning for EPMA analysis as the highly vesicular grains proved hard to analyse and needed to be analysed one by one. All analysed points were marked on the digital maps and cataloged.

5.4 Geochemical Analysis

Bulk or Grain-specific Analytical Methods

Tephra layers contain a juvenile volcanic component consisting of glass shards, pumice fragments and phenocrysts (eg. feldspar, pyroxenes, oxides). To analyse the composition of the magma it is necessary to analyse the glass shards only, and more specifically those glass shards that are free from microlites.

Analytical methods fall into two groups, grain discrete (Electron Microprobe analysis (EPMA), Ion Microprobe and Laser Ablation Inducitively Coupled Mass Spectrometry (LA-ICP-MS) and bulk sample methods. Bulk methods can again be

Figure 7. EPMA digital mapping method.

a) Probe plugs are scanned and labelled; b) Detailed images are taken under reflected light binocular microscope, points that are probed are added to these images; c) Images are taken when probing to get exact positioning and a clearer image and then labelled at 1000µm and d) at 200µm widths.

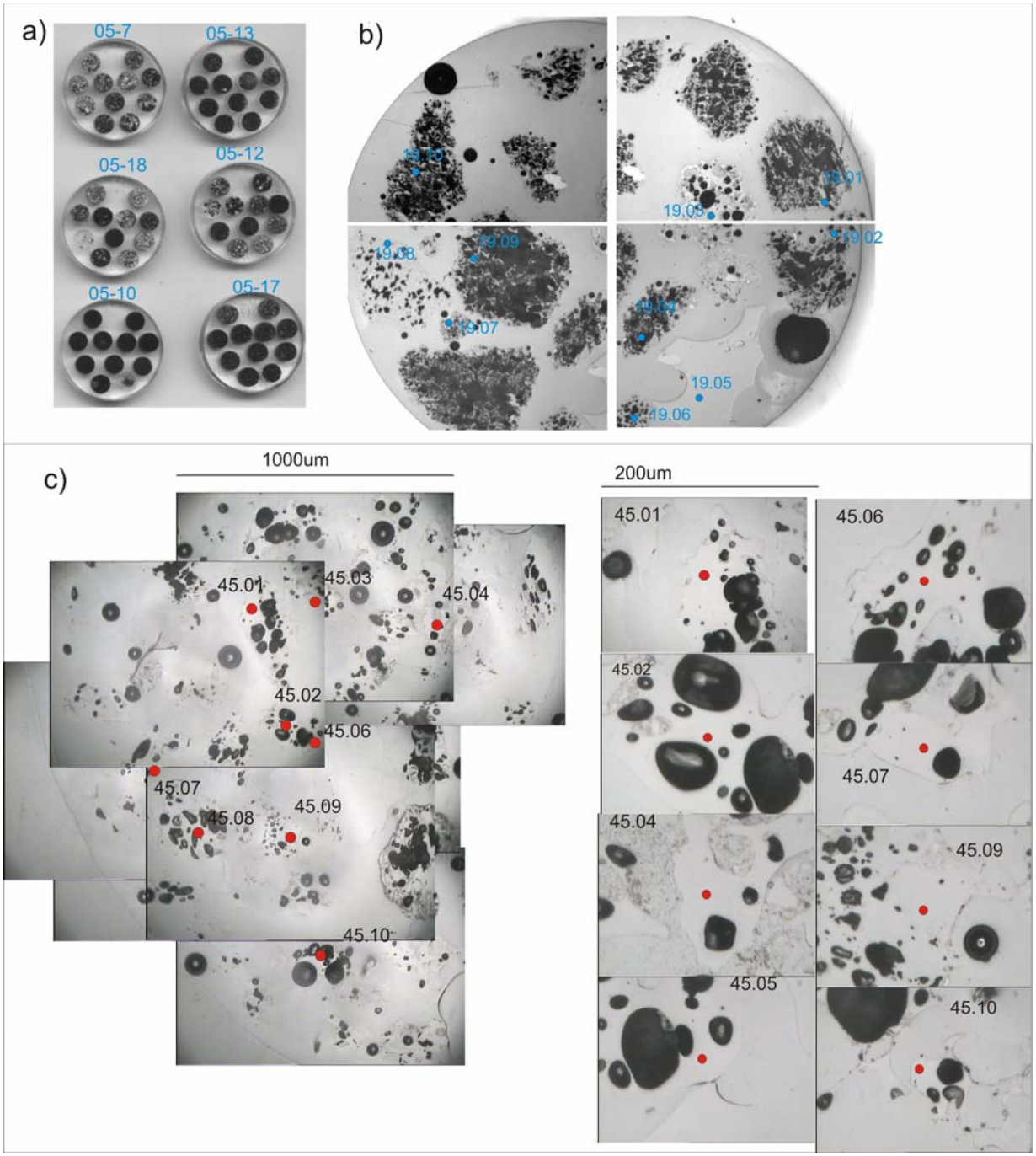

split into ‘‘dry’’ techniques such as X-ray Fluorescence spectrometry (XRF) and instrumental neutron activation analysis (INAA) or ‘‘wet’’ analysis by atomic absorption spectrophotometry (AAS), inductively coupled plasma mass spectrometry (ICP-MS) or inductively coupled plasma optical emission spectrophotometry (ICP-OES).

The bulk analysis of a tephra deposit will not reflect solely the primary magmatic component, and will not reflect the variation inherent within a tephra layer, rendering the analysis useless in terms of tephra correlation. As a result the use of grain specific methods is much preferred. Smith and Westgate (1969) used EPMA to characterise a variety of tephras based on their major elements and this approach is now common in tephra studies. Up until recently, trace element determination in tephra has relied on analysis of bulk material (either whole sample or a separated juvenile component) by XRF (Sverrisdóttir, 2007) or instrumental neutron activation (INAA; Sarna-Wojicicki et al., 1979; Westgate and Gorton, 1981). This was due to the achievable detection limits by EMPA not being low enough for reliable detection of trace elements. With the introduction of inductively coupled plasma mass spectrometry ICP-MS (Pearce et al. 1999), SIMS Ion microprobe proton (e.g. Hinton, 1995), and induced X-ray emission (PIXE, e.g. Fraser, 1995), LA-ICP-MS (Pearce et al. 2008) it has become possible to analyse single shards for trace elements. As yet these methods have not been applied widely to the analysis of volcanic glass.

In this project I used EPMA, as for a grain-specific method it is low cost and readily accessible. This is important in terms of making our work easier, but primarily it is important to use the methods that most studies will use if we are to create a useful resource for others to access. The main limitiation is that it is not possible to measure all trace elements and time is greatly increased per analysis if those trace elements that can be detected are measured.

Problems for all geochemical analytical methods

Post-depositional alteration of glass shards can occur, through hydration and alkali exchange (Shane, 2000); processes that are dependent upon the duration of any subaerial exposure and differences in depositional environment (Dugmore et al., 1992). Volcanic glass hydrates with time incorporating water within the polymer structure of the glass (e.g. Jezek and Nobel, 1978). As volcanic glasses form from

melts of residual liquid magma with a wide range of chemistry, temperature and internal states of order (Ewart and Fieldes, 1962) it is possible for shards from the same magma to have different states of polymerisation and to hydrate in different ways. Highly weathered glass shards often exhibit pitted surfaces with spherical etch pits. However, there is no evidence that this affects the interior of the shard until devitrification occurs. Therefore analyses should be made on freshly polished internal surfaces (Froggat 1992).

Alteration of volcanic glass also occurs as a result of biogenic grooving or microbiological activity on the glass surface and subsurface (Ross and Fisher, 1986; Thorseth et al., 1991, 1992). Microbiological activity is especially extensive in marine environments and is usually more marked on rhyolitic than on basaltic particles. In terrestrial deposits, such as peat bogs or lake sediments, extreme pH values can have a major influence on element mobility in both basaltic and rhyolitic volcanic glass shards (e.g. Thorseth et al., 1991, 1992) and can result in variations in the geochemical composition for a single tephra layer that exceed the variation related to natural inhomogeneity of the volcanic glass shards (Haflidason et al., 2000). Again polishing to reveal unweathered internal surfaces is sufficient. Previous studies in Iceland (eg. Jóhannsdóttir, 2007) have found little evidence of alteration in Holocene tephra deposits due to the short time periods and cooler temperatures suppressing the alteration process.

Problems specific to EPMA

EPMA analyses of volcanic glasses commonly have totals below 100 wt%. If all elements have been analysed totals under 98wt% cannot be accepted as a truly accurate representation of the chemistry as this implies instrumental error or lack of measurement of an important element or the area analysed contained a hole. As most samples are fully degassed the argument that retained volatiles are the cause for low totals cannot be correct. A minor effect in basaltic glasses is the measurement of total iron as FeO*, which will slightly under-represent iron because of the presence in most basaltic glasses of a minor Fe_2O_3 component (Hunt and Hill, 1993, 1996, 2001).

The quantification of sodium, especially in rhyolitic glass shards, has often been a problem during electron microprobe analysis, frequently resulting in a 50% underestimation of the original Na-concentration in the glasses. This results from

time-dependent loss in intensity following continuous electron bombardment from the electron gun (Nielsen and Sigurdsson, 1981). To correct for this loss, Nielsen and Sigurdsson (1981) recommended the use of an empirical technique that estimates the initial sodium concentration from the rate of decay of sodium counts. Another method commonly used has been to defocus the electron microprobe beam to reduce the electron bombardment per unit area, and in that way significantly reduce the loss of sodium. This method reduces the loss of sodium to around 10–15% of the original concentration (Haflidason 2000). This, however, reduces the accuracy of the measurements.

Advantages of EPMA are the ease of preparation and use of machine. It is also relatively low cost for a grain specific method. The main limitation of EPMA with respect to the issues concerning tephra deposit identification is that it is not suitable for determination of all trace elements.

5.4.1 EPMA analysis

VGHV and Hestvàtn

The groundmass glass of the VGHV and HST tephra layers was analysed by Thor Thordarson in 1997 using a the Cameca SX50 energy dispersive electron microprobe at CSIRO, Perth Australia. The following instrument settings were used: 15 kV acceleration voltage, 15 nA beam-current and 10 μm beam. Estimated precision is 1%. Inspection of the grains using BSE images was undertaken to ensure the analysis was of pristine and microlite free glass. Standards were analysed every 30 samples to check for drift and allow recalibration if necessary.

Hvítarvàtn

An analysis set up was produced for the Cameca SX100 energy dispersive electron microprobe that allows the measurement of the major and trace elements to detection limits in the range of 50-1400ppm (Table 1) for basaltic and silicic glasses at the NERC Tephra Analysis Unit at the University of Edinburgh. The analytical setup was established experimentally through analysis of an internationally recognised basaltic glass standard BHVO2g and the recommended standard for rhyolitic glasses of Lipari1. Beam size was reduced to the minimum possible without causing Na loss, as judged by comparison between our analyses and the ideal

composition quoted for the glass. Tests also show that even at the relatively high current densities used for minor and trace

Table 1. EPMA set-up being used at the Univeristy of Edinburgh on a Cameca SX100 electronprobe microanlyser using standard X-PHI corrections. There are two conditions for analysis to preserve Na_2O. Condition 1measures Al, Si, Ca, Ti, Fe, K, Na, Mg at 15kV, 2nA, with a 5µm beam, condition 2 measures F, Cl, P, S, Sr, Mn, Cr, at 15kV, 80nA, with a 5µm beam. Standards are BHV02G – USGS and Lipari1.

Element/ Oxide	SiO_2	TiO_2	Al_2O_3	FeO	MgO	MnO	CaO	Na_2O	K_2O	P_2O_5	F	Cl	S	Cr	Sr
Detection Limit (ppm)	1200-1400	380-410	640-720	2400-2700	300-330	163-170	550-750	680-800	370-420	50-60	440-450	60-70	49-52	85-90	229-238

element analysis, chemical modification of the sample during analysis does not occur. Minimising the beam diameter to a fifth of its original size (Figure 8) has two main advantages: 1) analysis of smaller areas is possible, reducing potential biases in data sets, and enabling repeat analysis on single shards; 2) a greater degree of automation of the analyses is possible, so that data production rates are improved. This set-up has been used for 95 (out of 164) of the Hvítarvàtn samples. The following instrument settings were used: 15 kV acceleration voltage, 2nA beam-current and 5µm beam for Al, Si, K, Ca, Ti, Fe, Na and Mg, and then 15 kV, 80nA and 5µm for F, Cl, P, S, Sr, Mn, Cr. However it is reasonably slow (8 mins per analysis) and it is not necessary to measure so many elements solely for correlating between tephra layers in different lakes. Therefore a faster set-up was developed for major elements and volatiles, which used the following settings 15 kV, 2nA and 5µm for Na, K, Mg, Al, Si, Ca, Ti, Fe, and 15 kV, 80nA and 5µm for F, Cl, P, S. This took about 4 minutes and so was far more efficient when only major elements and volatiles were needed and was used for the remaining 69 samples from Hvítarvàtn. Standards were analysed every 30 samples to check for drift and allow recalibration if necessary. PAP-ZAF matrix correction was applied to all analyses (e.g. Pouchou and Pichoir 1984). Comparison of the basaltic and silicic standard values of the data from this study, to the reported values of the standard, show no signigicant Na loss (Figure 9).

Table 2. Errors associated with EPMA data for each element analysed. The data collected from the standards is presented in appendix 1. These show the calculations for the errors given in table 2. These were calculated by finding the standard deviation and average of all data collected for every probe session. Two sigma was added and subtracted to the average to give the maximum and minimum values of the data within 95% confidence limits. These maximum and minimum values were then compared to the standard value given by USGS (BHVO2 and BIR-1) and Sparks (Lipari1). The differences are reported in the first 4 rows of the table for basaltic standards. The maximum difference in each case was taken to be the final uncertainty highlighted in red writing. All values are the fraction out of 100, i.e. 0.65 = 65%.

Standard	SiO_2	TiO_2	Al_2O_3	FeO	MnO	MgO	CaO	Na_2O	K_2O	P_2O_5
BHV02g	0.65	0.12	0.36	0.84	0.07	0.24	0.25	0.20	0.05	0.01
BHV02g	0.71	0.05	0.39	1.77	0.01	0.29	0.22	0.09	0.06	0.04
BIR-1	0.16	0.04	0.19	2.26	0.02	0.27	0.17	0.07	0.01	0.00
BIR-1	0.65	0.02	0.21	1.57	0.00	0.24	0.02	0.02	0.01	0.01
Basaltic max error	0.71	0.12	0.39	2.26	0.07	0.29	0.25	0.20	0.06	0.04
Lipari	0.93	0.03	0.62	0.03	0.00	0.07	0.09	0.17	0.17	0.02
Lipari	0.98	0.03	0.23	0.46	0.02	0.02	0.05	0.24	0.27	0.00
Silicic max error	0.98	0.03	0.62	0.46	0.02	0.07	0.09	0.24	0.27	0.02

The dataset collected from the standards is presented in Appendix 1. Calculation of the errors presented in table 2 are shown there. The errors were calculated by finding the standard deviation and average of all standards data collected for every probe session. Two sigma was added and subtracted to the average to give the maximum and minimum values of the data within 95% confidence limits. This was then compared to the standard value given by USGS in the case of BHVO2 and BIR-1, and Sparks in the case of Lipari1, and the difference is reported. The maximum difference in each case was taken to be the final uncertainty given in the table above.

Figure 8 (next page). All images have width of 200µm unless otherwise specified.
Top left image; a) size of area necessary for the initial analysis set-up ~100µm^2, b) the size of area necessary for the new analysis set-up ~ 20µm^2. Second on left; this image shows that whereas some areas might look like a large area of glass they are actually a very thin film of glass round the bubble with the rest filled with resin. 127.07 and 128.09 show nice basaltic grains with no microlites and large spaces to analyse. 132.04 and 130.05 show silicic highly vesicular grains which are very hard to analyse. The red dot shows the area analysed and is the biggest space found in that particular grain. The area analysed is slightly bigger than the red dot and as a result totals are often low due to there not being glass under the whole analysis area. 20.08 and 123.04 depict another problem with silicic grains. Often large holes are ripped out of the grain whilst polishing or they are not filled with resin due to the tiny vesicles. These show up as large black spaces. This affects the charging across the sample and therefore the results from the probe.

Figure 9 (page 41). Plots of Na_2O and K_2O; the red dot is the official standard value, the blue dots are the data from this study. The plots show no Na loss during EPMA analysis with the smaller beam size and longer counting times, for both basaltic (BHVO2 and BIR-1) and silicic (Lipari1) Standards.

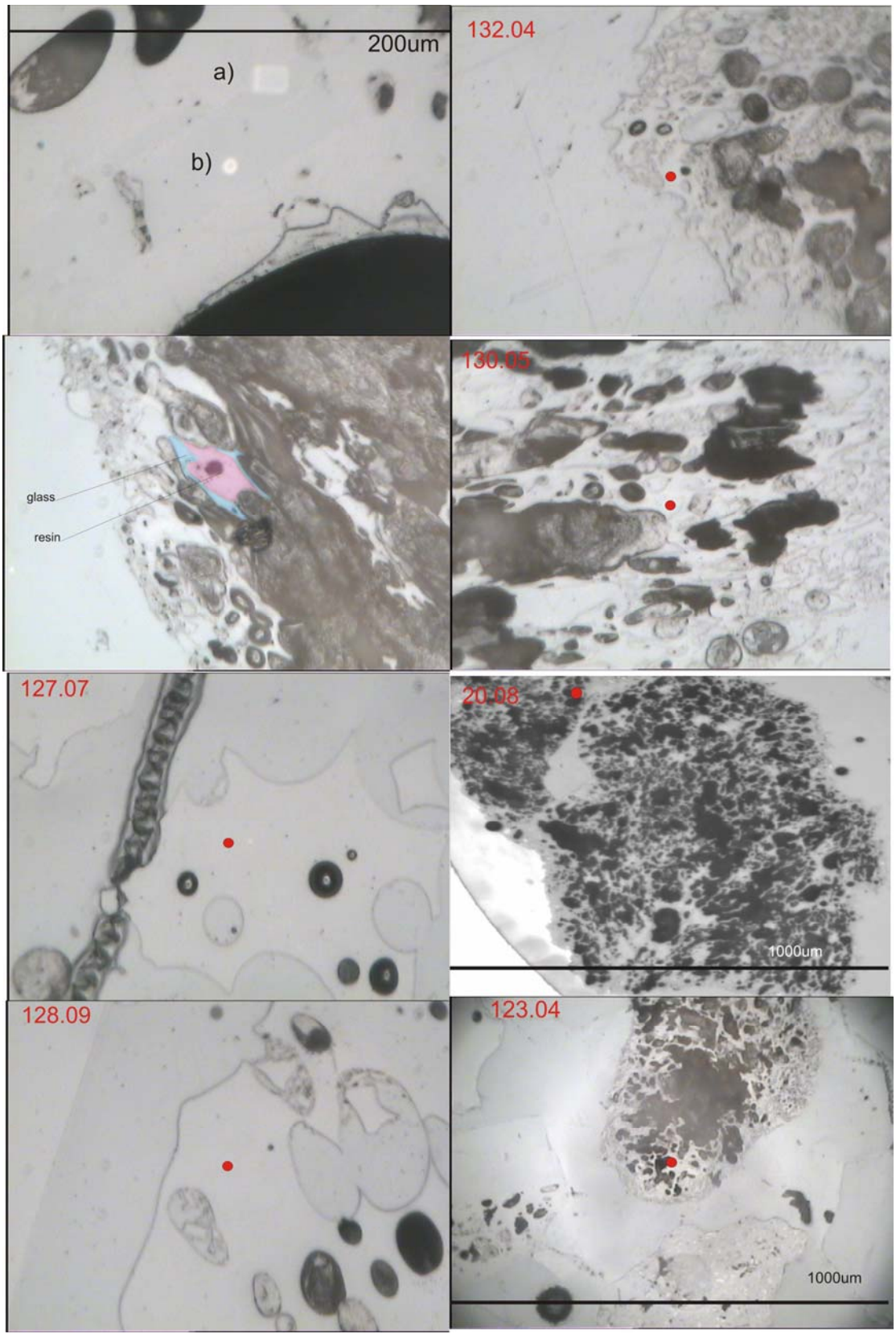
200um
a)
b)
132.04
glass
resin
130.05
127.07
20.08
1000um
128.09
123.04
1000um

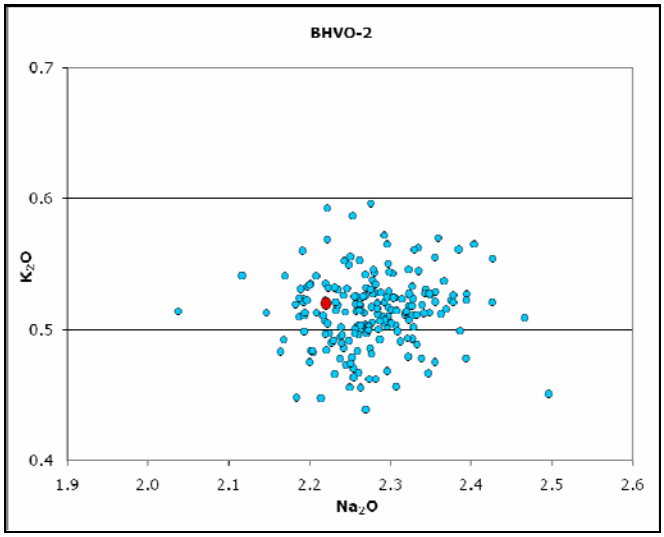
BHVO-2
0.7
0.6
0.5
0.4
K2O
1.9
2.0
2.1
2.2
2.3
2.4
2.5
2.6
Na2O

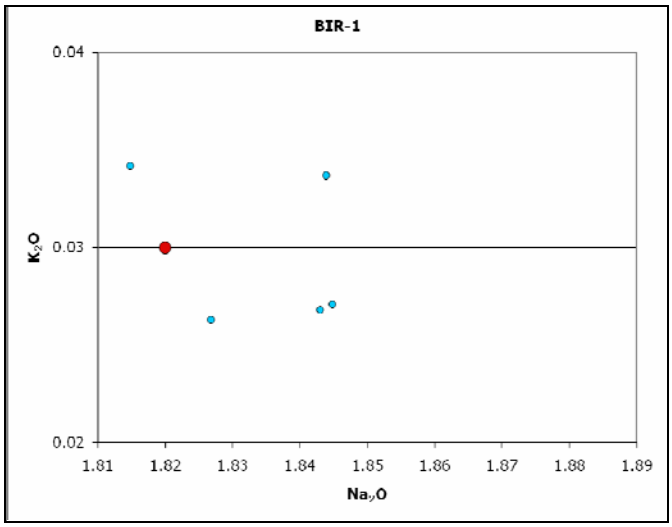
BIR-1
0.04
0.03
0.02
K2O
1.81
1.82
1.83
1.84
1.85
1.86
1.87
1.88
1.89
Na2O

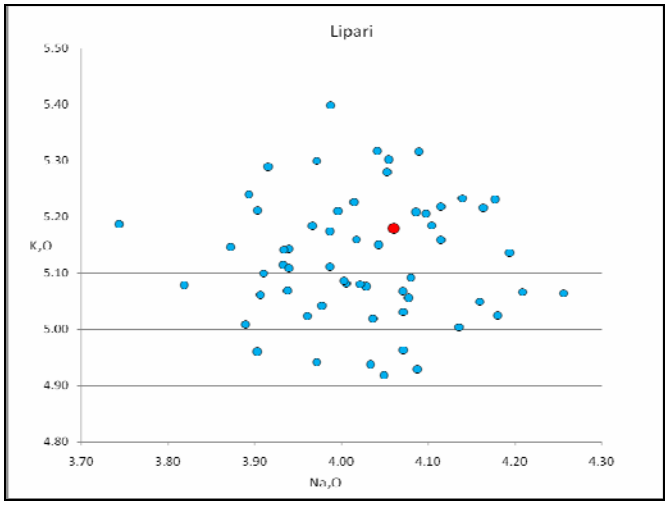
Lipari
5.40
5.30
5.20
K2O
5.10
5.00
4.90
4.80
3.70
3.80
3.90
4.00
4.10
4.20
4.30
Na2O

6. Results

6.1 Tephra Stratigraphy

Identification of key marker layers

In all of the lake cores the initial examination was for key marker layers. Table 3 shows the key marker layers found in the lake cores and their calendar (before 2000 AD) and ^{14}C ages. These marker layers were visually identified as the characteristics of the layers are well known in the area. Hekla layers are light in colour due to their silicic nature (Larsen et al. 1999). Katla layers, with the exception of the SILK layers, are basaltic and therefore black. SILK layers are silicic and pale in colour, often with needle shaped shards (Larsen et al. 2001). The Settlement layer has two parts, a basaltic and a silicic layer and so is very distinctive. The basaltic layer contains a distinctive population of plagioclase crystals (Dugmore et al. 1995).

For each lake, a log is constructed of the core. Key marker layers and the rock type of other layers which have been visually identified are shown. Only primary tephra layers are marked; redeposited tephra layers are excluded from the log. Where available, core images are shown in appendices. In addition it is possible to achieve an idea of composition by the colour of the layers; black layers are basaltic, brown layers are andesitic and white layers are rhyolitic.

Table 3. Key marker layers and calendar and C^{14} ages, following Hardardóttir, 1994.

Tephra Layer	**Source Volcano**	**^{14}C Age**	**Calendar Year (BP is years before 2000AD)**	**Reference**
K1500	Katla	360	1500AD / 500BP	Thorarinson 1975
Settlement Layer	Veiðivötn	1180 ±5	871 ±2 AD / 1129 BP	Grönvold et al. 1995
HA	Hekla	2500 ±100	2595 ±195 BP	Robertsdóttir, 1992a
HB	Hekla	2740 ±70	2845 ±70 BP	Robertsdóttir, 1992a
HC	Hekla	2800 ±50	2870 ±85 BP	
KE	Katla	2850 ±10	2975 ±60 BP	Robertsdóttir, 1992b
H3	Hekla	2880 ±30	3055 ±120 BP	Dugmore et al. 1995
KN	Katla	3300 ±100	3555 ±120 BP	Robertsdóttir, 1992b
H4	Hekla	3830 ±10	4275 ±10BP	Dugmore et al. 1995
T-tephra	Hekla	5765 ±55	6400 ±80 BP	Sveinbjornsdóttir et al. 1998
H5	Hekla	6200	7115 ±130 BP	Larsen and Thorarinson, 1977
SILK A8	Katla	6400	7320 ± 100 BP	Larsen, 2001

Vestra Gìsholtsvàtn

Table 4 gives the thickness and a description of each of the layers of the 94-VGHV01 core. No core images were available. Figure 10 shows a core log with the tephra type as it was identified via visual inspection.In addition, green squares mark C^{14} dates obtained by Jorunn Hardardóttir (2001). It is important to note that the C^{14} age for H4 is ~350 years older than dates obtained by Dugmore et al. (1995) suggesting that the ages in VGHV are too high due to the input of old carbon.See section 6.3, Sediment Accumulation Rates, for further discussion. Key marker layers of K1500, Settlement layer, HA, KE, H3, KN and H-T were identified by Gudrun Larsen.

Out of 60 layers, 57 appear dark in colour and only 3 are pale coloured. The thickest layers, which are in the region of 2cm thick, are the marker layers of HA, KE, KN, and H-T situated in the lower part of the core. The other layers are mostly 0.1-0.4cm thick. There are 60 primary layers in 5.3m of core; this is one layer approximately every 9cm. In general, the tephra layers are fairly regularly spaced throughout the core, although some clustering is apparent, such as at 3m in the vicinity of the HA tephra layer. The first 2m of the core has a low number of layers, with layers increasing in number from 2m to 4.5m and then decreasing again. However in terms of the time period during which the tephra layers are deposited, there are 12 layers during the 1180 years back to the Settlement layer and then 17 layers in the next approximately 1400 years back to HA showing that the increase in sedimentation rate after the Settlement layer was deposited is mostly responsible for the apparent low frequency of layers in the upper part of the core.

Hestvàtn

Appendix 2 shows the core photos and descriptions from the Hestvàtn GLAD4-HST03 core.

Table 4 gives the thickness and a description of each of the layers taken for sampling. The sediment stratigraphy and depositional history of the lake basins is documented in detail by Hardardóttir et al. (2001) and Hannesdóttir (2006). Geochemical data for the tephra layers has previously been reported in Hardardóttir et al. (2001). Figure 11 shows a core log with the tephra type as it was identified via visual inspection.

Table 4. Descriptions and thicknesses in cm of each layer sampled from the Vestra Gìsholtsvàtn and Hestvàtn cores.

Vestra Gìsholtsvàtn				**Hestvàtn**		
Layer Number	Thickness (cm)	Description		**Layer number**	Thickness (cm)	Description
G1	0.5	Black fine grained ash		**H1**	1.0	Black fine-med grained ash; spread over 4cm
G2	0.2	Black fine grained ash		**H2**	0.7	Black ash
G3	0.2	Black fine-med grained ash: interrupted		**H3**	2.8	Top-black ash
G4	0.2	Black ash		**H4**	2.8	Middle - mixture
G5	0.5	Black ash		**H5**	2.8	Bottom-light ash
G6	0.2	Black fine grained ash		**H6**	0.3	Black ash
G7	0.2	Light silty ash		**H7**	0.1	Black ash
G8	0.1	Black med grained ash		**H8**	0.2	Black ash
G9	0.2	Black med grained ash		**H9**	1.0	Black coarse ash
G10	0.7	Black ash		**H10**	0.2	Black ash grades coarse to fine
G11	0.7	Light ash		**H11**	0.1	Black ash
G12	0.3	Black fine-med grained ash: interrupted		**H12**	1.2	Black ash grades into silt
G13	0.2	Black fine-med grained ash: interrupted		**H13**	0.8	Black fine grained ash
G14	0.2	Black ash		**H14**	0.2	Black fine-med grained ash
G15	0.2	Black ash		**H15**	1.1	Light and black coarse/med grained ash
G16	0.2	Black ash		**H16**	0.4	Black fine to med grained ash
G17	1.1	Black fine-med grained ash: interrupted		**H17**	0.2	Black very coarse grained ash to silt
G18	0.4	Black fine-med grained ash		**H18**	2.4	Black ash grades from coarse to fine
G19	0.3	Black med grained ash		**H19**	0.3	Light
G20	0.3	Black ash		**H20**	0.7	Black coarse ash
G21	0.6	Black med grained ash		**H21**	4.5	Black med - fine grained ash with sharp bottom
G22	0.2	Black ash with sharp bottom		**H22**	4.5	Black med - fine grained ash with sharp bottom
G23	0.2	Black ash		**H23**	0.4	Black med - fine grained ash
G24	0.4	Black ash		**H24**	1.2	Black ash grades from med to fine
G25	1.7	Black fine grained ash to silt		**H25**	0.2	Black ash
G26	0.3	Light coloured silt		**H26**	0.5	Black fine grained ash
G27	2.3	Coarse black ash with lighter coloured grains		**H27**	0.2	Black ash
G28	0.1	Black very coarse ash >2mm, may include light grains		**H28**	3.4	Light mix
G29	2.9	Black ash		**H29**	3.4	Blackish
G30	0.2	Black ash		**H30**	3.4	Light
G31	0.4	Black ash		**H31**	0.6	Black coarse grained ash
G32	4.5	Black ash		**H32**	1.1	Black coarse to med grained ash
G33	4.5	Black ash		**H33**	0.2	Black coarse ash
G34	0.4	Black ash		**H34**	0.1	Black ash
G35	1.2	Black ash		**H35**	0.8	Black med grained ash with very sharp bottom
G36	0.4	Black ash		**H35**	0.8	Black med grained ash with very sharp bottom
G37	0.4	Black ash		**H36**	2.2	Black ash grades coarse to fine
G38	0.8	Black to dark brown ash		**H37**	2.2	Black ash grades coarse to fine
G39	0.4	Light greyish silt		**H38**	0.2	Black ash
G40	0.2	Black ash		**H39**	0.2	Black ash
G41	1.3	Black ash		**H40**	0.4	Black ash
G42	0.2	Black ash		**H41**	0.6	Black coarse ash
G43	0.3	Black ash		**H42**	0.4	Brown ash
G44	0.5	Black ash				
G45	0.2	Black ash				
G46	0.3	Black ash				
G47	1.3	Black ash				

Figure 10. (next page) Core log of Vestra Gìsholtsvàtn with only the primary tephra layers identified. Colour denotes rock type. Key marker layers that it is possible to identify visually are shown. The three green squares are C^{14} dates from Hardardóttir (2001).

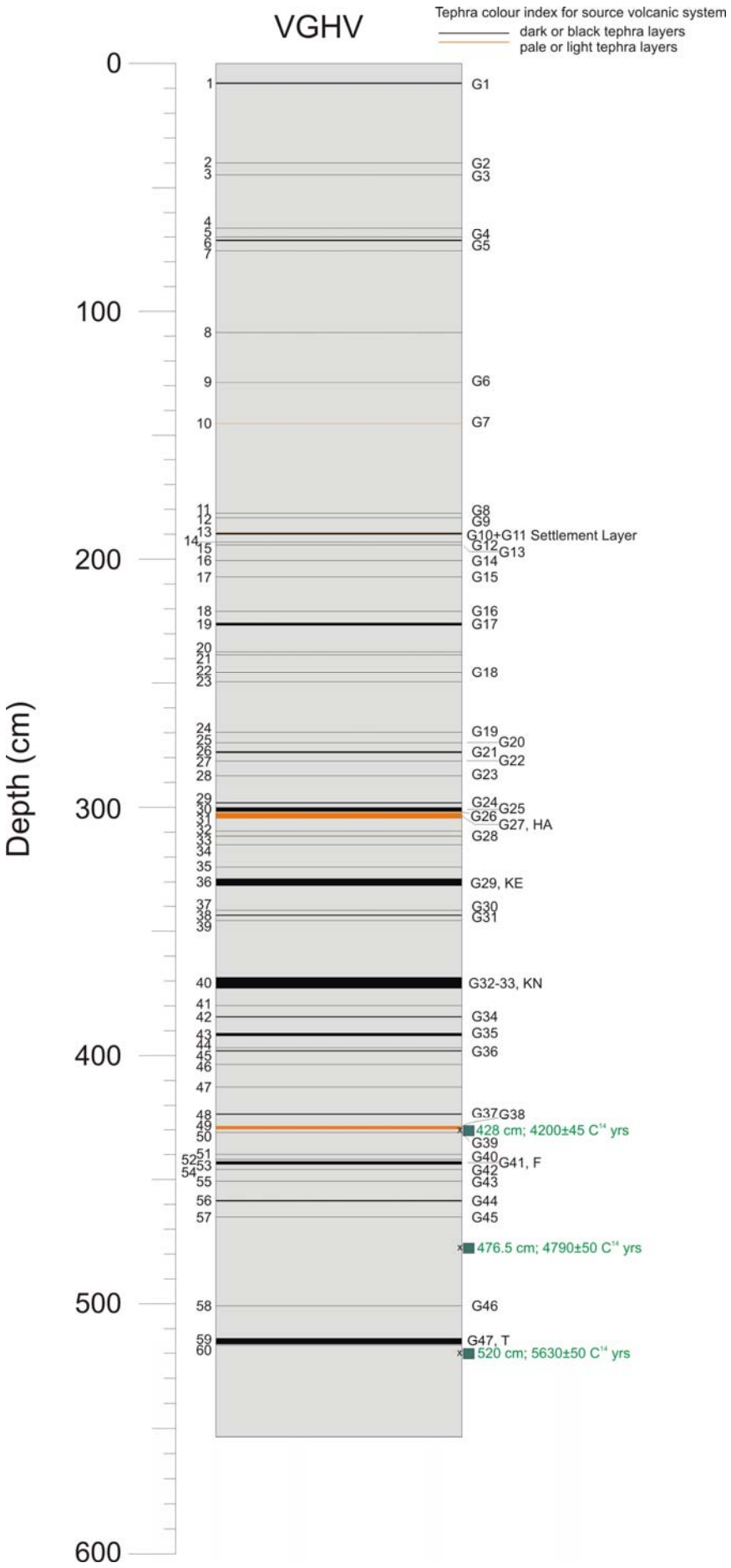
VGHV
Tephra colour index for source volcanic system
dark or black tephra layers
pale or light tephra layers
Depth (cm)
0
100
200
300
400
500
600
G1
G2
G3
G4
G5
G6
G7
G8
G9
G10+G11 Settlement Layer
G12
G13
G14
G15
G16
G17
G18
G19
G20
G21
G22
G23
G24
G25
G26
G27, HA
G28
G29, KE
G30
G31
G32-33, KN
G34
G35
G36
G37
G38
428 cm; 4200±45 C14 yrs
G39
G40
G41, F
G42
G43
G44
G45
476.5 cm; 4790±50 C14 yrs
G46
G47, T
520 cm; 5630±50 C14 yrs

Figure 11. Core log of Hestvàtn with only the primary tephra layers identified. Colour denotes rock type. Key marker layers that it is possible to identify visually are shown.

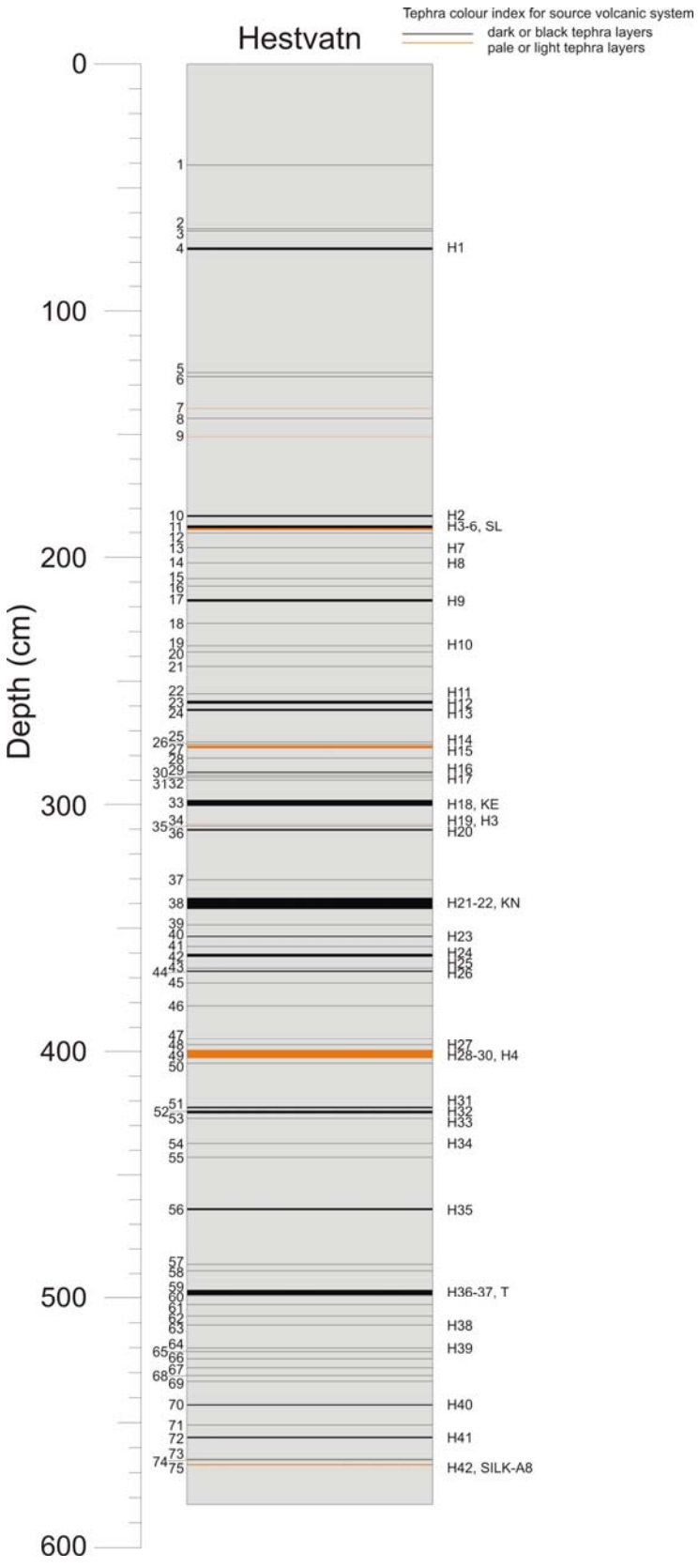

Key marker layers of K1500, Settlement layer, KE, H3, KN, H4, H-T and a SILK layer were identified by Thorvaldur Thordarson and Gudrun Eva Jóhannsdóttir. It is important to note that the initial visual identification of H5 (Layer 42 from Hestvàtn) reported in Hardardóttir et al. 2001 was shown to be incorrect after geochemical analysis. This was corrected in Jóhannsdóttir (2007) to be a SILK layer (a silicic layer from Katla) (see section 6.2.2 Geochemical check of the identification of key marker layers).

Out of 75 layers, 68 appear dark in colour and only 7 are pale coloured. The thickest layers, which are between 2 to 4cm thick, are the marker layers of the Settlement layer, KE, KN, H4 and H-T. Apart from the Settlement layer these layers are situated in the lower part of the core. The other layers are mostly 0.1-0.4cm thick. There are 75 layers in 5.8m of core. This is one layer approximately every 8cm. For the first 2m of the core the tephra layers are not regularly spaced with two main areas of tephra layers at 40-70cm and 120-150cm. Below 2m, the tephra layers are fairly regularly spaced throughout the core, although clustering is apparent around 2.8m. The first 2m of the core has a low number of layers. Layers increase in frequency from 2m to 4m, with the peak around 2.8 to 3.1m where there are 11 tephra layers within 30cm. Tephra layer frequency then decreases again until 5m. Below 5m there is a significant increase in frequency of tephra layers; 15 tephra layers over an interval of 75cm. However, in terms of time, 11 layers were deposited during the 1180 years back to the Settlement layer, and then 16 layers in the next approximately 1400 years back to HA. Again, this demonstrates that the increase in sedimentation rate following settlement in Iceland is mostly responsible for the apparent low frequency of layers in the upper part of the core. Despite the high frequency of tephra layers per depth of sediment between HA and KN, there is a similar frequency per year as there are 10 layers in about 800 years.

Hvítarvàtn

Descriptions of samples of tephra taken from the Hvítarvàtn core are given in Appendix 3 along with core photos from Hvítarvàtn, which are annotated to provide information on correlation and key marker layers. In this project the Hvítarvàtn core is only examined from present until H5, the cores older than this are presented in Jóhannsdóttir (2007). Figure 12 shows a core log with the tephra type as it was identified via visual inspection. Erosion and slumping areas are also noted. An example of slumping is in 3B-1H-1 from 75-90cm. Erosion is apparent in core 3A-2H-1 at about 110cm, where the layer H1104 is not identified, yet it is highly visible in the cores to either side. This

Figure 12. Core log of Hvítarvàtn with only the primary tephra layers identified. Colour denotes rock type. Key marker layers that it is possible to identify visually are shown.

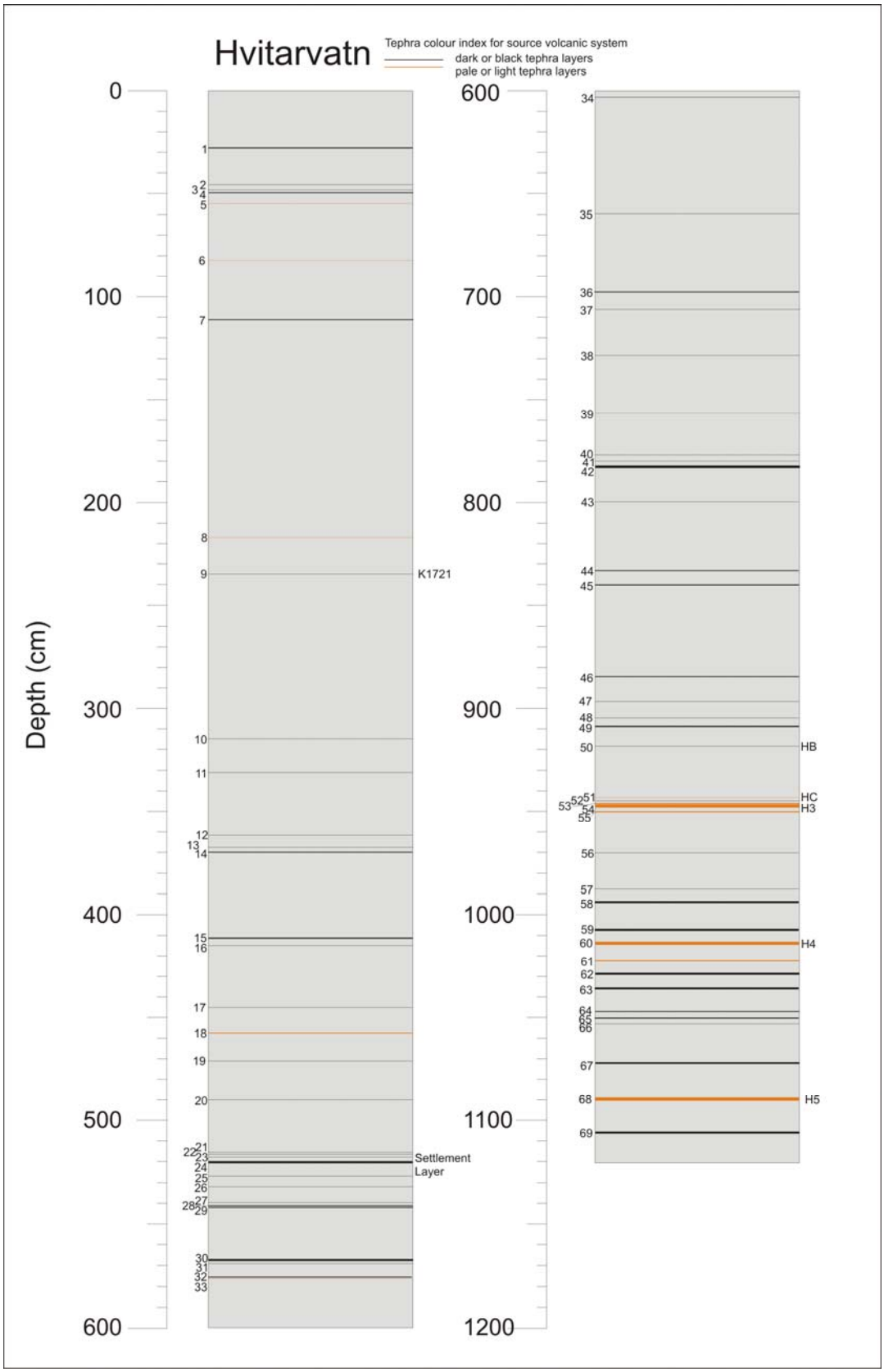

indicates the importance of multiple cores. Significant folding that is apparent in some cores is formed during core retrieval, as the end of each fold points down the core. An example is around 20-40cm in core 1A-1H-1 and most of the core section 3A-1H-2. This shows there is no need to worry about disruption of the sediment record whilst it was in-situ. Also notable is the Hekla layer which has been disturbed by coring. It has been transported up the top side of the core in the image, redepositing layers in extension cracks in the core, at 60-65cm, 95-109cm and 130-142cm. There is evidence of ice-rafted debris above K1721 (D. Larsen pers comm. 2008).

The marker layers identified in Hvítarvàtn are K1500, Settlement Layer, HB, HC, H3, H4 and H5. A detailed log of the Settlement layer, and of H4 from the Hvítarvàtn cores are presented in Figure 13.

Out of 69 layers, 57 appear dark in colour and 12 are pale coloured. The thickest layers, which are between 1 to 2 cm thick, are the marker layers of the Settlement layer, H3, H4 and H5. Apart from the Settlement layer these layers are situated in the lower part of the core. Layer 42, which is a dark Katla layer, is also notable at 1.2cm thick, as are layers 58 (Hekla), 59 (Hekla), 62 (Katla) and 69 (Katla) which are all dark and 1cm thick. The other layers are mostly 0.1-0.4cm thick.

There are 69 layers in 11.2m of core. This is one layer approximately every 15cm. For the first 4m of the core the tephra layers are not regularly spaced with two main clusters of tephra layers at 45-55cm and 360-370cm. Below 4m, the tephra layers are fairly regularly spaced throughout the core, although clusters do appear, such as around 5.3m near the Settlement layer, and 9.5m around H3. The first 3.5m of the core has a low number of layers, with layers increasing in frequency from 3.5m to 6m. The peak is from 5.1-5.4m where there are 9 tephra layers within 30cm. Tephra layer frequency then decreases again until 9m. Below 9m there are high numbers of tephra layers; 22 tephra layers in 2m.

There are 22 layers during the 1180 years back to the Settlement layer and then 30 layers in the next approximately 1700 years back to H3, which again demonstrates that the increase in sedimentation rate following settlement is mostly responsible for the apparent low frequency of layers in the upper part of the core. Below H3 there is a marked decrease in the number of tephra layers per 1000yrs. In the 1000years between H3 and H4 there are 6 layers and in the next 2500years to H5 there are only 8 layers.

Figure 13 (next page). Detailed logs of two of the key marker layers in the Hvítarvàtn core. H4 is characterised by a very thick pale coloured deposit, the Settlement layer by the distinctive black and white layers with the black layers containing plagioclase crystals.

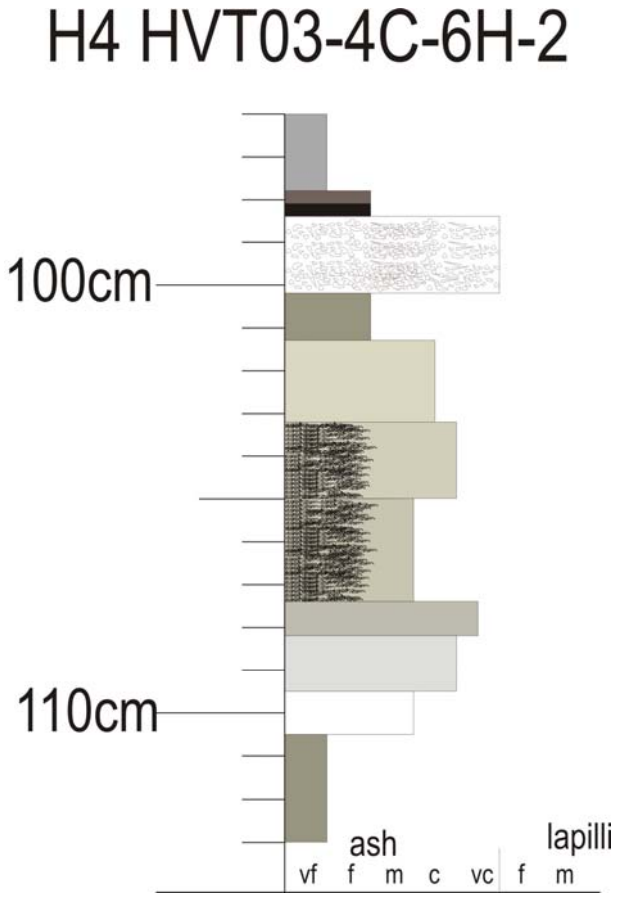

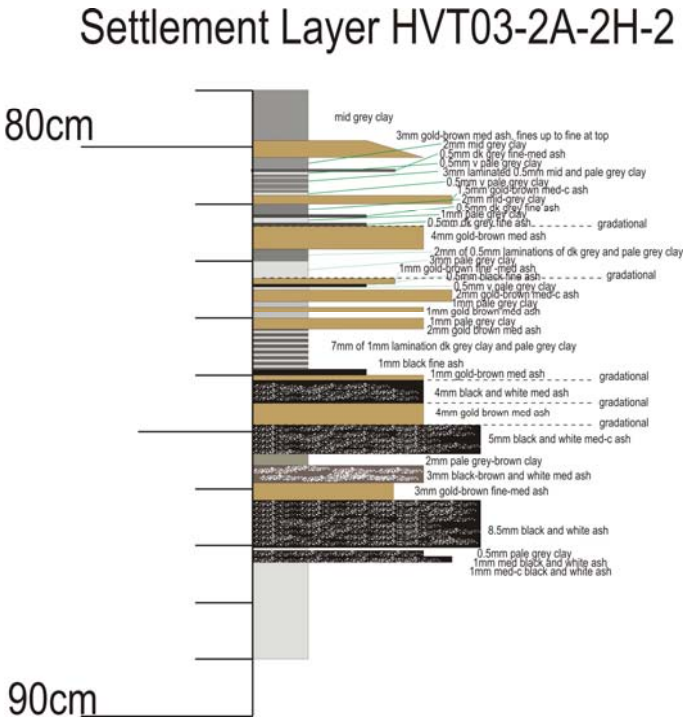

6.2 Geochemistry

All geochemical data is presented in Appendix 4. It is very useful to see the range of geochemistry in a tephra layer as it is characteristic and therefore averages are not presented here.

6.2.1 Identification of Source Volcano for each tephra layer

When dealing with large data sets a systematic and accurate way of classifying tephra layers according to their physical properties and chemical composition is essential. Jóhannsdóttir (2006) developed a step by step scheme for identifying Icelandic tephra layers and their source volcanoes, which is primarily based on using major element glass composition and in particular the incompatible element concentrations. This scheme is developed further here. The main development is a more comprehensive set of distinguishing plots to reduce possibility of confusion between layers of similar chemistry e.g. Hekla and Katla layers. It also avoids splitting data from layers into many different chemical groups which are pre-assigned to a volcanic source as this process is very time consuming and difficult to automate and it does not examine the tephra layer dataset as a whole.

An existing dataset consisting of the chemistry of known tephra layers was constructed (Björck and Wåstegaad, 1999, Boygle, 1994, Devine et al, 1984, Dugmore et al. 2000, Einarsson, 1982, Gee et al. 1998, Grönvold, 1984, Grönvold and Johanneson, 1984, Haflidason, 1992, Hannon et al., 1998, Hardarson et al. 1993, Hemmond et al. 1993, Jakobsson 1968, 1979a,b, Jakobsson et al. 1978, Lacasse et al. 1995, Larsen, 1982, Larsen et al. 1999, 2001, Metrich et al. 1991, Meyer et al., 1985, Mork, 1982, Nordahl and Haflidason, 1992, Óladóttir, 2004, Óladóttir et al. 2005, Siggurdson, 1970, Sigvaldson, 1974, Sinton et al, 2005, Slater et al., 1998, Steinthorson, 1978, Thordarson and Self, 1998, Thordarson et al. 1996, 1998, 2001, Thordarson, unpublished, 1999, 2002, Tronnes, 1990, Turney et al. 1997, Wåstegaad et al. 2000, 2001). This was then examined fully in order to find the best bivariate plots for the discrimination of the different volcanic systems using both oxides, or ratios of oxides. All of the data from each tephra layer is compared to the appropriate plots for its chemistry. This gives the range of geochemistry which in itself is diagnostic and avoids confusion caused by averaging data of very different chemistries.

Figure 14 and Table 5 depict the flow chart and set of plots used in ascribing a source volcano for the tephra layer. The first step is to decide whether the tephra layers are basaltic (under 52 wt%), and/or are between 52 and 65 wt% and/or are over 65 wt%. The appropriate path is then followed for each set of data. For

example, if some of the data for layer 1 is basaltic and subalkaline, a plot of Al_2O_3 – SiO_2/CaO is used to work out whether it is either RVZ and WVZ, or Veiðivötn, Grímsvötn, Askja and Krafla. Then another 4 different plots (SiO_2/TiO_2-FeO/CaO, MgO/K_2O-CaO/P_2O_5, K_2O-FeO, SiO_2-MgO/CaO) are used to distinguish between Veiðivötn, Grímsvötn, Askja and Krafla. If some data for his tephra layer has >65 wt% SiO_2 then the appropriate path is followed for this data starting with SiO_2-CaO. This process has been semi-automated through the construction of a matlab code to reduce time consuming steps and make it more accessible to other studies.

A caveat in the method described here is that it does not allow for effective discrimination between mafic tephra layers from the Hekla and Katla volcanic systems. The most evolved component of Hekla basalts is identical to Katla basalts, but Hekla basalts are less evolved on average and typically exhibit a greater range in compositon than Katla basalts. Consequently these patterns can be used to differentiate between basaltic tephra layers from these two volcanic systems. Figure 15 shows an example of this for two layers from VGHV, one from Katla forming a tight cluster and one from Hekla which is spread out over a wide range of values.

Plots were constructed to establish whether errors from the EPMA analyses (see table 2) would cause too much overlap of the fields of geochemistry of each source volcano and therefore make distinguishing problematic. Two are shown; an example for basaltic tephras in figure 16 and an example for silicic tephras in figure 17. For the basaltic plot, aTiO_2 –K_2O plot of Hekla, Katla, Snæfellsjökull and Vestmannæyjar, the maximum error of $\pm$0.12 for TiO_2 and of $\pm$0.03 for K_2O is shown. It is still possible to discriminate between the fields. For the silicic plot, a CaO-TiO_2 plot of Veiðivötn, Askja, Katla, Hekla and Öræfajökull, the maximum error of $\pm$0.09 for CaO and of $\pm$0.03 for TiO_2 is shown. It is again still possible to discriminate between the fields. Similar results are seen for all elements and plots and therefore the errors in EPMA analysis do not affect the result of the identification.

In order to check that this scheme is worthwhile the extra effort over the simpler TiO_2-FeO approach, the source volcano was identified using the TiO_2-FeO plot for each tephra layer from the overall stratigraphy. The results show that only 59 layers were correctly identified from the 109 analysed layers. In other words, the source volcano was not correctly identified for 45% of the tephra layers using TiO_2- FeO plot alone. This is almost entirely due to the difficulty in identifying Hekla on the TiO_2- FeO plot.

Table 5. Discrimination of source volcano using geochemistry flow chart (to be used in conjunction with Figure 14).

For groups	Plot	Comments
All analyses	SiO_2-Alkali	Divide into Alkaline, Subalkaline, Andesitic, Rhyolitic
Plot 1. Alkaline	K_2O-TiO_2	Splits into Hekla+Katla or Snæfellsjökull +Vestmanneyjar which have lower TiO_2
Plot 1. Alkaline (Hekla+Katla)	K_2O-TiO_2	Clustering plot; Hekla is spread out, Katla clustered
Plot 2. Hekla and Katla	SiO_2/Na_2O - Al_2O_3/P_2O_5	Hekla has higher SiO_2/K_2O and slightly higher Al_2O_3/FeO
Plot 3. Hekla and Katla	SiO_2/Na_2O – MgO/CaO	Hekla has higher MgO/CaO on the whole
Plot 4. Hekla and Katla	TiO_2/Na_2O- FeO/CaO	Hekla has lower FeO/CaO
Plot 5. Snæfellsjökull and Vest	FeO/Na_2O – Na_2O/K_2O	Snæfellsjökull has lower Na2O/K2O and higher FeO/Na_2O.
Plot 6. Subalkaline – all	FeO-SiO_2	Separates RVZ and WVZ from Askja, Veiðivötn, Krafla and Grimsvötn (lower Al_2O_3)
Plot. 7 RVZ, WVZ,	SiO_2/Al_2O_3 – SiO_2/CaO	RVZ higher SiO_2/CaO and less spread
Plot 8. Askja, Veiðivötn, Krafla and Grimsvötn	SiO_2/TiO_2 – FeO/CaO	Distinguishes Krafla or Grimsvötn (due to tight cluster) and Askja and Veiðivötn
Plot 9. Askja, Veiðivötn Krafla and Grimsvötn	MgO/K_2O– CaO/P_2O_5	Distinguishes Veiðivötn+Askja from Krafla or Grimsvötn
Plot 10. Askja +Veiðivötn	K_2O-FeO	Veiðivötn has lower K_2O than Askja
Silicic	SiO_2-Alkali	Split into andesite (52-65 wt%SiO2) and rhyolite (>65wt% SiO_2)
Plot 11. Andesite – all	FeO-MgO	Öræfajökull is separated by high FeO and low MgO.
Plot 12. Andesite – Katla, Hekla, Veiðivötn, Askja	SiO_2/MgO– K_2O/P_2O_5	Hekla and Katla have higher SiO_2/MgO than Veidivotn. Not possible to differentiate Hekla and Katla from Askja.
Plot 13. Andesite	SiO_2/MgO – TiO_2/P_2O_5	Askja has higher TiO_2/P_2O_5 than Hekla or Katla
Plot 14. Andesite	TiO_2/P_2O_5- FeO/MgO	Hekla has higher FeO/MgO than Katla
Plot 15. Andesite	FeO/MgO – K_2O/P_2O_5	Katla has a larger range of K2O/P2O5 than Hekla
Plot 16. Rhyolite -all	SiO_2-CaO	Snæfellsjökullfjökull, Törfajökulll, Eyafjallajökull all have low CaO
Plot 17. Rhyolite -all	SiO_2-K_2O	Snæfellsjökullfjökull, Törfajökulll, Eyafjallajökull all have K_2O
Plot 18. Snæfellsjökulll, Törfajökull, Eyafjallajökull	SiO_2 – Na_2O	Eyafjallajökull has high Na_2O, Törfajökull has mid Na_2O, Snæfellsjökullfjökull has lower Na_2O
Plot 19. Rhyolite -all	SiO_2-TiO_2	Askja and Krafla have higher TiO_2 at higher SiO_2
Plot 20.Askja, Krafla	SiO_2/MgO- SiO2/TiO2	Askja has wide spread, Krafla is defined in a line across middle
Plot 21. Katla, Hekla, Öræfajökull, Veiðivötn	SiO_2 – CaO/K_2O	Hekla is always higher in CaO/K2O
Plot 22. Katla, Öræfajökull, Veiðivötn	SiO_2-FeO/K_2O	Veiðivötn has lower SiO_2 and FeO/K_2O. Oræfajökull is tightly clustered, Katla has higher SiO_2 and FeO/K_2O.

Figure 14 (following 5 pages). a) Source volcano identification method. Flow chart depicting the methodology for identifying the source volcano of the tephra layer. Fields of colour represent the spread of geochemical data for a specific volcano. Depending on the geochemistry of the layer being dealt with, a path is followed through the diagram until there is only one possible volcano it can be. As paper size is limited to A4 which means the plots are very small, each section of the flow chart is shown enlarged on the following pages. b) Alkaline methodology; c) Subalkaline methodology; d) Andesitic Methodology; e) Rhyolitic methodology.

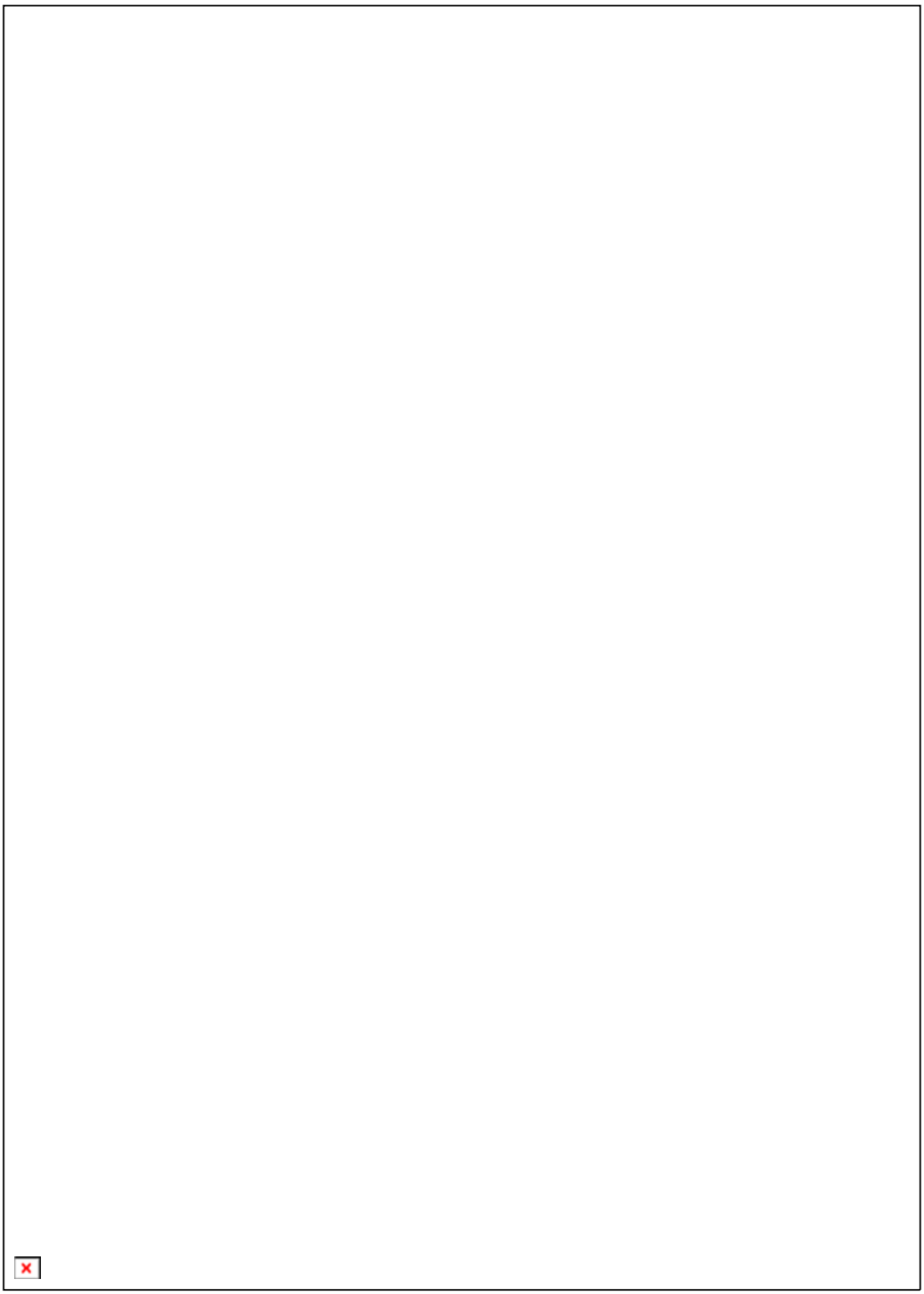

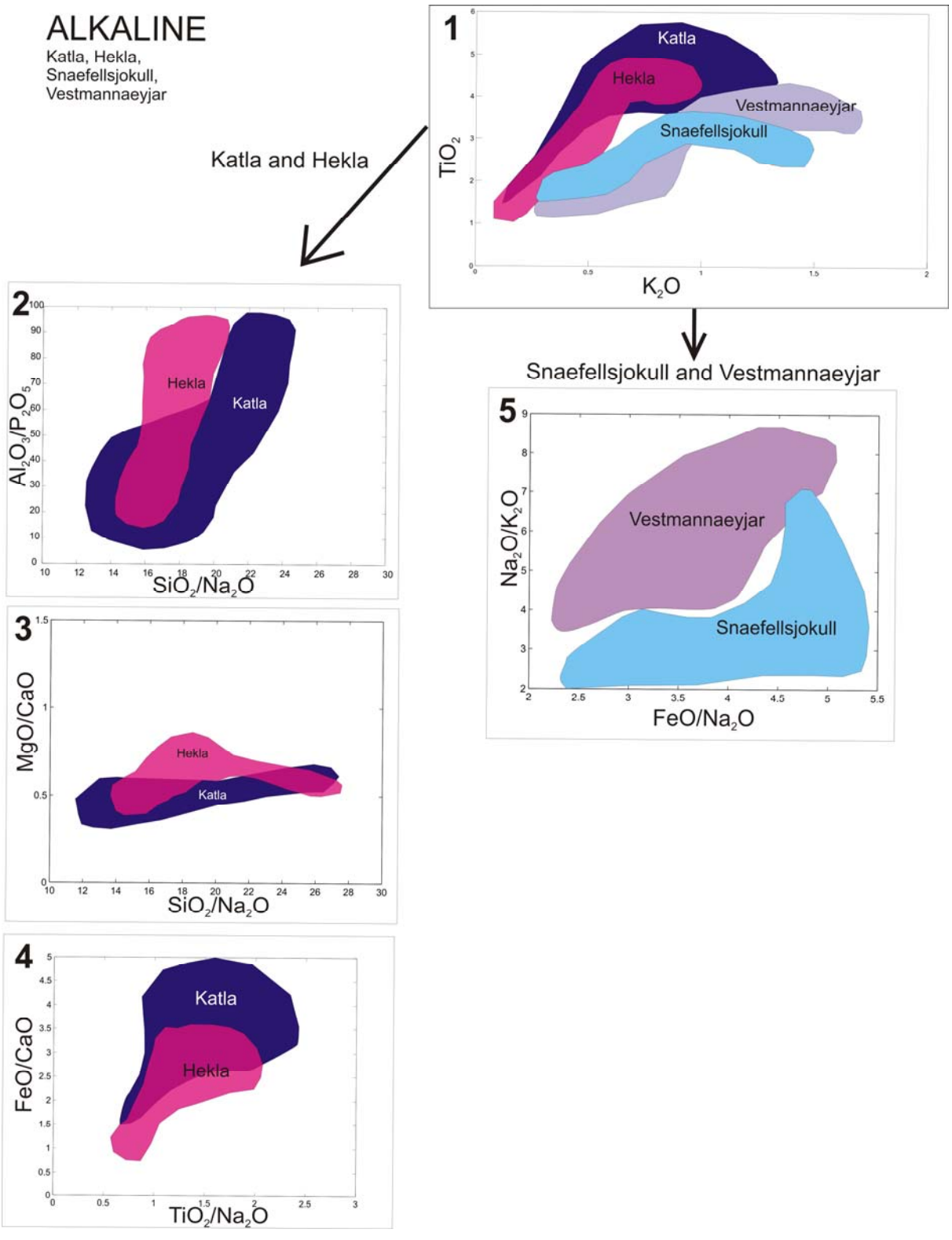
ALKALINE
Katla, Hekla,
Snaefellsjokull,
Vestmannaeyjar
Katla and Hekla
1
Katla
Hekla
Vestmannaeyjar
Snaefellsjokull
TiO2
K2O
Snaefellsjokull and Vestmannaeyjar
2
Hekla
Katla
Al2O3/P2O5
SiO2/Na2O
5
Vestmannaeyjar
Snaefellsjokull
Na2O/K2O
FeO/Na2O
3
Hekla
Katla
MgO/CaO
SiO2/Na2O
4
Katla
Hekla
FeO/CaO
TiO2/Na2O

SUBALKALINE

Grimsvotn, Veidivotn,WVZ, RVZ, Askja

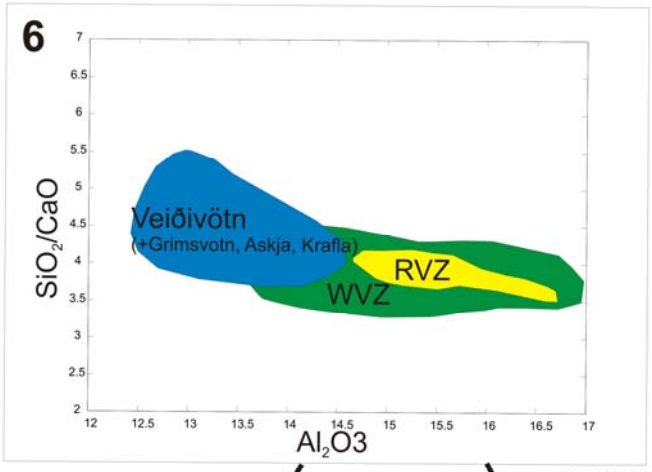

WVZ/RVZ

Veiðivötn, Grimsvotn, Askja, Krafla

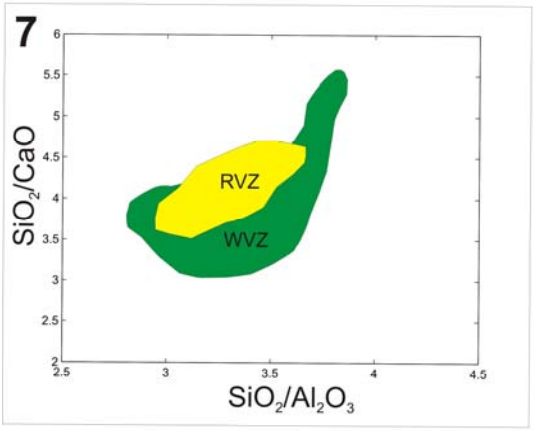

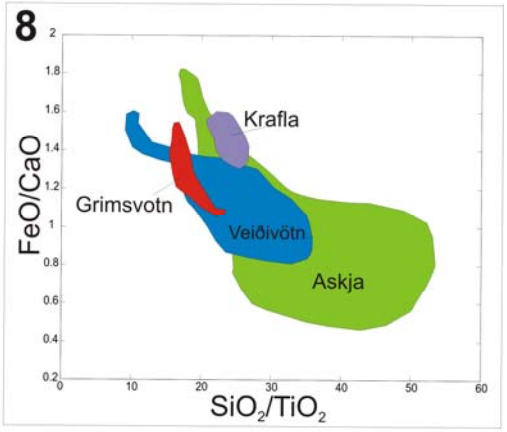

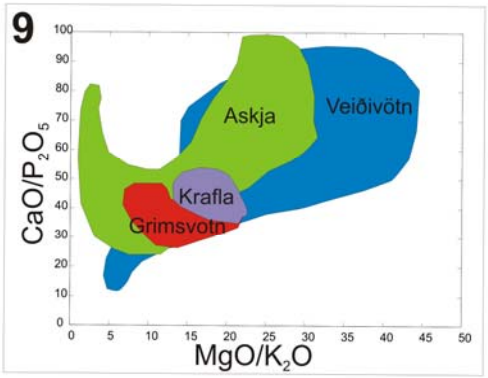

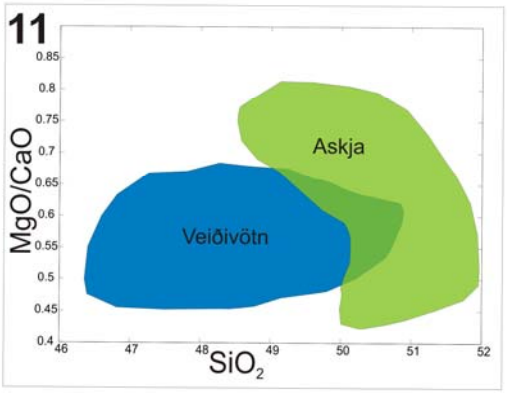

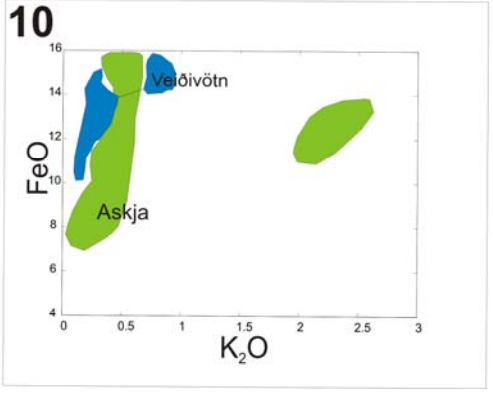

SILICIC-Andesitic

Katla, Hekla, Veidivotn, Askja, Oraefjokull

11

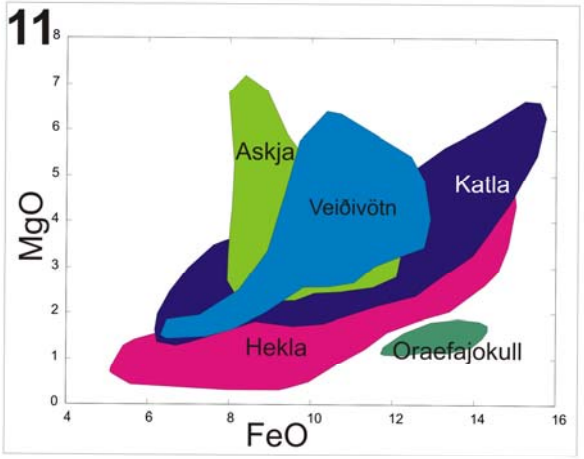

14

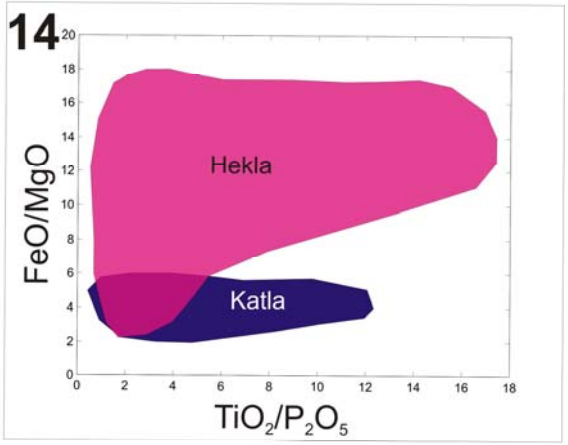

12

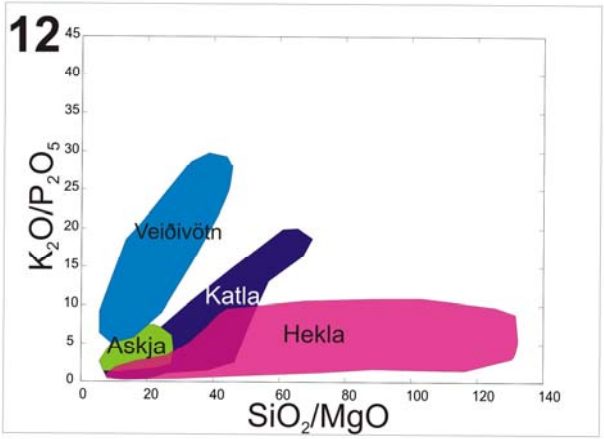

15

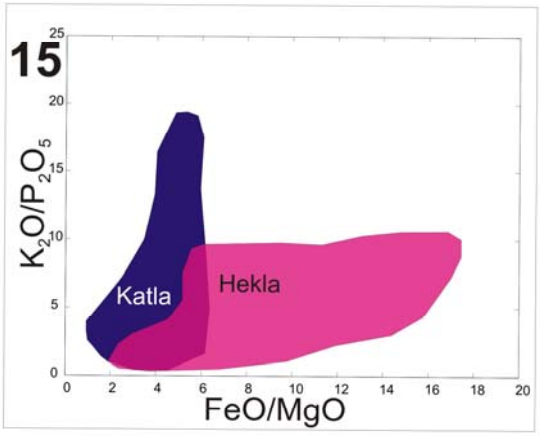

13

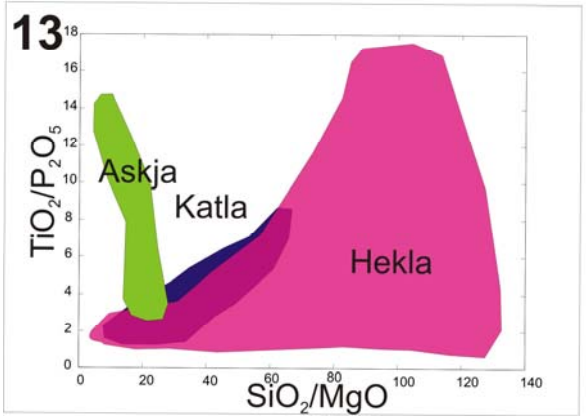

SILICIC - Rhyolitic

Katla, Hekla, Veidivotn,
Askja, Eyafjell, Snaefjellsjokull,
Torfajokull, Oraefjokull, Krafla

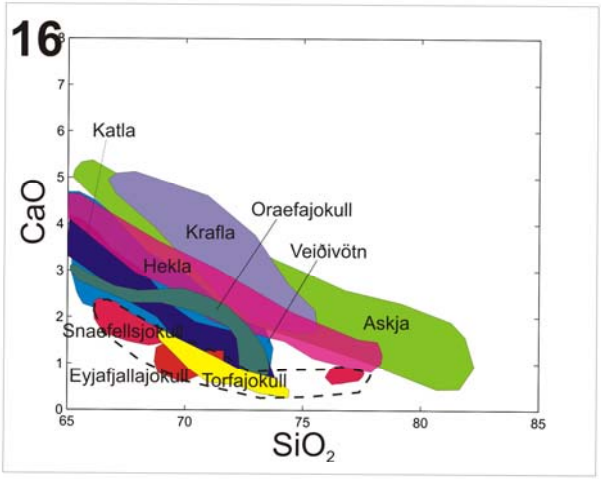

Snaefellsjokull, Torfajokull, Eyafjallajokull

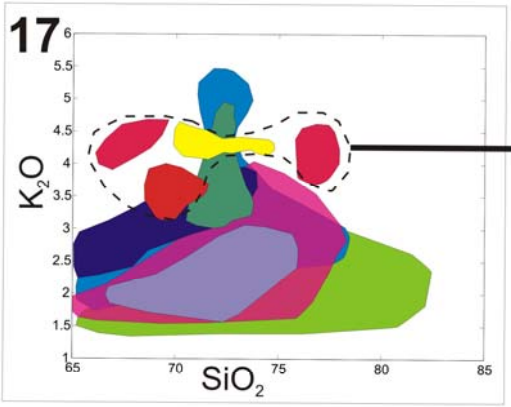

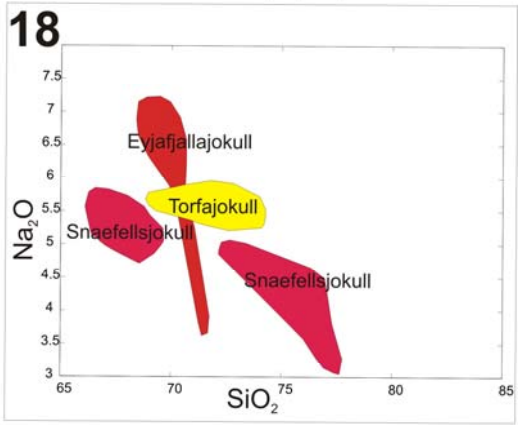

Askja and Krafla

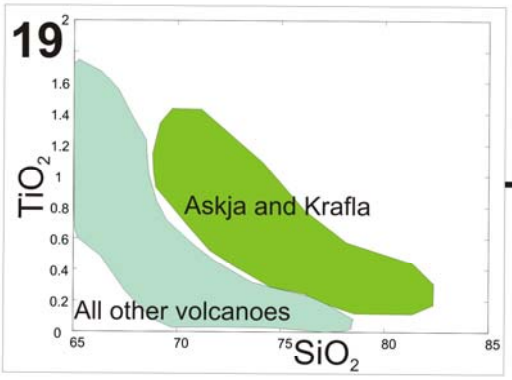

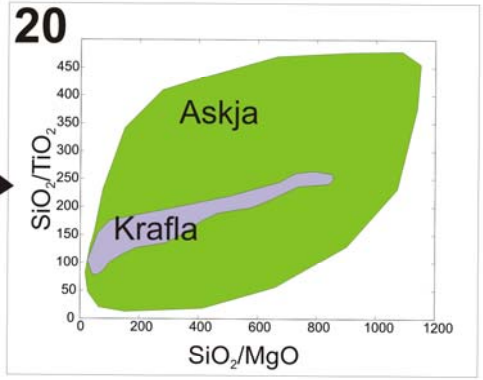

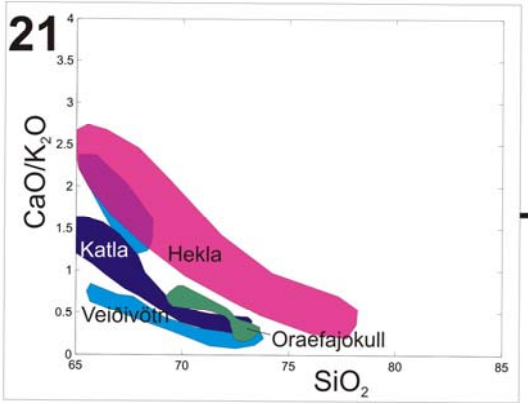

Oraefajokull, Katla, Veidivotn

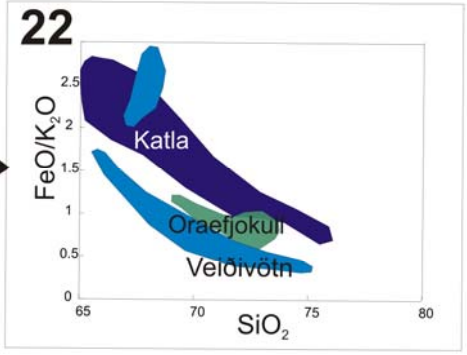

Figure 15. TiO_2 and FeO plot of a Katla layer and a Hekla layer showing the difference in their range of values. This was found to be characteristic.

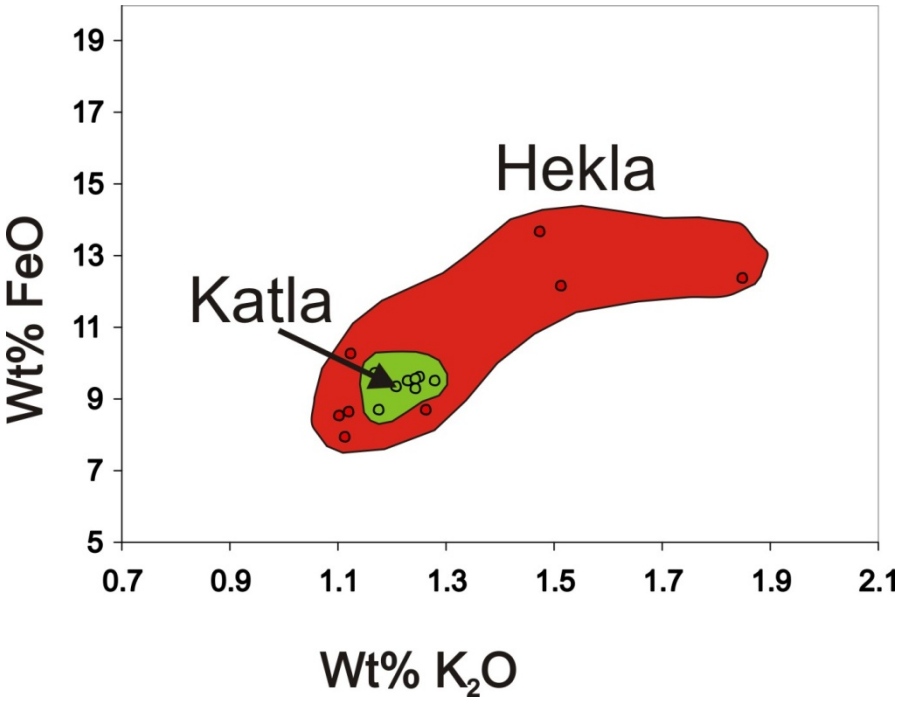

Figure 16. TiO_2 –K_2O plot of Hekla, Katla, Snæfellsjökull and Vestmannæyjar. Maximum error of ±0.12 for TiO_2 is shown and maximum error of ±0.03 for K_2O is shown. It is still possible to discriminate between the fields.

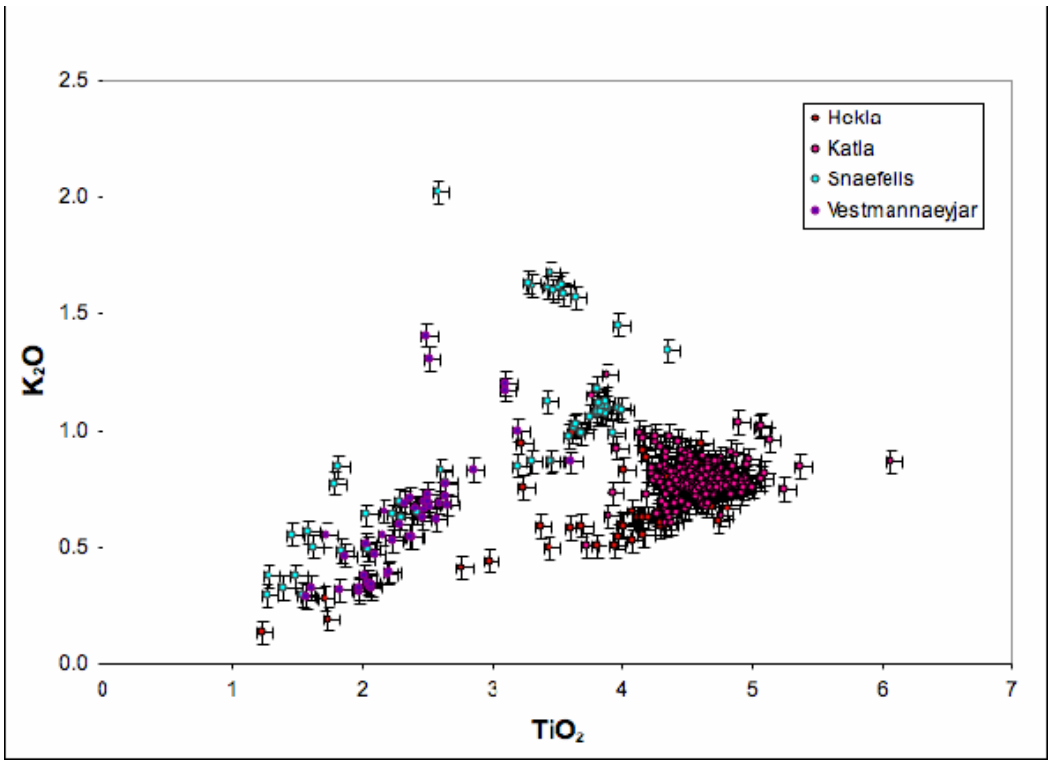

Figure 17. CaO-TiO_2 plot of Veiðivötn, Askja, Katla, Hekla and Öræfajökull. Maximum error of ±0.09 for CaO is shown and maximum error of ±0.03 for TiO_2 is shown. It is still possible to discriminate between the fields.

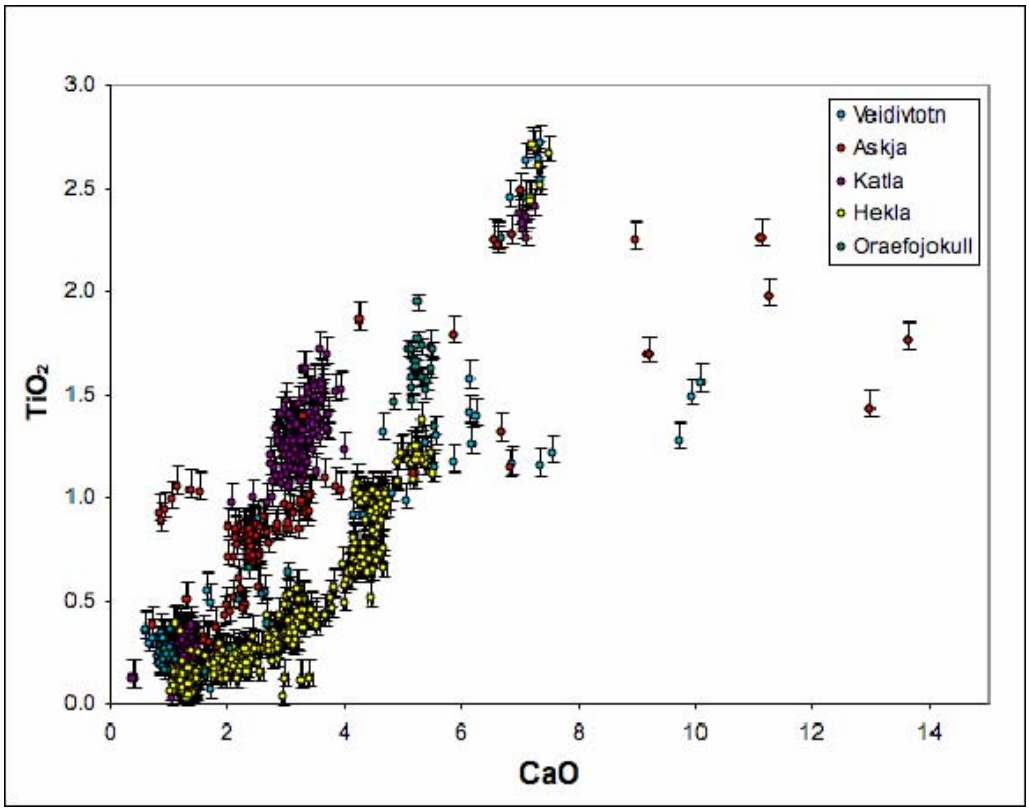

6.2.2 Geochemical Check of the Identification of Key Marker Layers

In order to check that the identification of the key marker layers was correct, each of the marker layers identified visually was plotted against data from a known source of that particular marker layer, or layers that could be similar.

As mentioned in section 6.1 (Tephra Stratigraphy), the SILK layer (Hestvàtn layer 42) was mis-identified as H5 in Hestvàtn prior to geochemical analysis. The procedure taken for this layer is a good example as to how it was ascertained whether this was indeed the marker layer that had been identified visually. Figure 18 demonstrates how geochemical analysis showed the layer is a SILK layer; Ca and Fe were far higher than would be expected for H5. Also, the total alkalis are higher than expected for Hekla tephra layers with SiO_2 content around 65%. In contrast, the results are a perfect match with the composition of dacitic Katla tephras.

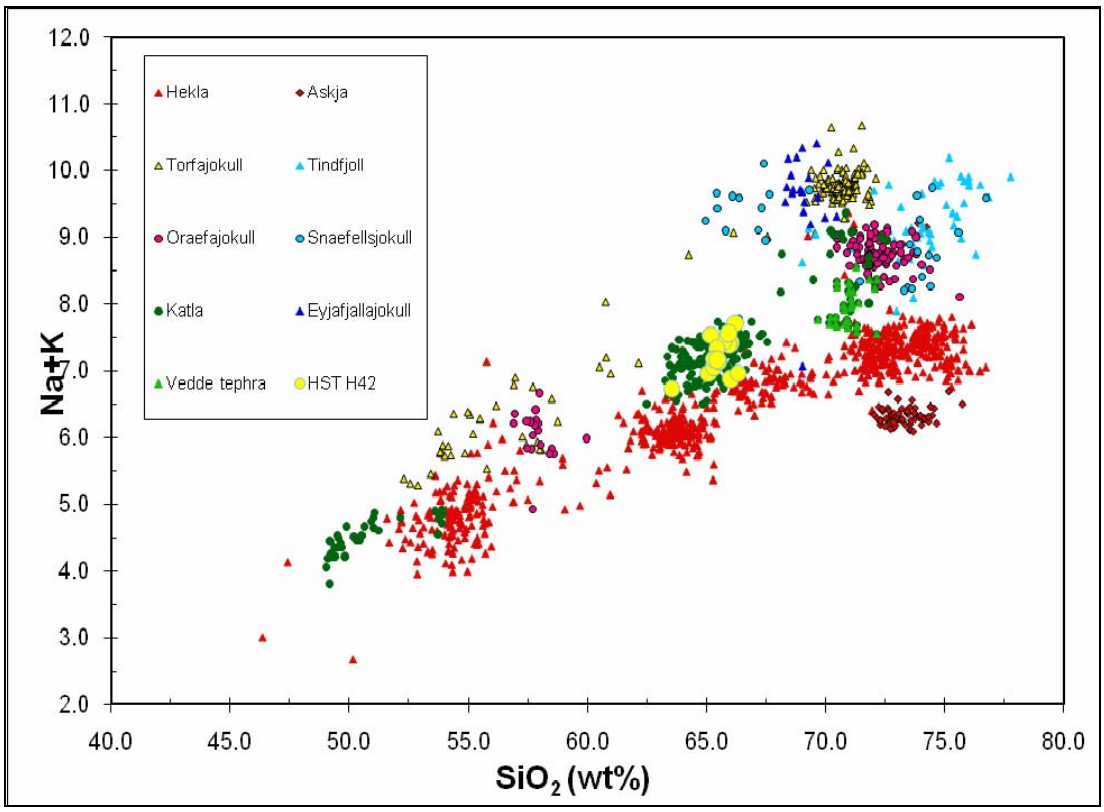
Hekla
Askja
Torfajokull
Tindfjoll
Oraefajokull
Snaefellsjokull
Katla
Eyjafjallajokull
Vedde tephra
HST H42
Na+K
SiO2 (wt%)
12.0
11.0
10.0
9.0
8.0
7.0
6.0
5.0
4.0
3.0
2.0
40.0
45.0
50.0
55.0
60.0
65.0
70.0
75.0
80.0

a)

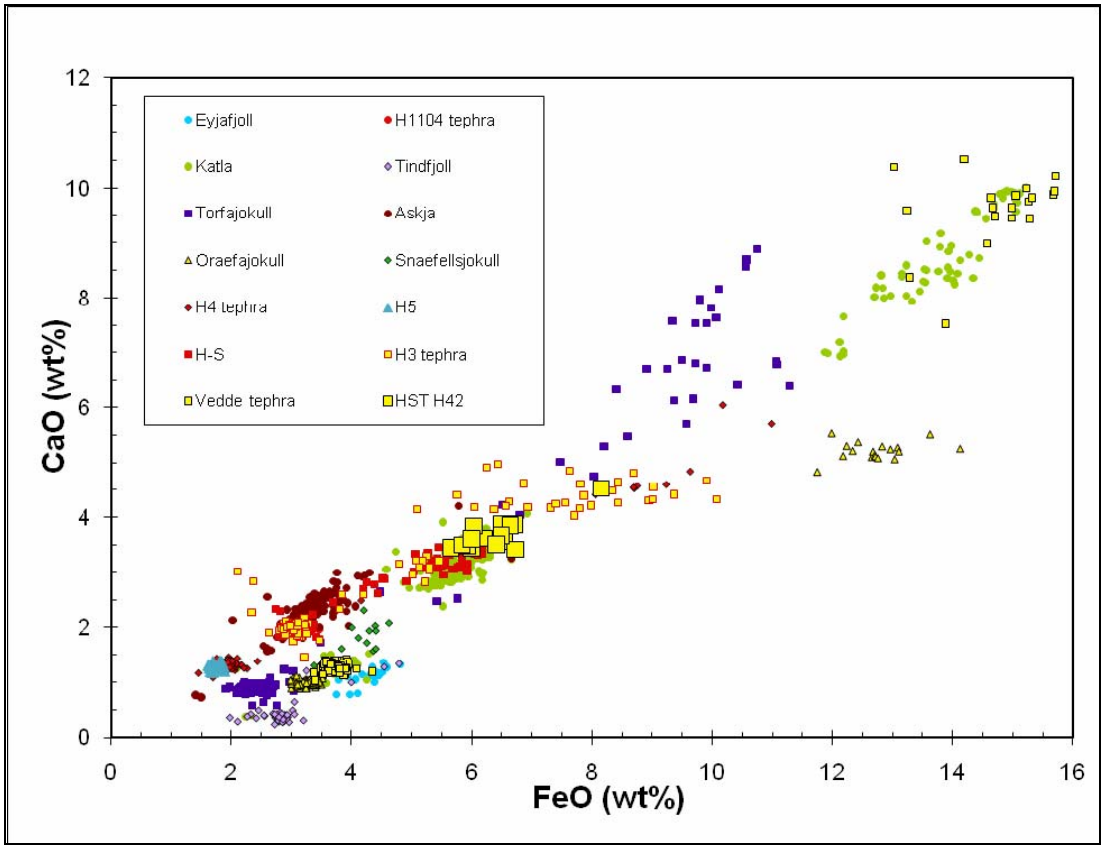
Eyjafjoll
H1104 tephra
Katla
Tindfjoll
Torfajokull
Askja
Oraefajokull
Snaefellsjokull
H4 tephra
H5
H-S
H3 tephra
Vedde tephra
HST H42
CaO (wt%)
FeO (wt%)
12
10
8
6
4
2
0
0
2
4
6
8
10
12
14
16

b)

Figure 18 (previous page)

a) Alkali- Silica plot of all of the possible silicic producing volcanoes; Hekla, Askja, Törfajökulll, Tindfjoll, Öræfajökull, Eyafjalljökull, Snæfellsjökullsfellsjökull, Katla and also including the Vedde tephra. HST layer 42 is shown to correlate with Katla rather than Hekla therefore showing the initial identification of the layer as H5 is wrong.

b) FeO-CaO plot of the major silicic producing volcanoes including in particular most of the main Hekla layers for comparison. Hekla, Askja, Törfajökulll, Tindfjoll, Öræfajökull, Eyafjalljökull, Snæfellsjökullsfellsjökull, Katla products are shown. Also shown are H1104, H-S, H4 and H5. This clearly shows that the layer cannot be H5 as both CaO and FeO are much higher. It confirms the source as being Katla as the Alkali-Silica plot has ruled out the possibility of it being either a Hekla or Törfajökulll layer which are the other possibilities there. Silicic layers from Katla are called SILK layers.

Figure 19. The following plots show that the layer HST42 has the most similarities with SILK A-8. Data for SILK A-8 and 9 is from Larsen (2001) and for K7180BP is from Óladóttir (2009). a) K_2O-TiO_2 plot shows slightly higher TiO_2 for HST42 and SILK A-8 in comparison to the other two layers; b) CaO-TiO_2 plot shows slightly higher CaO for HST42 and SILK A-8 in comparison to the other two layers; c) MgO-TiO_2 plot shows higher MgO and TiO_2 for HST42 and SILK A-8 in comparison to the other two layers.

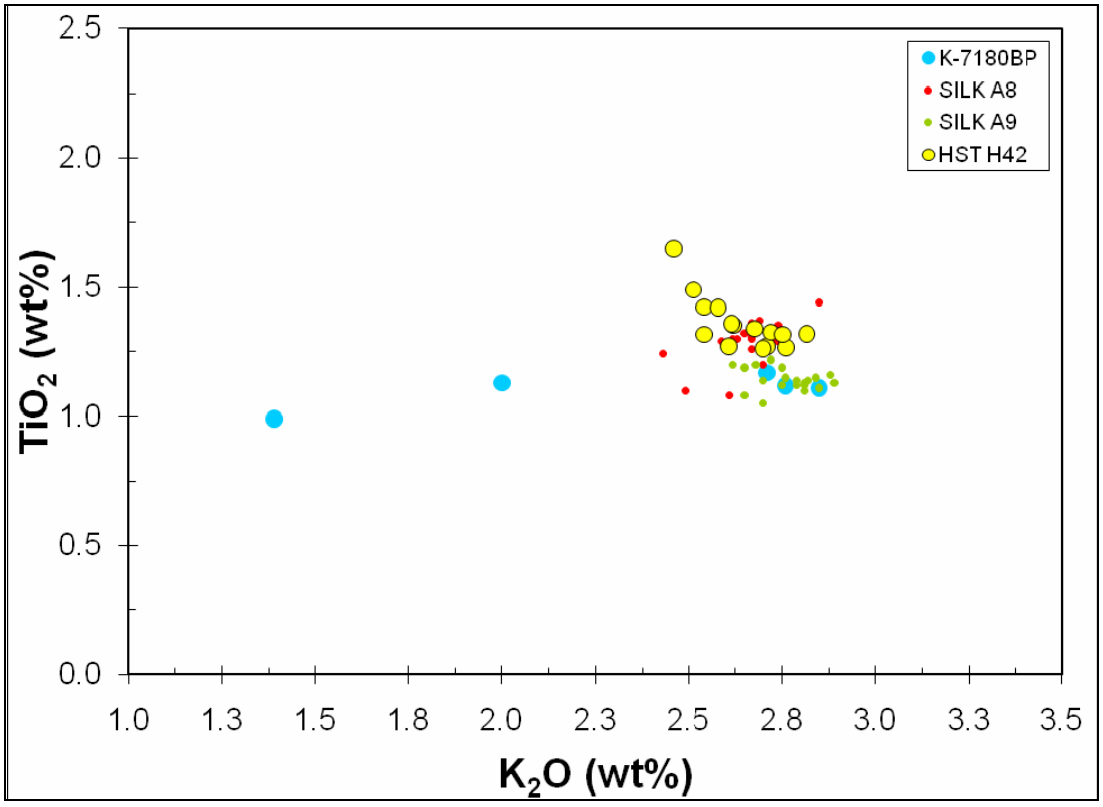

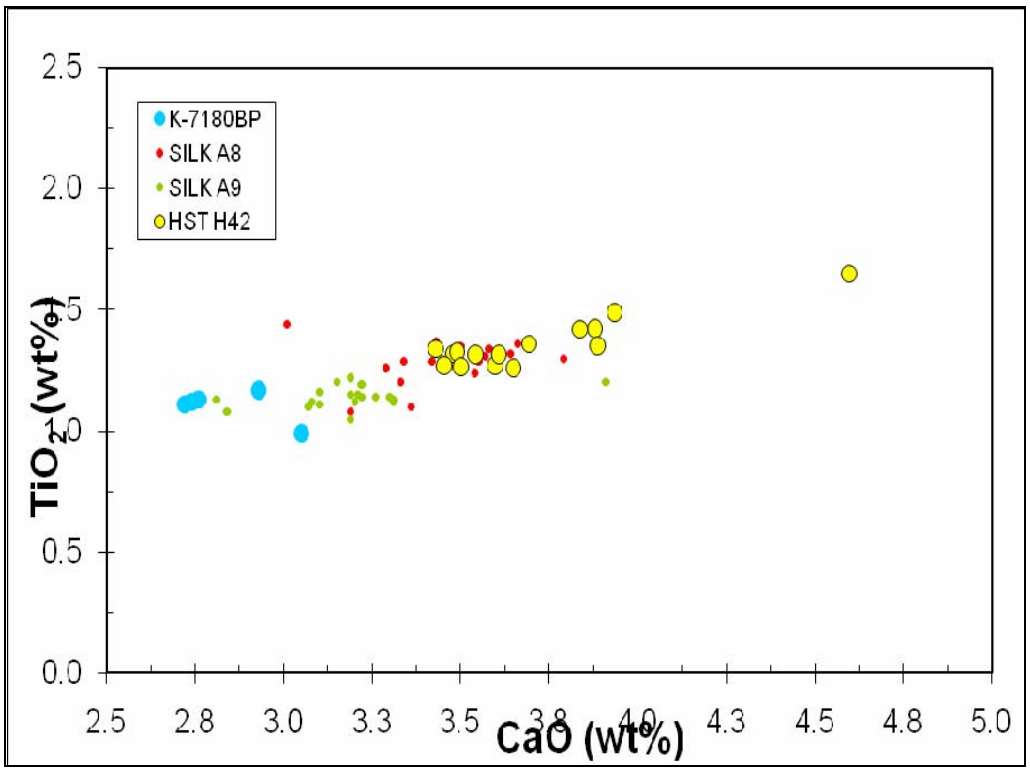
K-7180BP
SILK A8
SILK A9
HST H42
TiO2 (wt%)
CaO (wt%)
2.5
2.0
0.5
0.0
2.5
2.8
3.0
3.3
3.5
4.3
4.5
4.8
5.0

b)

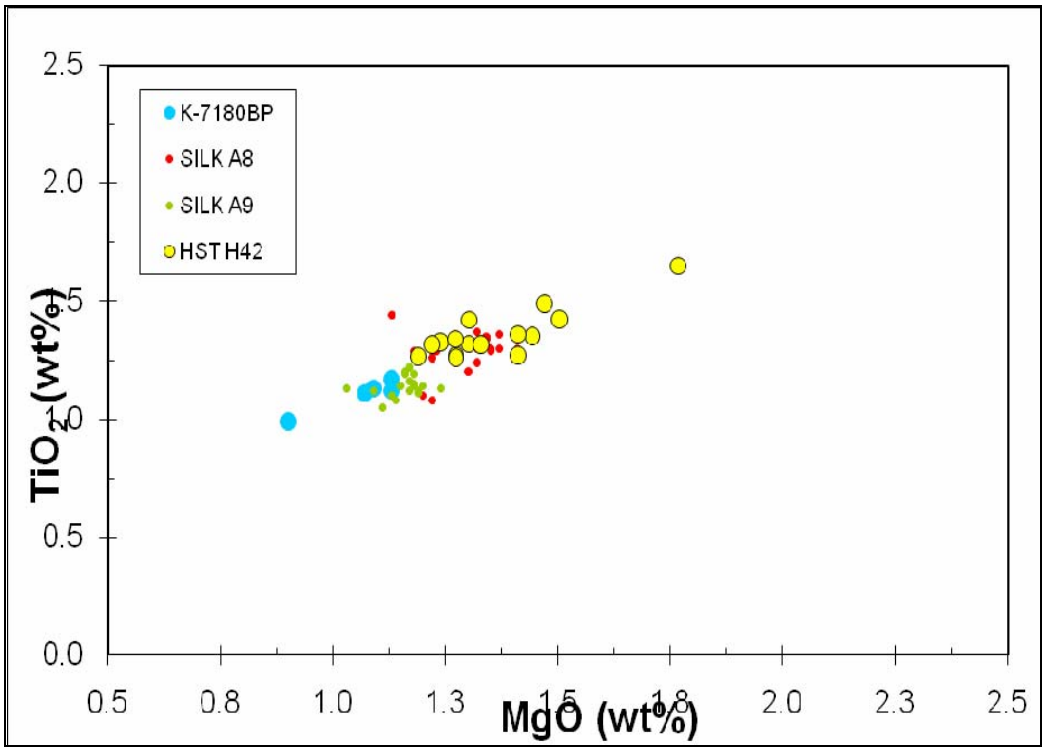
K-7180BP
SILK A8
SILK A9
HST H42
TiO2 (wt%)
MgO (wt%)
2.5
2.0
0.5
0.0
0.5
0.8
1.0
1.3
2.0
2.3
2.5

c)

Once it is established that HST42 is a rhyolitic Katla tepha there are only four options, as the layer must be significantly older than ~6000years as it is well below the T-tephra (6400yrs BP) in the core. These are SILK A-7, A-8 and A-9 and K7180BP. Geochemical data exist for SILK A-8 and 9 is from Larsen (2001) and for K7180BP data is from Óladóttir (2009) identified to the East of Katla. Unfortunately there is no data for SILK A-7. HST42 is similar to SILK A-8 in terms of composition (Figure 19) with differences in TiO_2, CaO and MgO from SILK A-9 and K7180BP. Therefore, we conclude that this layer corresponds to SILK A-8, although it is not possible to rule out SILK A-7. Another possibility is that it is a previously un-identified tephra layer of similar age to SILK A-7, 8 and 9 and of similar composition to SILK A-8 but dispersed to the west of Katla.

6.2.3 Correlation of Layers

Correlation was achieved through the comparison of geochemical analyses. Layers from all the Hvítarvàtn cores were correlated into one combined stratigraphy which was then correlated to VGHV and HST. All data from the two possible matching layers was plotted on a series of bivariate plots containing all ten oxides (Figure 20). This was sufficient to decide that some layers at similar depth and with similar colour and grain size were geochemically very different and should not be correlated. This was backed up and checked through matching known marker layers, colour and grain size of tephra layers and stratigraphic position of the layer in the succession.

6.2.4 Stratigraphy of primary tephra layers

Individual sections at each lake have been constructed (Figure 21 (Hvítarvàtn)) and Figure 22 (Vestra Gìsholtsvàtn and Hestvàtn). These were then correlated (Figure 23).

135 primary Holocene tephra layers were identified in the combined stratigraphy which includes 42 layers from Hestvàtn, 49 layers from Vestra Gìsholtsvàtnand 69 layers from Hvítarvàtn. 106 of these tephra layers were analysed for major element geochemistry. Not all tephra layers were analysed due to time and expense of EPMA analysis. Appendix 5 gives the geochemical data for each layer in the combined stratigraphy.

Vestra Gìsholtsvàtn and Hestvàtn are described together due to their proximity. Table 6, summarises the correlation of the 7 different cores at Hvítarvàtn. Table 7.

Figure 20. SiO_2 on x-axis plotted against all other elements on y-axis. Layer G12 is red dots, Layer G13 is green and Layer H7 is blue. Therefore H7 is correlated to G13, not G12.

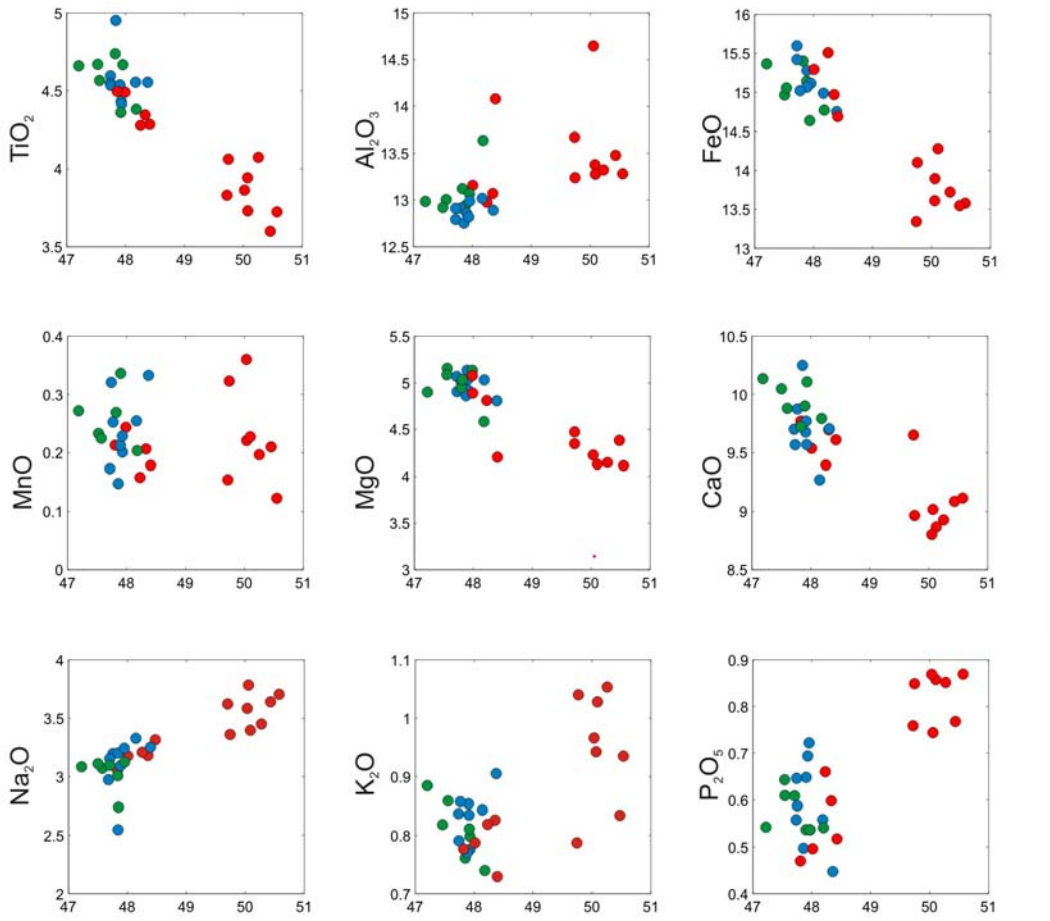

summarises the tephra layer depth, location, composition and source volcano for the combined stratigraphy. It also notes ages of layers from SAR models and uses these to propose an identification of the historical tephra layers. There was usually only one possible choice of identification for the tephra layer given the approximate age from the SAR and so reliability for this depends on the accuracy of records of tephra producing eruptions from Thordarson and Höskuldsson (2008). As previously mentioned, (Section 3.6 Dating in Iceland) historical records are thought to be very good since 1500AD, less detailed from 1000AD to 1500AD and very patchy from 870-1000AD. This should be kept in mind when using these tables. If an eruption is missing from the records it cannot have been considered here.

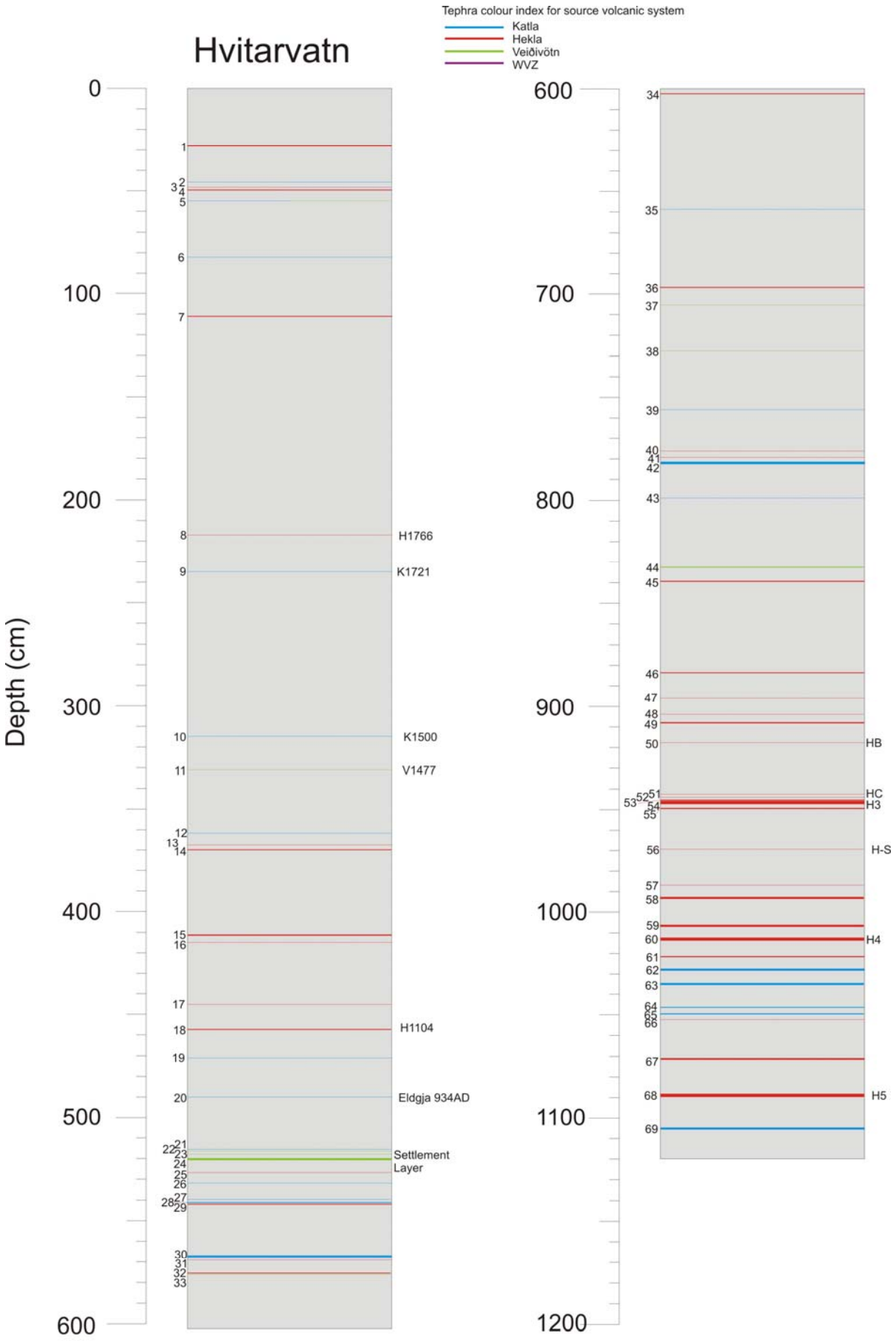
Tephra colour index for source volcanic system
Katla
Hekla
Veiðivötn
WVZ
Hvitarvatn
Depth (cm)
0
100
200
300
400
500
600
600
700
800
900
1000
1100
1200
H1766
K1721
K1500
V1477
H1104
Eldgja 934AD
Settlement Layer
HB
HC
H3
H-S
H4
H5

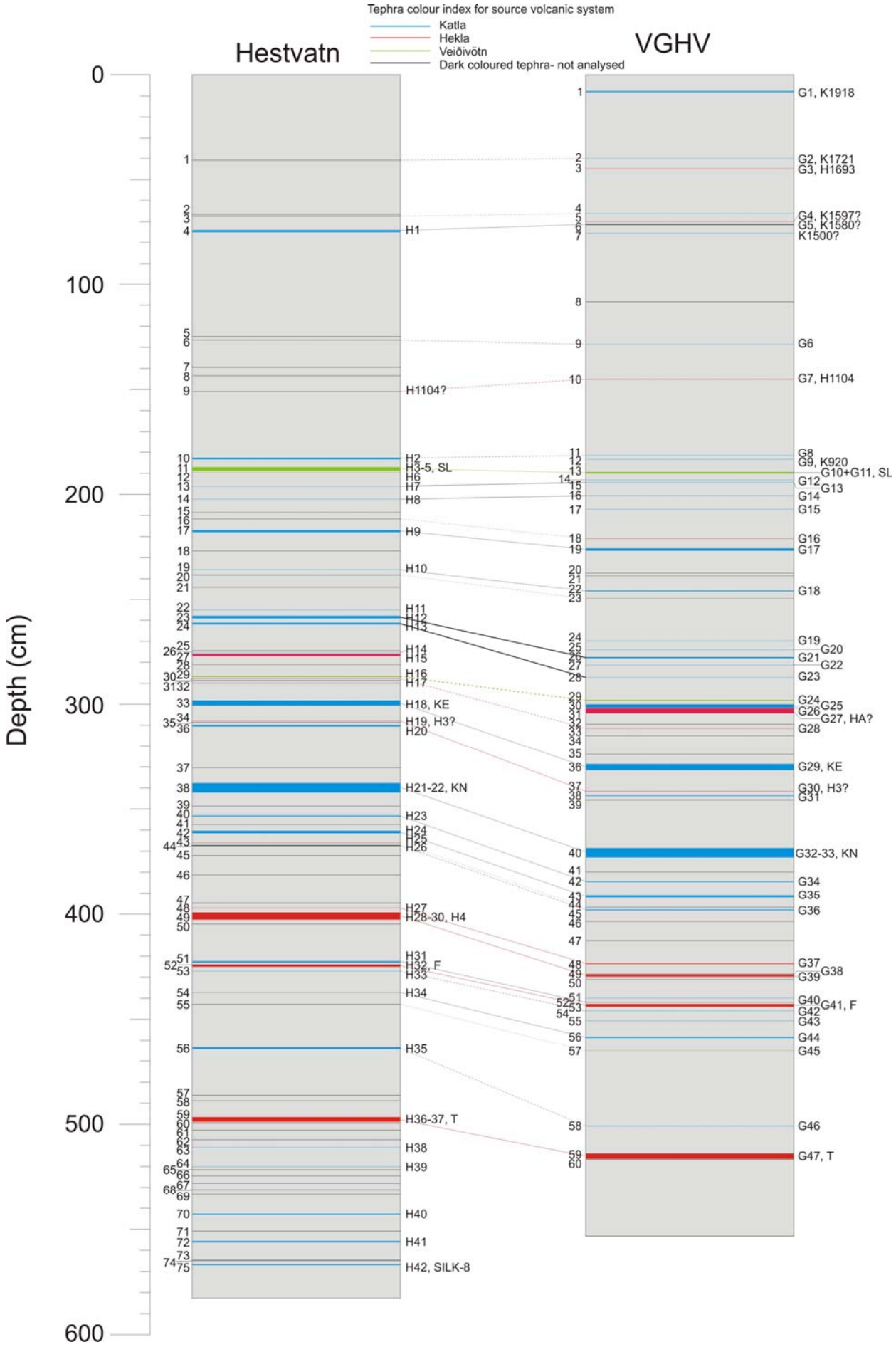
Tephra colour index for source volcanic system
Katla
Hekla
Veiðivötn
Dark coloured tephra- not analysed
Hestvatn
VGHV
Depth (cm)
0
100
200
300
400
500
600
H1
H1104?
H2
H3-5, SL
H6
H7
H8
H9
H10
H11
H12
H13
H14
H15
H16
H17
H18, KE
H19, H3?
H20
H21-22, KN
H23
H24
H25
H26
H27
H28-30, H4
H31
H32, F
H33
H34
H35
H36-37, T
H38
H39
H40
H41
H42, SILK-8
G1, K1918
G2, K1721
G3, H1693
G4, K1597?
G5, K1580?
K1500?
G6
G7, H1104
G8
G9, K920
G10+G11, SL
G12
G13
G14
G15
G16
G17
G18
G19
G20
G21
G22
G23
G24
G25
G26
G27, HA?
G28
G29, KE
G30, H3?
G31
G32-33, KN
G34
G35
G36
G37
G38
G39
G40
G41, F
G42
G43
G44
G45
G46
G47, T

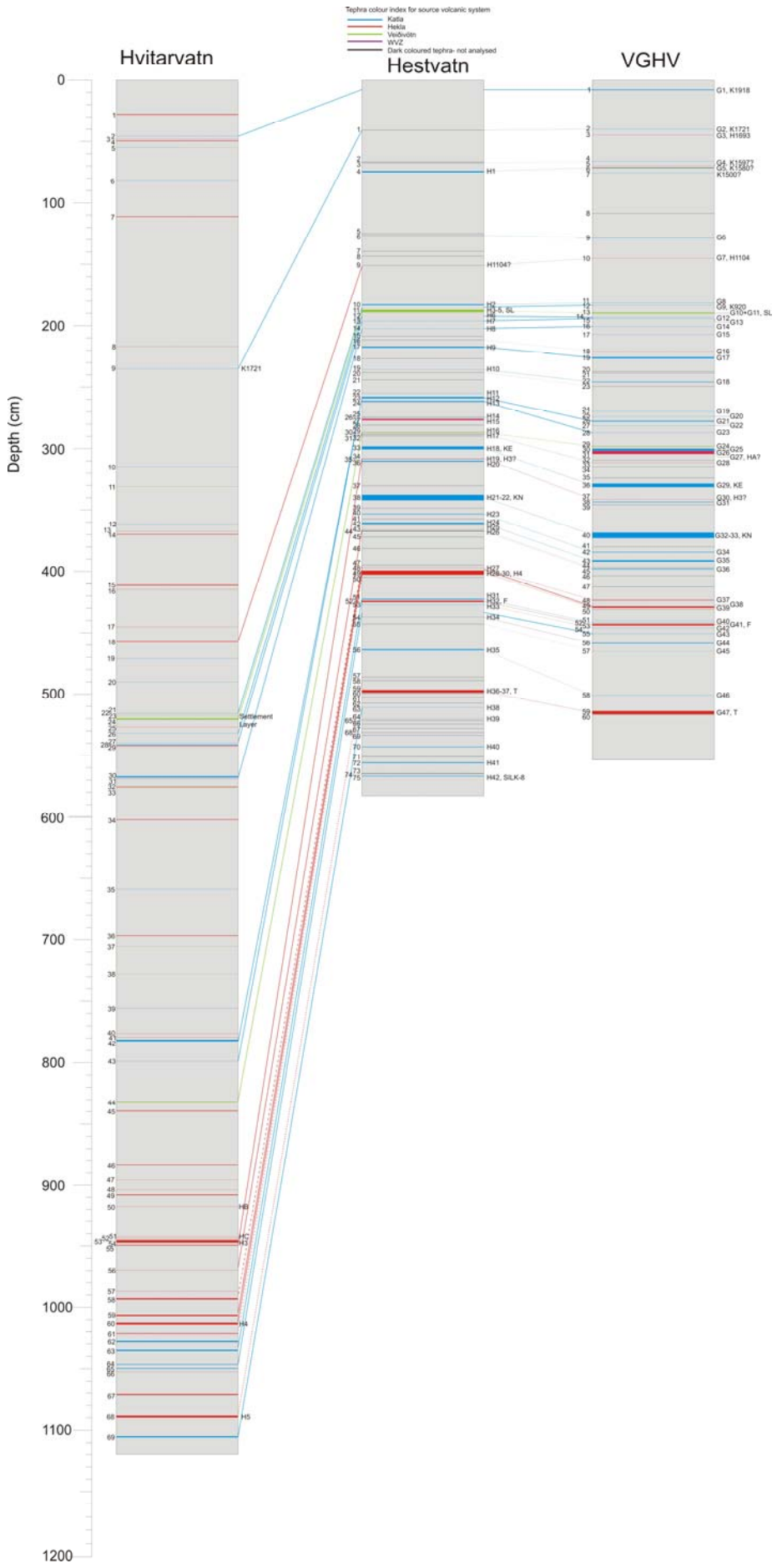
Tephra colour index for source volcanic system
Katla
Hekla
Veiðivötn
WVZ
Dark coloured tephra- not analysed
Hvitarvatn
Hestvatn
VGHV
Depth (cm)
0
100
200
300
400
500
600
700
800
900
1000
1100
1200
K1721
Settlement Layer
H1
H1104?
H18, KE
H21-22, KN
H26-30, H4
H35
H36-37, T
H42, SILK-8
G1, K1918
G2, K1721
G3, H1693
G6
G7, H1104
G29, KE
G32-33, KN
G47, T

Figure 21 (page 66). Core log showing the source volcano of each layer from Hvítarvàtn. Identified key marker layers are labeled. The colour of the line indicates the source volcano of the tephra layer.

Figure 22 (page 67) Correlation of Vestra Gìsholtsvàtn and Hestvàtn. Strong correlations are shown in a continuous line, correlations that are less certain are shown with dashed lines. Colour of the line indicates the source volcano of the tephra layer.

Figure 23 (previous page). Correlation of Vestra Gìsholtsvàtn and Hestvàtn, and Hvítarvàtn. Strong correlations are shown in a continuous line, correlations that are less certain are shown with dashed lines. The colour of the line indicates the source volcano of the tephra layer. Dashed lines in the Hestvàtn core are layers that are not present in the Hestvàtn core but the layers are correlated from Hvítarvàtn to Vestra Gìsholtsvàtn.

Table 6 (next pages). A summary of the Hvítarvàtn cores. There are 7 cores, 1A, 1B, 2A, 2B, 2C, 3A, 3B. This correlates the cores and shows where samples were taken. Cores 1A, 1B, 2A, 2B are in the first table. Cores 2C, 3A and 3B are in the second table. In an ideal presentation the second table would follow to the right of the first but space does not allow this here. If a tephra layer is not visible in any core, a reason is given as to why it is not there. Varve ages are given by Darren Larsen. Age in yrs BP is worked out from Sediment Accumulation Rate graphs (see section 6.3). Overall tephra layer number is given so that samples can be related to the final stratigraphy. Source volcano determined by geochemical analysis is shown (see section 6.2.1). The identification of the tephra layer is shown where known, either through geochemical analysis, or a combination of the age given by SAR and varve dating and the knowledge of which volcano was the source volcano (see Section 6.4). Finally the average thickness of the tephra layer is given.

1A				1B				2A				2B			
Sample No.	**Depth**	**Varve Age (yrs AD)**	**Age (yrs BP)**	**Sample No.**	**Depth**	**Varve Age (yrs AD)**	**Age (yrs BP)**	**Sample No.**	**Depth**	**Varve Age (yrs AD)**	**Age (yrs BP)**	**Sample No.**	**Depth**	**Varve Age (yrs AD)**	**Age (yrs before 2000BP)**
	27.9		30	**17**	27.9	x	30		26.9		30		27.8		30
x	disturbed				56		44	**x**	disturbed			**x**	too small		
x	disturbed				58.7		45	**x**	disturbed				48.1		45
	69.2		53		63		53		56.1		53		49.6		53
	78.1		61	**18**	75.8	1969	61	**x**	disturbed				54.8		61
	149.1		140	**19**	140	1889	140	**x**	disturbed			**x**	not distinct enough		
1	185.8	1859	155	**x**	no core				101.6		155		111.7		155
	279.1		234	**20**	274.8	1766	234		176.1		234		216.9		234
	303.2		279	**21**	299.5	1721	279		195.7		279		234.8		279
x	no core			**x**	disturbed			**35**	268.5	1518	500		315.8		500
	410.5		523	**x**	411.8		523	**36**	286.3	1491	523		332		523
x	disturbed			**x**	disturbed			**37**	346	1337	584	**x**	not distinct enough		
x	disturbed			**x**	disturbed			**38**	351.2	1330	611	**x**	not distinct enough		
x	disturbed			**x**	disturbed			**39**	354.2	1323	659		370.2		659
	489		700		490.8		700		364.7		700		411.1		700
x	no core			**x**	disturbed				375.2		778		414.9		778
x	not distinct enough			**x**	not distinct enough			**40,41**	393.2	1206	794	**82**	445.2	1153	794
	547.3		896		547.8		896	**42,43**	410	1094	896	**83**	457	1104	896
	565.3		1040		566.8		1040	**44,45**	426.1	1043	1040	**84,85**	471.9	1043	1040
2	592	949	1066		595.1		1066	**46**	443.1	950	1066		490.3		1066
3	611.1	890	1080		619.9		1080	**47**	468.8	887	1080		515.1		1080
4	613.6	884	1120		621.1		1120	**48**	470	881	1120		516.6		1120
	too small			**x**	too small			**49**	471.8	872	1128	**86,87**	517.8	872	1128
5,6	621.4	871	1130	**x**	627.3		1130	**50,51**	475.1	870	1130	**88,89**	520.6	871	1130
	not distinct enough			**x**					482.5		1140	**90**	526.5	860	1140
7	633	823	1150		644.1		1150	**52**	488	833	1150	**91**	531.6	833	1150
	640.3		1194		653.1		1194		494.7		1194	**92**	539.7	806	1194
	641.7		1197		654.4		1197	**53**	496.2	803	1197		541		1197
	642.9		1201		655.2		1201		497		1201	**93**	541.9	799	1201
8	674.7	687	1313	**x**	no core			**54**	521.2	704	1313	**94**	567	704	1313

x	not distinct enough			**22**	685.2		1322		530.1		1322		569.1		1322
	686.1		1346	**23**	691		1346	**x**	no core				575.5		1346
9	687	651	1349		691.5		1349	**x**	no core				575.9		1349
	720		1397		721.2		1397	**55**	561.2	556	1397	**95**	603.1	603	1397
x	no core				777.1		1444	**56**	622	303	1444	**96**	659.8	556	1444
	810.4		1832		811.2		1832	**x**	653.6		1832	**97**	697.7	168	1832
	824		1856	**x**	no core			**57**	661.3	144	1856		706.6	144	1856
10	861.2	63	1933		861.7		1933	**58**	681.1	67	1933	**x**	no core		
11	914.1	-112	2112	**24**	912.8	-112	2112	**59**	725.2	-100	2100	**98**	756.8	-100	2100
x	too small			**25**	935.6	-184	2184	**x**	too small				776.8		2184
12	935.8	-184	2184	**26**	936.9	-188	2188	**60**	747.3	-179	2179		780		2188
13	940.7	-194	2194	**27**	941.5	-194	2194	**61**	752.6	-194	2194	**99**	782.5	-194	2194
	958		2270	**x**	no core			**62**	770.2	-270	2270	**100**	799.8	-270	2270
14	999.5		2425		995.2		2425	**63**	804.2		2425	**101**	833.2		2425
15	1007.9		2465	**28**	1003.8		2465	**64**	811.2		2465	**102**	840.1		2465
	1059.1		2664	**29**	1055.1		2664		859.8		2664	**103**	884.1		2664
16	1063.7		2703		1061.9		2703		868.9		2703		896		2703
x	disturbed			**30**	1073.8		2758		878.7		2758		904.6		2758
x	disturbed			**31**	1092		2813		885.6		2813	**104**	908.2		2813
	1094.1		2841	**32,33,34**	1094.7		2841	**65**	892.3		2841	**105,106**	918		2841
	1121.1		2954		1120.8		2954		917.8		2954	**107**	943.5		2954
x	not distinct enough			**x**	not distinct enough			**66**	924.1		3007	**x**	not distinct enough		
x	not distinct enough			**x**	not distinct enough			**67,68**	929.6		3007	**108**	945.9		3007
x	not distinct enough			**x**	not distinct enough			**69,70**	935.1		3007	**109**	946.7		3007
	1129.5		3007		1129.2		3007		946.9		3007	**110**	950.1		3007
	1181.4		3802		1183		3802	**x**	953.5		3802	**x**	970		3802
	1202.9		3915.5		1199.8		3915.5	**71,72**	974.9		3915.5		987.5		3915.5
	1211.2		3977		1207.9		3977		990.3		3977	**111,112**	993.7		3977
	1327.3		4163.333		1319.1		4163.333	**x**	not distinct enough			**113**	1007		4163.333
	1328.9		4196		1326.2		4196	**73,74**	996.8		4196	**114**	1013.8		4196
	1332.6		4214.2		1331.6		4214.2	**75,76**	1007.6		4214.2	**115**	1022.1		4214.2
	1334.1		4320.8		1334.8		4320.8	**x**	not distinct enough			**116**	1028		4320.8
	1350.7		4611.2		1350.1		4611.2		1018.2		4611.2		1036.7		4611.2
x	not distinct enough			**x**	not distinct enough			**x**	not distinct enough			**x**	not distinct enough		
	1353		4911.25	**x**	1353.1		4911.25	**x**	not distinct enough			**x**	not distinct enough		
	1354.1		5036.4		1354.7		5036.4	**77,78**	1037.4		5036.4	**117,118**	1052.8		5036.4

	1414.1		5812.5	**x**	disturbed			**79,80**	1057.7		5812.5	**119,120**	1072.2		5812.5
	1435		6200	**x**	disturbed			**x**	no core			**121**	1089.8		6200
	1452.9		6786.667	**x**	disturbed			**81**	1102.2		6786.667	**x**	no core		

2C				3A				3B										Thickness (cm)
Sample No.	**Depth**	**Varve Age (yrs AD)**	**Age (yrs BP)**	**Sample No.**	**Depth**	**Varve Age (yrs AD)**	**Age (yrs BP)**	**Sample No.**	**Depth**	**Varve Age (yrs AD)**	**Age (yrs BP)**	**Overall**	**Source Volcano**	**Layer Name**		**Age(BP)**	**Error**	
	26.6		30		21.8		30		22.3		30	**1**	**Hekla**	1970/1980	1970	30	30	0.6
123	50	1937	44	**x**	too small			**x**	too small			**2**	**WVZ+K**	K1955-not possible	1955	44	44+-1	0.1
124	50.8	1936	45	**x**	too small			**x**	too small			**3**	**WVZ+H**	Mixed-reworked?		45	45+-2	0.1
125	54	1929	53		53.7		53		49.6		53	**4**	**Hekla**	H1947	1947	53	1947	0.4
	64.2		61	**x**	disturbed			**x**	disturbed			**5**	**Veid/Katla**	Mixed-reworked?				0.2
	92.1		140	**x**	not distinct enough			**x**	disturbed			**6**	**Katla**	K1860	1860	140	140	0.2
	113.1		155		86		155		106		155	**7**	**Hekla**	H1845	1845	155	155	0.4
	182.8		234	**126**	204.2		234		215.7		234	**8**	**Hekla**	H1766	1766	234	234	0.3
	202.8		279	**127**	229.1	x	279		232.2		279	**9**	**Katla**	K1721	1721	279	279	0.1
x	no core			**x**	no core				297.6		500	**10**	**Katla**	K1500	1500	500	500	0.1
x	no core			**x**	no core			**137**	311.9	x	523	**11**	**Veid**	V1477	1477	523	523	0.05
x	no core			**x**	disturbed				361		584	**12**	**Katla**	K1416	1416	584	584	0.1
x	no core			**x**	disturbed				366.2		611	**13**	**Hekla**	H1389	1389	611	611	0.1
x	no core				343.4		659		370		659	**14**	**Hekla**	H1341	1341	659	659	0.3
x	no core				354.2		700	**138**	380.4	1300	700	**15**	**Hekla**	H1300	1300	700	700	0.7
x	no core				370		778	**139,140**	390.7	1259	778	**16**	**Hekla**	H1222	1222	778	778	0.1
x	no core			**x**	not distinct enough			**x**	not distinct enough			**17**	**Hekla**	H1206	1206	794	794	0.3
x	no core			**x**	not present			**141**	433.1	1104	896	**18**	**Hekla**	H1104	1104	896	896	0.2
x	no core				430.3		1040	**x**	no core			**19**	**Hekla**	K960	960	1040	1040	0.1
x	no core				441.8		1066		445.8		1066	**20**	**Katla**	Eldgja	934	1066	1066	0.1
x	no core			**x**	not distinct enough			**x**	disturbed			**21**	**Veid/K**	Katla920	920	1080	1080	0.2
x	no core				468.8		1120	**x**	disturbed			**22**	**Veid**	Bardabunga	880	1120	1120	0.1
x	no core			**x**	too small			**x**	too small			**23**	**Veid**	?				0.1
x	no core			**x**	472.7		1130	**x**	478		1130	**24**	**Veid**	Settlement	870	1130	1130	1.1
x	no core				476.8		1140		481.5		1140	**25**	**Hekla**			1140	1140	0.2
x	no core				482.7		1150		489.1		1150	**26**	**Katla**	Katla 9th C	850	1150	1150	0.2
x	no core				488.1		1194		493.5		1194	**27**	**Katla**			1194	1194	0.2
x	no core				490		1197		495.2		1197	**28**	**Katla**			1197	1197	0.3
x	no core				491.1		1201		496.1		1201	**29**	**Hekla**			1201	1201	0.3
x	no core				506.2		1313		511.8		1313	**30**	**Katla**			1313	1313	0.9

x	no core			**x**	not present			**x**	not present			**31**	**WVZ**			1322	1322+-2	0.1
x	no core				529.4		1346		525.9		1346	**32**	**Hekla**			1346	1346	0.3
x	no core				529.6		1349		526.1		1349	**33**	**Veid**			1349	1349	0.1
x	no core				541.2		1397		547.5		1397	**34**	**Hekla**			1397	1397	0.05
x	no core			**x**	no core				602		1444	**35**	**Katla**			1444	1444	0.1
x	no core				622.1		1832		631.3		1832	**36**	**Hekla**			1832	1832	0.3
x	no core				630.1		1856		634.4		1856	**37**	**Veid**			1856	1856	0.2
x	no core				648.2		1933		658		1933	**38**	**Veid**			1933	1933	0.1
x	no core				685.7		2100	**x**	no core			**39**	**Katla**			2100	2100	0.1
x	no core			**x**	too small			**x**	no core			**40**	**Hekla**			2184	2184	0.1
x	no core				704		2188	**x**	no core			**41**	**Hekla**			2188	2188	0.2
x	no core				706.3		2194	**x**	no core			**42**	**Katla**			2194	2194	1.2
x	no core				720		2270	**x**	no core			**43**	**Katla**			2270	2270	0.2
x	no core			**128**	750.1		2425	**142**	750.9		2425	**44**	**Veid**			2425	2425+-20	0.3
x	no core			**129**	756.2		2465	**143,144**	756.9		2465	**45**	**Hekla**			2465	2464+-30	0.5
x	no core			**130**	795.9		2664	**145**	797		2664	**46**	**Hekla**			2664	2664+-30	0.3
x	no core				802.5		2703		805.2		2703	**47**	**Hekla**			2703	2702+-40	0.1
x	no core				811.8		2758		813.3		2758	**48**	**Hekla**			2758	2758+-35	0.2
x	no core				816.7		2813		818		2813	**49**	**Hekla**			2813	2813+-70	0.4
x	no core			**135,136**	825		2841	**146,147**	825.7		2841	**50**	**Hekla**	HB		2842	2842+-45	0.1
x	no core				844.1		2954		846.1		2954	**51**	**Hekla**	HC		2955	2955+-55	0.1
x	no core			**131**	848		3007	**148,149**	849.7		3007	**52**	**Hekla**	H3		3007	3007	0.2
x	no core			**132**	850.2		3007		850.2		3007	**53**	**Hekla**	H3		3007	3007	0.8
x	no core			**133**	852.6		3007		850.4		3007	**54**	**Hekla**	H3		3007	3007	2
x	no core			**134**	854.9		3007	**150,151,152**	851.2		3007	**55**	**Hekla**	H3		3007	3007	0.5
x	no core			**x**	891.3		3802	**153,154**	890.4		3802	**56**	**Hekla**	H-S?		3802	3802	0.2
x	no core				902		3915.5		901		3915.5	**57**	**Hekla**			3916	3916	0.2
x	no core				902.6		3977		902.8		3977	**58**	**Hekla**			3977	3977	1
x	no core			**x**	too small			**x**	too small			**59**	**Hekla**			4163	4163	1
x	no core			**x**	too small			**x**	too small			**60**	**Hekla**	H4		4196	4196	1.5
x	no core			**x**	906.1		4214.2	**x**	906.3		4214.2	**61**	**Hekla**			4214	4214	0.5
x	no core			**x**	919.8		4320.8	**155**	920.3		4320.8	**62**	**Katla**			4321	4321	1

x	no core				945.2		4611.2	**156**	939.7		4611.2	**63**	**Katla**			4611	4611	0.6
x	no core				989.2		4906.75	**157**	965.1		4906.75	**64**	**Katla**			4907	4907	0.4
x	no core				992.8		4911.25	**158**	968.4		4911.25	**65**	**Katla**			4911	4911	0.5
x	no core			**x**	998		5036.4	**159**	970.8		5036.4	**66**	**Hekla**			5036	5036	0.1
x	no core				1041.1		5812.5		1026.1		5812.5	**67**	**Hekla**			5813	5813	0.8
x	no core				1058.6		6200		1036.2		6200	**68**	**Hekla**	H5		6200	6200	1.6
x	no core				1092.1		6786.667		1098.2		6786.667	**69**	**Katla**			6787	6787	1

Depth	HVT tephra layer number	Age(BP)	Layer Name	VGHV	Base of tephra layer from surface (cm)	HST	Base of tephra layer from surface (cm)	VGHV + HST tephra layer number	Age (years BP)	Most likely historical eruption	Overall layer	Name	Age (yrs BP)	Source Volcano	Rock type			Overall Rock Type
27.8	**1**	30	**1970/1980**								**1**	**1970/1980**	30	Hekla	basaltic		silicic	mixed
45.5	**2**	45	**K1955?**	G1	8.2			1	47	K1955	**2**	**K1955 – not possible**	45	Katla	basaltic	andesitic	silicic	mixed
48.1	**3**	46	**mixed**								**3**	**Mixed-reworked?**	46	WVZ+H	basaltic	andesitic		mixed
49.6	**4**	53	**H1947**								**4**	**H1947**	53	Hekla	basaltic	andesitic		mixed
54.8	**5**		**?**								**5**	**Mixed – reworked?**		Veid/Katla			silicic	silicic
82.1	**6**	140	**K1860**								**6**	**K1860**	140	Katla			silicic	silicic
111.7	**7**	155	**H1845**								**7**	**H1845**	155	Hekla	basaltic			basaltic
216.9	**8**	234	**H1766**								**8**	**H1766**	234	Hekla		andesitic	silicic	mixed
234.8	**9**	279	**K1721**	G2	40.1		40.9	2	279	K1721	**9**	**K1721**	279	Katla	basaltic			basaltic
				G3	44.9			3	307	H1693	**10**	**H1693**	307	Katla		andesitic		andesitic
					66.3		65.6	3a	382	K1625	**11**	**K1625**	382	Katla	n/a	n/a	n/a	n/a
				G4	70.1			4	403	H1597	**12**	**H1597**	403	Hekla	basaltic	andesitic		mixed
				G5	71.6	H1	75	5	423	K1580	**13**	**K1580**	423	Katla	basaltic			basaltic
315.8	**10**	500	**K1500**		75.6			5a	445	K1500	**14**	**K1500**	500	Katla	basaltic			basaltic
332.0	**11**	523	**V1477**								**15**	**V1477**	523	Veid	basaltic			basaltic
361.1	**12**	584	**K1416**								**16**	**K1416**	584	Katla	basaltic		silicic	mixed
367.2	**13**	611	**H1389**								**17**	**H1389**	611	Hekla	basaltic		silicic	mixed

					108.6			5b	632	K1357	**18**	**K1357**	643	Katla	n/a	n/a	n/a	n/a
370.2	**14**	659	**H1341**								**19**	**H1341**	659	Hekla	basaltic			basaltic
411.1	**15**	700	**H1300**								**20**	**H1300**	700	Hekla		andesitic		andesitic
							125.1	5c	731	K1262	**21**	**K1262**	738	Katla	n/a	n/a	n/a	n/a
				G6	128.8		126.6	6	746	K1245	**22**	**K1245**	755	Katla	basaltic			basaltic
414.9	**16**	778	**H1222**								**23**	**H1222**	778	Hekla	basaltic		silicic	mixed
445.2	**17**	794	**H1206**								**24**	**H1206**	794	Hekla	basaltic		silicic	mixed
							139.6	6a	842	H1158	**25**	**H1158**	842	Hekla	n/a	n/a	n/a	n/a
							143.6	6b	847	reworked?	**26**	**reworked?**	847	x	n/a	n/a	n/a	n/a
457.0	**18**	896	**H1104**	G7	145.3		151.1	7	896	H1104	**27**	**H1104**	896	Hekla	basaltic		silicic	mixed
471.9	**19**	1040	**K960**								**28**	**K960**	1040	Hekla	basaltic		silicic	mixed
490.3	**20**	1066	**Eldgja**								**29**	**Eldgja**	1066	Katla	basaltic			basaltic
				G8	181.6	H2	183.4	8	1080	?	**30**	**?**	1070	Hekla	basaltic			basaltic
515.1	**21**	1080	**Katla920**	G9	183.5			9	1097	K920	**31**	**Katla920**	1080	Katla	basaltic			basaltic
516.6	**22**	1120	**Bardabunga**								**32**	**Bardabunga**	1120	Veid	basaltic			basaltic
517.8	**23**		**?**								**33**	**?**		Veid	basaltic		silicic	mixed
520.6	**24**	1130	**Settlement**	G10	190.1	H3	189.9	10	1130	Settlement	**34**	**Settlement**	1130	Veid	basaltic		silicic	mixed
526.5	**25**	1140									**35**		1140	Hekla	basaltic		silicic	mixed
531.6	**26**	1150	**Katla 9th C**	G12	193.3			11	1164		**36**	**Katla 9th C**	1150	Katla	basaltic			basaltic
539.7	**27**	1194									**37**		1194	Katla	basaltic			basaltic
541.0	**28**	1197		G13	194.2	H7	196.2	12	1208		**38**		1197	Katla	basaltic			basaltic
541.9	**29**	1201									**39**		1201	Hekla	basaltic	andesitic		mixed

567.0	**30**	1313		G14	200.7	H8	202.4	13	1301		**40**		1313	Katla	basaltic			basaltic
569.1	**31**	1322									**41**		1322	WVZ	basaltic			basaltic
575.5	**32**	1346									**42**		1346	Hekla		andesitic		andesitic
575.9	**33**	1349									**43**		1349	Veid	basaltic		silicic	mixed
				G15	207.2		208.6	14	1388		**44**		1388	Katla	basaltic			basaltic
603.1	**34**	1397									**45**		1397	Hekla	basaltic	andesitic	silicic	mixed
659.8	**35**	1444									**46**		1444	Katla		andesitic		andesitic
				G16	221.1		211.6	15	1511		**47**		1511	Hekla	basaltic	andesitic		mixed
				G17	226.7	H9	217.9	16	1596		**48**		1596	Katla	basaltic			basaltic
					237.4			16a	1733		**49**		1733	x	n/a	n/a	n/a	n/a
					238.4			16b	1760		**50**		1760	x	n/a	n/a	n/a	n/a
697.7	**36**	1832									**51**		1832	Hekla	basaltic			basaltic
				G18	246	H10	235.8	17	1853		**52**		1853	Katl	basaltic			basaltic
706.6	**37**	1856									**53**		1856	Veid	basaltic			basaltic
					249.6			17a	1913		**54**		1913	x	n/a	n/a	n/a	n/a
728.6	**38**	1933									**55**		1933	Veid	basaltic			basaltic
756.8	**39**	2100									**56**		2100	Katla	basaltic			basaltic
				G19	270			18	2157		**57**		2157	Katla	basaltic			basaltic
776.8	**40**	2184									**58**		2184	Hekla	basaltic	andesitic		mixed
780.0	**41**	2188									**59**		2188	Hekla	basaltic	andesitic	silicic	mixed
				G20	274.2			19	2208		**60**		2192	Katla	basaltic			basaltic
782.5	**42**	2194				H11	255.6	20	2210		**61**		2194	Katla	basaltic			basaltic

799.8	**43**	2270		G21	278.1	H12	259.1	21	2262		**62**		2270	Katla	basaltic			basaltic
				G22	281.5			22	2292		**63**		2292	Katla	basaltic			basaltic
				G23	284.4	H13	262	23	2338		**64**		2338	Katla	basaltic			basaltic
							274.6	23a	2526		**65**		2397	x	n/a	n/a	n/a	n/a
						H14	275.6	24	2541		**66**		2412	Katla	basaltic			basaltic
						H15	277.7	25	2546		**67**		2417	Hekla		andesitic		andesitic
833.2	**44**	2425		G24	298.4	H16	287	26	2554		**68**		2425	Veid	basaltic		silicic	mixed
840.1	**45**	2464.833									**69**		2465	Hekla	basaltic	andesitic	silicic	mixed
				G25	301.7			27	2556		**70**		2556	Katla	basaltic			basaltic
				G26	302			28	2569		**71**		2569	Katla	basaltic	andesitic		mixed
884.1	**46**	2664.167									**72**		2664	Hekla	basaltic	andesitic		mixed
				G27	304.3			29	2609	HA	**73**		2609	Hekla		andesitic		andesitic
					309.7			29a	2670		**74**		2670		n/a	n/a	n/a	n/a
896.0	**47**	2702.5									**75**		2703	Hekla	basaltic	andesitic		mixed
				G28	311.5	H17	288	30	2724		**76**		2724	Hekla		andesitic		andesitic
904.6	**48**	2757.8									**77**		2758	Hekla			silicic	silicic
					315.1			30a	2761		**78**		2761	x	n/a	n/a	n/a	n/a
908.2	**49**	2813.2									**79**		2813	Hekla	basaltic		silicic	mixed
918.0	**50**	2841.5	**HB**								**80**		2842	Hekla	basaltic	andesitic		mixed
					324.2			30b	2867		**81**		2867	x	n/a	n/a	n/a	n/a
943.5	**51**	2954.5	**HC**								**82**		2955	Hekla	basaltic	andesitic	silicic	mixed
				G29	331.5	H18	300.6	31	2962	KE	**83**	**KE**	2962	Katla	basaltic			basaltic

944.4	**52**	3007	**H3**								**84**	**H3**	3007	Hekla		andesitic	silicic	mixed
945.9	**53**	3007	**H3**								**85**	**H3**	3007	Hekla		andesitic	silicic	mixed
946.7	**54**	3007	**H3**								**86**	**H3**	3007	Hekla		andesitic	silicic	mixed
950.1	**55**	3007	**H3**	G30	341.7	H19	308.1	32	3007	H3	**87**	**H3**	3007	Hekla	basaltic	andesitic	silicic	mixed
							308.7	32a	3008		**88**		3008	x	n/a	n/a	n/a	n/a
				G31	343.8	H20	310.6	33	3031		**89**		3031	Katla	basaltic			basaltic
							330.5	33a	3352		**90**		3352	x	n/a	n/a	n/a	n/a
				G32	373	H21	342.2	34	3533	KN	**91**	**KN**	3533	Katla	basaltic			basaltic
					380		348.7	34a	3586		**92**		3586	x	n/a	n/a	n/a	n/a
				G34	384.6	H23	353.4	35	3663		**93**		3663	Katla	basaltic			basaltic
				G35	392.1	H24	361.5	36	3749		**94**		3749	Katla	basaltic			basaltic
970.0	**56**	3802	**H-S?**		396.9	H25	366.2	37	3790		**95**	**H-S**	3802	Hekla		andesitic	silicic	mixed
				G36	398.3	H26	367.6	38	3821		**96**		3821	Katla	basaltic			basaltic
					403.6		372.2	38a	3878		**97**		3878	x	n/a	n/a	n/a	n/a
987.5	**57**	3916									**98**		3916	Hekla		andesitic	silicic	mixed
993.7	**58**	3977			412.7		381.4	38b	3976		**99**		3977	Hekla		andesitic	silicic	mixed
							394.8	38c	4096		**100**		4096	x	n/a	n/a	n/a	n/a
				G37	423.7	H27	397.3	39	4128		**101**		4128	Katla	basaltic	andesitic		mixed
1007.0	**59**	4163		G38	429.3			40	4178		**102**		4163	Hekla	basaltic	andesitic	silicic	mixed
1013.8	**60**	4196	**H4**	G39	429.8	H28	402.7	41	4192	H4	**103**	**H4**	4196	Hekla	basaltic	andesitic	silicic	mixed
1022.1	**61**	4214			430.6		404.8	41a	4238		**104**		4214	Hekla		andesitic	silicic	mixed
1028.0	**62**	4321									**105**		4321	Katla	basaltic			basaltic

					440			41b	4508		**106**		4508	x	n/a	n/a	n/a	n/a
1036.7	**63**	4611		G40	442	H31	423	42	4621		**107**		4611	Katla	basaltic			basaltic
				G41	444	H32	425.1	43	4739	H-F	**108**	**H-F**	4739	Hekla	basaltic			basaltic
				G42	446.1	H33	427.2	44	4784		**109**		4784	Katla	basaltic			basaltic
1047.3	**64**	4907		G43	450.8			45	4908		**110**		4907	Katla	basaltic			basaltic
1050.1	**65**	4911		G44	458.8	H34	437.3				**111**		4911	Katla	basaltic			basaltic
				G44	458.8	H34	437.3	46	5020		**112**		5020	Katla	basaltic			basaltic
1052.8	**66**	5036									**113**		5036	Hekla	basaltic	andesitic	silicic	mixed
				G45	465.2		442.9	47	5156		**114**		5156	Veid	basaltic			basaltic
				G46	501	H35	464.3	48	5656		**115**		5656	Katla	basaltic			basaltic
1072.2	**67**	5813									**116**		5813	Hekla	basaltic	andesitic	silicic	mixed
							487.3	48a	6142		**117**		6142	x	n/a	n/a	n/a	n/a
1089.8	**68**	6200	**H5**				490	48b	6243		**118**	**H5**	6200	Hekla			silicic	silicic
				G47	515.1	H36	498.8	49	6409		**119**		6409	Hekla	basaltic	andesitic		mixed
							499.5	49a	6459		**120**		6459	x	n/a	n/a	n/a	n/a
							502.8	49b	6529		**121**		6529	x	n/a	n/a	n/a	n/a
							507.4	49c	6668		**122**		6668	x	n/a	n/a	n/a	n/a
1106.9	**69**	6787				H38	511	50	6721		**123**		6787	Katla	basaltic			basaltic
						H39	520.2	51	6924		**124**		6924	Katla	basaltic			basaltic
							521.6	51a	6957		**125**		6957	x	n/a	n/a	n/a	n/a
							525.5	51b	7042		**126**		7042	x	n/a	n/a	n/a	n/a
							528.1	51c	7111		**127**		7111	x	n/a	n/a	n/a	n/a

							531.2	51d	7169		**128**		7169	x	n/a	n/a	n/a	n/a
							533.5	51e	7241		**129**		7241	x	n/a	n/a	n/a	n/a
						H40	543.1	52	7470		**130**		7470	Katla	basaltic			basaltic
							551	52a	7650		**131**		7650	x	n/a	n/a	n/a	n/a
						H41	556.2	53	7782		**132**		7782	Katla	basaltic			basaltic
							564.6	53a	7926		**133**		7926	x	n/a	n/a	n/a	n/a
							565	53b	7960		**134**		7960	x	n/a	n/a	n/a	n/a
						H42	567	54	8000	SILK A8	**135**	**SILK A8**	8000	Katla			silicic	silicic

Table 7. A summary of the correlation between the Vestra Gìsholtsvàtn, Hestvàtn and Hvítarvàtn cores. Overall tephra layer number is given so that tephra layers in individual cores can be related to the final stratigraphy. Age, probable identity of historical tephra layers and source volcano (see table x (one before this) are given, as described previously. Rock type is also noted. In cases where there are both silicic and basaltic grains but by far the majority are silicic then the layer is described as silicic as this is its main characteristic. If there is a more even distribution between silicic and basaltic, the layer is described as mixed. The identification of the tephra layer is shown where known, either through geochemical analysis, or a combination of the age given by SAR and varve dating and the knowledge of which volcano was the source volcano (see Section 6.4).

Vestra Gìsholtsvàtnand Hestvàtn

Of those that have been analysed, 80% of the layers (44) are basaltic in composition, 7% (4) intermediate to silicic and 13% (7) are mixed basalt and silicic composition. Following the methodology outlined in section 4.5, the sources of all tephra layers are three volcanic systems within the East Volcanic Zone (EVZ); 36 layers from Katla (65%), 14 layers from Hekla (25%), 5 layers from Veiðivötn-Bárðarbunga (9%).

Hvítarvàtn

Of the 69 tephra layers, 35% of the layers (24) are basaltic in composition, 4% intermediate (3), 6% silicic (4) and 55% (38) are mixed basalt and silicic composition.

The sources of the the tephra layers are nearly all from within the EVZ; 20 layers from Katla (30%), 37 layers from Hekla (54%), 9 layers from Veiðivötn-Bárðarbunga (13%). There are also 2 layers from the WVZ (3%). The presence of the 2 WVZ layers is probably explained by the proximity of Hvítarvàtn to the WVZ. Hence, tephra fall from smaller eruptions are more likely to be recorded than in VGHV and HST. Again tephra layers from Grimsvötn are not seen for the same reasons as VGHV and HST. The change from Katla being dominant in VGHV and HST to Hekla being dominant in HVT is also probably a product of their relative distances from volcano to lake. The change to a greater proportion of mixed layers is likely to be a result of the increased contribution from Hekla. In terms of hazard predictions the record shows that Hekla is the volcano most likely to directly affect this area of Iceland.

Combined Stratigraphy for South-West Iceland

Of the 135 layers in the combined stratigraphy (Table 7), 105 have been analysed. Of those, 47.5% of the layers (50) are basaltic in composition, 6.5% (7) intermediate, 5% silicic (5) and 41% (43) are mixed basalt and silicic composition. In the combined stratigraphy there are 47 layers from Katla (45%), 46 layers from Hekla (44%), 10 layers from Veiðivötn-Bárðarbunga (9%) and 2 layers from the WVZ (2%). This indicates Katla and Hekla eruptions are equally likely to spread tephra over South-West Iceland.

Figure 24. Chemistry of tephra layers with time. Y-axis shows tephra layer number ie. age increases down the plot. X-axis shows oxide concentration. Blue dots show all the data for each layer, pink dots are the mean of each layer. Blue shading covers range of data for each layer that is determined to be from Katla showing the variation in this composition and particularly the range in composition with time.

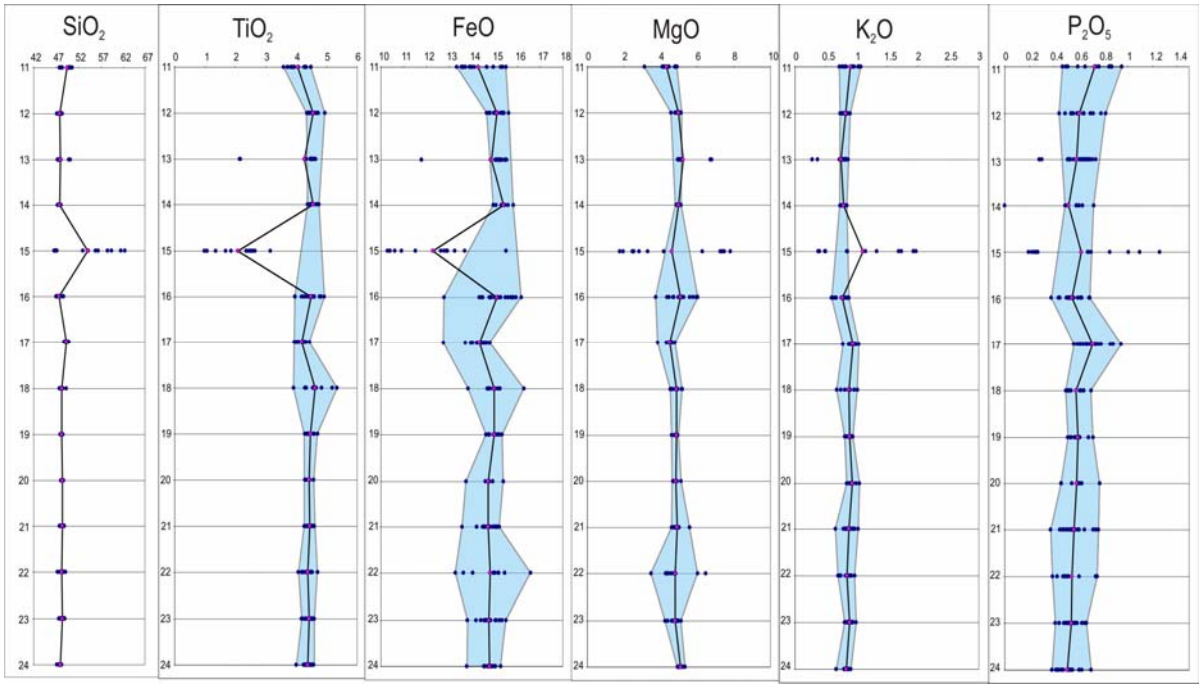

6.2.5 Identification of individual eruptions

In most cases it is not possible to identify different eruptions from the same volcano solely using major element geochemistry. This is the same finding as Westgate and Gorton (1981). For example if all Katla layers from VGHV and HST are plotted on a bivariate plot there are distinct areas for different layers but the overlap between each is too great for effective discrimination. However it is possible to identify series of layers or even individual layers by examining changes in chemistry with time (Figure 24). VGHV and HST layers 11-24 are all from Katla with the exception of layer 15 which is from Hekla. Layer 13 can also be distinguished easily as it has some grains of SiO_2 ~50wt%, whereas SiO_2 is very similar for the rest of the Katla layers at ~47.7wt%. However a pattern can be established by looking at the range of values for each layer; Layer 19 has the smallest range in oxide concentrations, whereas Layer 22 has the largest range. Range increases from 24 to 22, then decreases to 19, then increases to 16, decreases to 14 and increases to 11. This pattern can then be matched to future records to allow more precise correlation.

6.2.6 Trace element content of tephras

Cr_2O_3, NiO and SrO were measured in 96 (out of 164) of the HVT samples to see if they helped in the discrimination of source volcano (Appendix 4). The vast majority of the Cr_2O_3 and NiO data were under detection limits and so of no use. SrO was detected a sufficient number of times but was of no use in the discrimination of Hekla and Katla; the values being very similar.

6.2.7 Volatile content of tephras

F, Cl, SO_2 were measured in all HVT tephra layers (Appendix 4). F is constant with increase in SiO_2, Cl increases with increase in SiO_2 and SO_2 decreases with increase in SiO_2. Volatile contents have a greater range in Hekla layers than in Katla layers particularly in Cl and F. In terms of discrimination between the two volcanoes they have values that are too similar to be of any additional help than simply using major elements. However as the values here represent concentrations after partial (or full) degassing), no correlation with other incompatible elements can be expected because S, Cl and F values have been modified by phase separation.

6.3 Sediment Accumulation Rate

For each lake the Sediment Accumulation Rate (SAR) was calculated for each interval using dated tephra layers as boundary markers. For VGHV and HST there are seven identified tephra layers that have been dated by the C^{14} method. These are Settlement, KE, KN and H-F (e.g. Hardardóttir et al., 2001), H3 and H4 (Dugmore et al., 1995a) and K-A8 (Larsen et al., 2001). For Hvítarvàtn there are ten identified layers; H1766, K1721, V1477, H1300, H1104, Eldgja, Settlement, H3, H4, H5.

Assuming constant SAR throughout each interval, the age of each tephra layer was calculated using its depth in the sediment. The dates of geochemically and physically correlated layers were then compared and averaged when discrepancies arose. As discussed by Óladóttir (2005) there are assumptions and uncertainties inherent in this method. However it gives a relative age for each layer that is useful for calculating the frequency of tephra fallout during the Holocene and provides chronological constraints for studies aimed at investigating the long term magmatic evolution at individual systems and is the most appropriate method when the number of dates available is limited as in this study (Telford et al. 2004).

Sediment Accumulation Rate models were constructed for each lake and shown on Figure 25.

a)

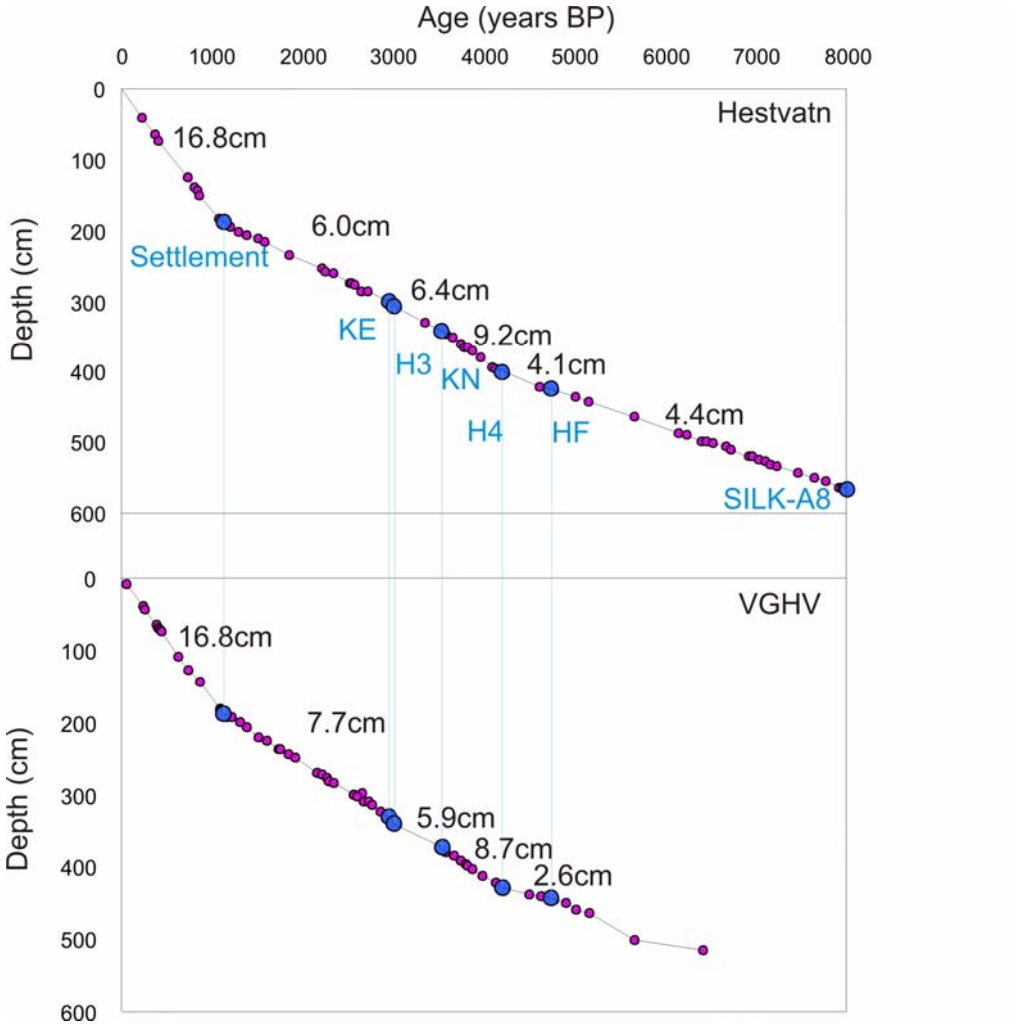
Age (years BP)
0
1000
2000
3000
4000
5000
6000
7000
8000
Hestvatn
Depth (cm)
16.8cm
6.0cm
Settlement
6.4cm
KE
9.2cm
H3
KN
4.1cm
H4
HF
4.4cm
SILK-A8
VGHV
16.8cm
7.7cm
5.9cm
8.7cm
2.6cm

b)

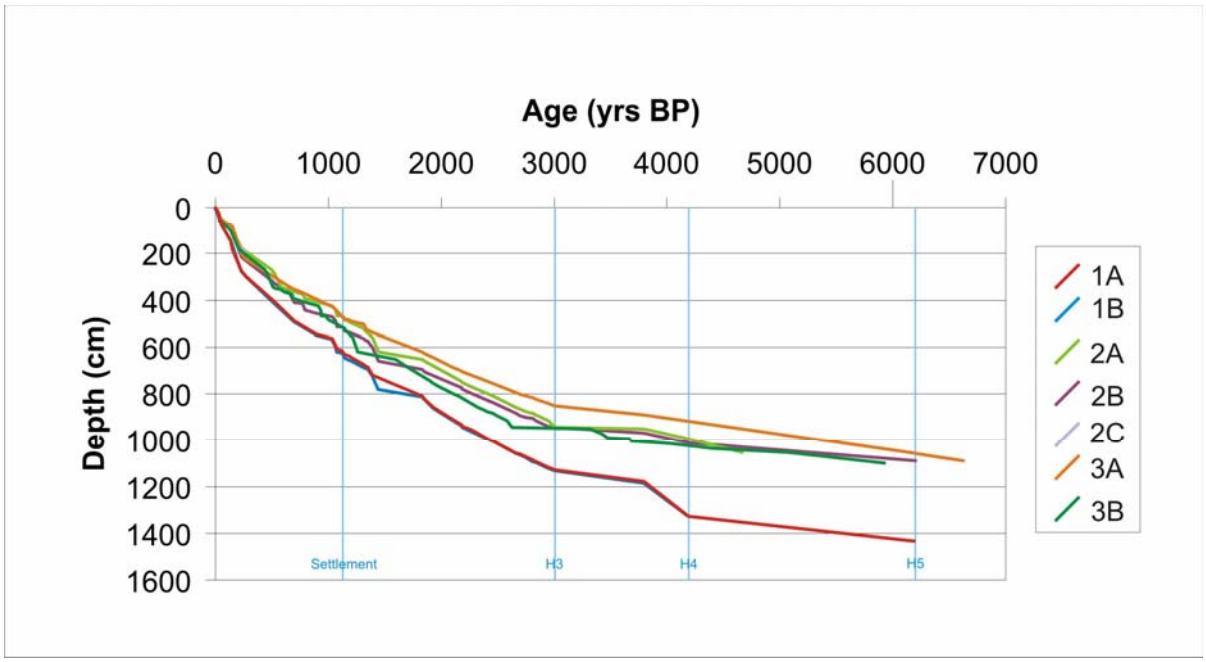
Age (yrs BP)
0
1000
2000
3000
4000
5000
6000
7000
Depth (cm)
Settlement
H3
H4
H5
1A
1B
2A
2B
2C
3A
3B

Figure 25 (previous page). a) Age-Depth models for Hestvàtn (upper) and Vestra Gìsholtsvàtn (lower) showing sediment accumulation rate in cm/100yrs for each section. Blue dots represent marker layers which are labelled. Pink dots are the other layers that are given an estimated age from this model. b) Age depth model for Hvítarvàtn. Blue vertical lines represent key marker layers. Each core is represented by a different coloured line on the age depth model.

Vestra Gìsholtsvàtn and Hestvàtn

SAR range from 2.6cm/100yr (in VGHV from ~4700-4200BP) to 16.8cm/100yr (in both lakes from 1130-0 BP). SAR are lower in VGHV than HST for the same period apart from ~2900-1130BP. Sediment accumulation generally appears to increase throughout the Holocene from 4.4cm/100yr (HST) from 8000 to ~5000BP, to 16.8cm/100yr (both lakes) from 1130-0 BP. No concurrent increase in density is noticed (Geirsdóttir pers. comm. 2009) leading to the conclusion that it is a real sediment accumulation rate increase. There are 2 periods of particularly high accumulation rates, after Settlement (1130BP) and after H4 (~4200BP) (Figure 25a).

As mentioned in section 6.1 (Tephra Stratigraphy) there are three C^{14} dates for the VGHV core. The C^{14} age for H4 is ~350 years older than dates obtained by Dugmore et al. (1995) suggesting that the ages in VGHV are too high due to the input of old carbon. Hence, the C^{14} age of 5630±50 for the T-tephra might be expected to be too old as well. This can be tested using the SAR models for the VGHV core (Figure 25a). They show the age of the T-tephra to be ~6400BP which equates to ~5700 C^{14} age. This is almost within the error of the age obtained by Hardardóttir (2001) of 5630±50 C^{14} yrs and also similar to that obtained by Sveinbjornsdóttir et al. 1998. Therefore it seems likely that it is only the date near to H4 that was affected by the input of old carbon.

Hvítarvàtn

SAR range from 3.8cm/100yr (6200-4196BP in core 2B) to 55.5cm/100yr (in from 1130-0 BP in core 1B). SAR are highest in cores 1A and 1B, lower in 2A, 2B, 3A and 3B. Again sediment accumulation generally appears to increase throughout the Holocene from 3.8cm/100yr from 6200 to 4196BP to 55.5cm/100yr (Settlement to 0BP). SAR in the last ~300 years has been as high as 108.7cm/yr (K1721-present in core 1A). The main perturbations to the smooth curve of increase throughout the Holocene are seen after H4 and after Settlement (Figure 25b). If SAR estimates are

examined in more detail in the historic period (1130-0BP), the largest SAR is 130.6cm/100yr (in core 2A from 1947 to present) with SAR above 100cm/100yr from K1721 onwards.
SAR was a main contributor in helping to identify the ages of the tephra layers. Estimates are given in Table 6 (summary of HVT cores).

6.4 Identification of historic tephra layers

Using the estimated ages from the SAR model it is possible to get an idea of the frequency of tephra fall in the area which can give information about eruption frequency and paleowind directions. Table 7, gives estimated ages of each tephra layer. This can then help identify particular layers. For example Layers 5a and 5b from Vestra Gìsholtsvàtn and Hestvàtn were not analysed for geochemistry. Therefore a tentative identification can be made for 5a to K1500 and for 5b to K1357, considering dates given by SAR model and distributions of tephra from Larsen (1978), Sigurgeirsson (1992) and Thorarinsson (1947). The first 5 layers in the combined stratigraphy present the most problems. Following these there was only one choice of tephra layer with the correct source volcano and correct approximate age. It is not possible to tell from the records whether Layer 1 is H1970 or H1980. Layer 2 is from Katla and has an age around that of K1955 but this eruption produced no tephra, only a flood so the tephra layer is not a product of this. There are no other recorded Katla layers around this period. Layers 3 and 5 are of mixed source leading to the conclusion that they are reworked layers. Layer 3 has geochemical affinities to WVZ and Hekla and Layer 5 to Veiðivötn and Katla.

Comparing identification of historical eruptions with the dates given by the SAR method gives a measure of its accuracy. Predictably, there is no consistent offset and ages vary from 0 to 55 years between the Vestra Gìsholtsvàtn and Hestvàtn cores, which is to be expected as the SAR method assumed a constant rate for 1130 years, which is not realistic. The eruption ages tend to be older than the ages derived from the SAR method by on average 14 years, implying that SAR is over-estimated for this period.
The ages from Hvítarvàtn have an additional age control. Darren Larsen has counted varves throughout the cores for the last 2300years using the following tephra layers as age controls: K1721, H1766, H1300, H1104, Settlement. Age differences from the varve age to the actual age range between 0 and 96 years and

again are not consistent. However if core 2B is ignored, then age differences are not greater than 30 years with an average deviation of 4 years. Presumably something went wrong with the varve counting in core 2B and the use of varve counting does improve the age record providing there are multiple checks on age from known tephra layers.

6.5 Frequency of Tephra Fall

The average number of tephra layers in the period 0-8200yr BP is 4.4 layers/500yr at Hestvàtn, 3.4 layers/500yr at Vestra Gìsholtsvàtnand 4.3layers/500yrs at Hvítarvàtn. However from the combined stratigraphy of VGHV and Hestvàtn the average is 5.6 layers/500yr, and from the combined stratigraphy from all three lakes it is 8.4layers/500yrs, emphasising the importance of correlating multiple sites in producing records. The frequency of tephra layers in the record varies greatly between different time periods, with rates of tephra fall and preservation as low as 4 layers/500yr (from 5500-6000yr BP) to 19 layers/500yr (1000-1500yrBP). Tephra layer frequency was evaluated using periodicities of 200, 400, 500, 700 and 1000yrs and the results show that frequency distribution is characterised at all periodicities by three peaks at 2.5-3Ka, 3.5-4Ka and 7-7.5Ka. If the data from Hvítarvàtn are included there is no peak at 7-7.5ka due to the tephra layers only being analysed up to ~6200yrs in VGHV and HST. Eruptions appear to occur in clusters, but there is no pattern to whether a Hekla, Katla or Veiðivötn eruption starts the cluster of eruptions (Figure 26).

6.6 Presence of Tephra Layers in Lakes

<u>Vestra Gìsholtsvàtn and Hestvàtn</u>

There are considerable differences in the tephra record at the two sites despite their proximity (Figure 22, Table 7). Only 3 layers are present in the Hestvàtn core in the first 100cm depth (~700yr BP), compared to 8 in Vestra Gíslholtsvàtn. There are 16 more layers present at the bottom of the Hestvàtn core than the Vestra Gìsholtsvàtn core extending it for another ~1600yrs. Before 6000BP, the core from Hestvàtn commonly does not include Katla layers recorded in the Vestra Gìsholtsvàtn core whereas after 6000BP Katla layers are missing from the Vestra Gìsholtsvàtn core. Vestra Gìsholtsvàtn preserved all the Hekla layers found in the combined stratigraphy but did not include all the Veiðivötn-Bárðarbunga layers whereas Hestvàtn preserved all the Veiðivötn-Bárðarbunga but did not include the Hekla

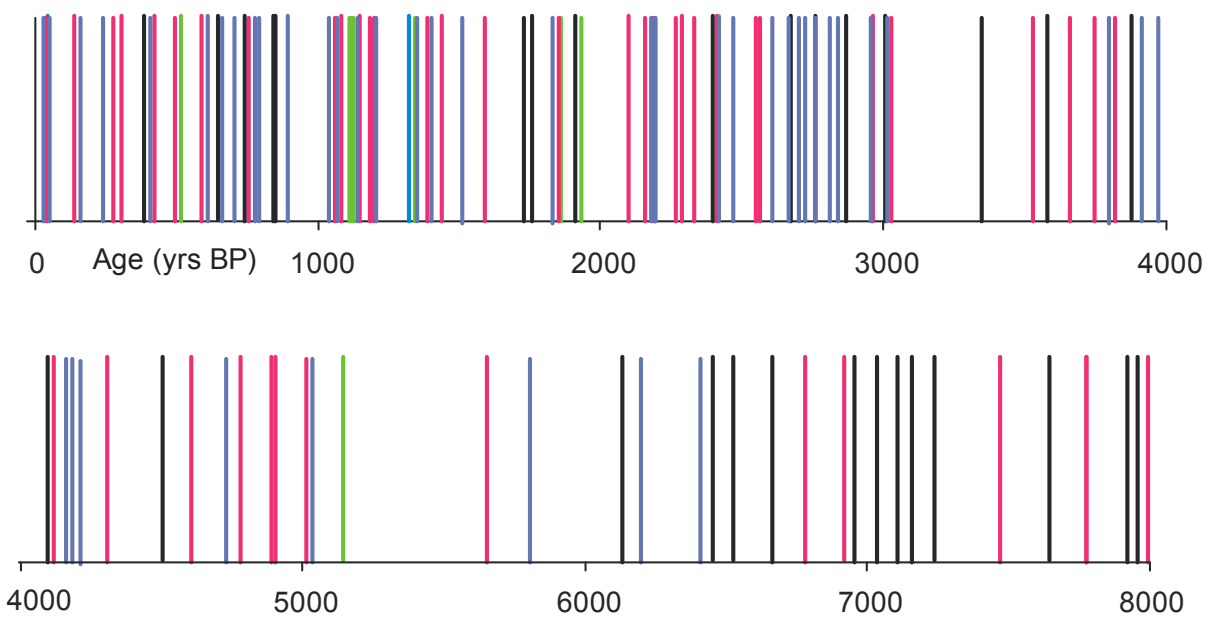

Figure 26. Tephra layer frequency plot. Age in years BP along y-axis. Pink line represents Katla eruption, purple line represents Hekla eruption, green line represents Veiðivötn eruption and light blue line represents a WVZ eruption.

layers on several occasions.

Hvítarvàtn

There are 7 cores from Hvítarvàtn so the differences in the presence and absence of tephra layers within one lake can be examined in detail (Table 6). In most cases when a layer cannot be verified in other cores it is because the layer is too thin (eg. Layer 2 in 2B), the core is disturbed in that area (eg. Layer 2. in 1A), the layers are not distinct enough (eg. Layer 6 in 3A) or it is a section where the core was not retrieved (eg. Layer 10 in 1A). This emphasises the value of multiple core sites from a lake. If only one core was examined the number of tephra layers visibly identified ranged from 72.5 – 87% of the total number of layers.

Combined Stratigraphy

There are 20 layers in the historical section of the combined stratigraphy with a known source. Of these 14 are from Hekla, 12 from Katla and 4 from Veiðivötn. 71% of the Hekla layers are not present in VGHV and HST, 25% of the Katla layers and 75% of the Veiðivötn layers. 12% of the Hekla layers are not present in Hvítarvàtn,

as are 42% of the Katla layers. However none of the Veiðivötn layers are missing. These figures are not suprising given the location of lakes and volcanoes; Hvítarvàtn is closer to both Hekla and Veiðivötn. This shows that most tephra layers are not widely dispersed.

7. Discussion

7.1 Stratigraphy

An initial visual inspection of the cores is a very important aspect of the analysis and capable of extracting a great deal of information. However, a geochemical check of tephra identity is also necessary, as shown by the mis-identification of H5 in the Hestvàtn core. K1500, Settlement Layer and H3 are the only marker layers identified visually in all lakes. This emphasizes their importance throughout the area of South-Central Iceland in terms of tephra stratigraphy. More of the key Hekla layers are found in Hvítarvàtn probably due to its proximity to Hekla in comparison to the other two lakes. A higher proportion of layers from Vestra Gìsholtsvàtn are mafic (95%) compared to Hestvàtn (91%) and Hvítarvàtn (83%). This can lead to initial conclusions that Katla was a more important source volcano for Vestra Gìsholtsvàtn and Hestvàtn as Katla is known to produce more mafic tephra layers.
All lakes show an increase in sedimentation rate after the Settlement Layer is deposited. The average sedimentation rate in Hvítarvàtn is a lot higher than in Hestvàtn and Vestra Gìsholtsvàtn. This is probably due to the environment around Hvítarvàtn being very erodible due to a lack of vegetation because of its altitude and position, therefore producing a large amount of potential deposit material. See Section 7.3 (Sediment Accumulation Rate) for further discussion.

7.2 Geochemistry

7.2.1 Identification of Source Volcano for each tephra layer

It was found that this step by step scheme produced better results than the commonly used FeO-TiO_2 plots as it was possible to identify nearly twice as many layers. FeO-TiO_2 plots discriminate well between a few of the main tephra producing volcanoes (Katla, Veiðivötn and Grímsvötn), but are not capable of distinguishing between all of the potential volcanoes, potentially leading to errors. The main problem are the Hekla layers as the plot does not effectively discriminate them from the compositional fields defined by the other volcanic systems. Additional problems in these cores were the presence of some WVZ layers which the FeO-TiO_2 plot would not differentiate from Veiðivötn.

This method is only as good as the database upon which it is based. Not all the data we used was EPMA data as for some volcanoes there is not available published

EPMA data (e.g. Vestmannæyjar data fromJakobsson, 1968). In adddition some data (e.g. RVZ data from Jakobsson et al. 1978) is not from glass, but from lavas, as glass data does not exist for these volcanoes. The use of solely aphyric lavas has helped to ensure that the lava composition is the nearest to melt composition that is available.Therefore there is potential for significant improvement within the database and the on-going collection of more geochemical data from known sources will improve and provide a more robust database. Once that is achieved this method then needs checking and re-evaluating.

Additionally there are still areas on the plots used where the result can be ambiguous for certain volcanoes at certain chemistries, for example figure 27. Here Veiðivötn, Katla and Öræfajökull rhyolitic tephras are plotted using SiO_2 and FeO/K_2O. The Katla field overlaps the Veiðivötn field and the Öræfajökull field in places. Usually data points will cover a range of values which can help distinction. However, if data points only plotted in these areas of overlap it would be impossible to distinguish between the volcanoes. This is one of the advantages of this method as several plots are produced for each rock type, increasing the chances of one of the plots being more discriminatory. Additionally the tephra layer may contain basaltic grains or andesitic grains which can either positively identify one of these volcanoes or at least rule out a volcano. Inevitably there are some tephra layers which it is not possible to identify robustly.

Petrological Processes

The distinction between the volcanoes, noticeable from the plots outlined in the method (figure 14), can offer insight into the petrological processes and magma evolution trends in Iceland.

The apparent bimodality of the basaltic end of the Alkali-Silica plot is an artefact of there being far more Hekla and Katla data than from any other of the basaltic tephra producing eruptions. At the evolved side of the plot once the melts reach the residua system of quartz and nepheline, there appears to be a trend towards more alkali rich rhyolites from Snæfellsjökull, Törfajökulll and Eyafjallajökull.

Figure 28 (which is the same plot as plot 1 from figure 14 showing the methodology) of K_2O and TiO_2 and Hekla, Katla, Snæfellsjökull and Vestmannæyjar shows two

Figure 27. This is the same as plot 22 from figure 14 showing the methodology. Veiðivötn, Katla and Öræfajökull rhyolitic tephras are plotted using SiO_2 and FeO/K_2O. The Katla field overlaps the Veiðivötn field and the Öræfajökull field in places. If data points only plot in the areas of overlap, emphasized by the red circles, it would be impossible to distinguish between the volcanoes.

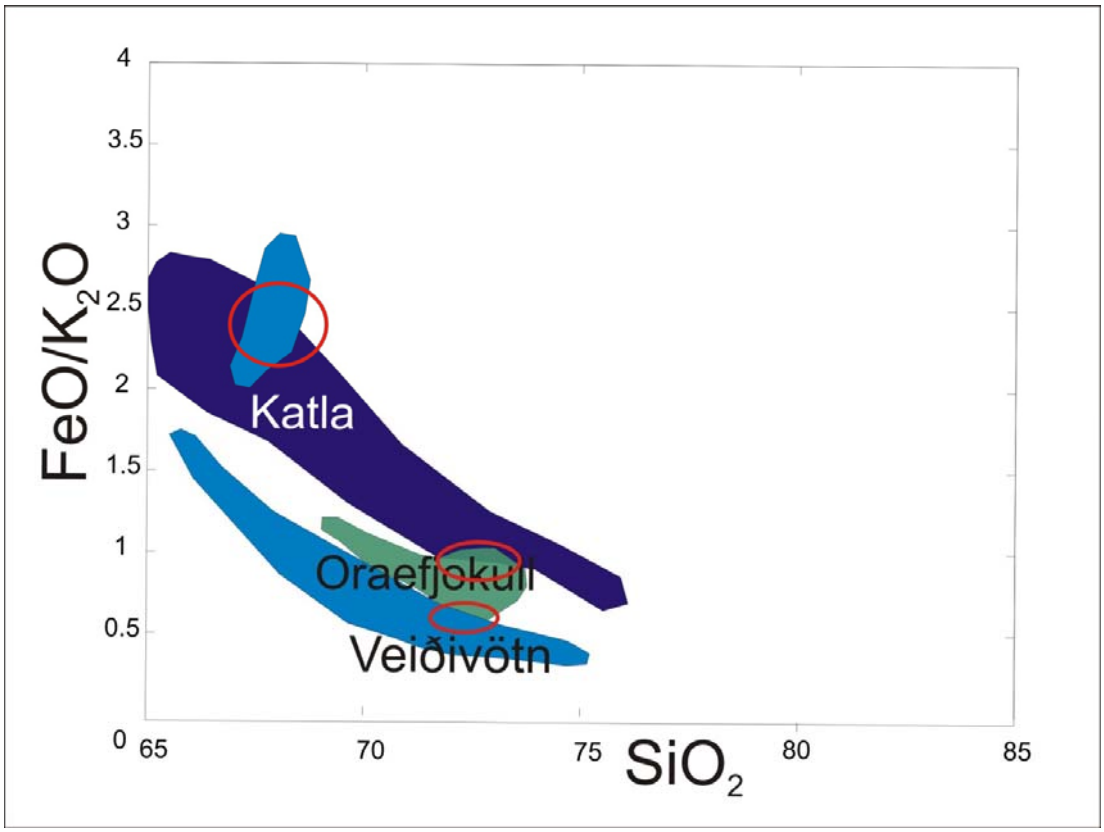

distinct trends. Hekla and Katla have a steeper trend of increasing K_2O with increasing TiO_2, with TiO_2 levelling off at about 4.5 wt%. The increase in K_2O and TiO_2 shows olivine and plagioclase crystallisation as both minerals contain little of these elements. The levelling off of TiO_2 shows the point at which magnetite is starting to crystalise. The Snæfellsjökull and Vestmannæyjar trend is shallower with TiO_2 levelling at about 2.5 wt%. This implies that pyroxene is being crystallised during the evolution of the Snæfellsjökulls and Vestmannæyjar magmas as this contains TiO_2, therefore reducing the increase in TiO_2. In addition the Snæfellsjökull/Vestmannæyjar magmas start at higher K_2O than the Katla/Hekla magmas. The higher incompatible content implies a smaller melt fraction producing the Snæfellsjökull/Vestmannæyjar magmas.

Figure 28. (which is the same plot as plot 1 from figure 14 showing the methodology) of K_2O and TiO_2 and Hekla, Katla, Snæfellsjökull and Vestmannæyjar shows two distinct trends. Hekla and Katla have a steeper trend of increasing K_2O with increasing TiO_2, with TiO_2 levelling off at about 4.5 wt%. The Snæfellsjökull and Vestmannæyjar trend is shallower with TiO_2 levelling at about 2.5 wt%. In addition the Snæfellsjökull/Vestmannæyjar magmas start at higher K_2O than the Katla/Hekla magmas. K_2O and TIO_2 plot of basaltic alkaline magmas from Hekla, Katla, Vestmannæyjar and Snæfellsjökull.

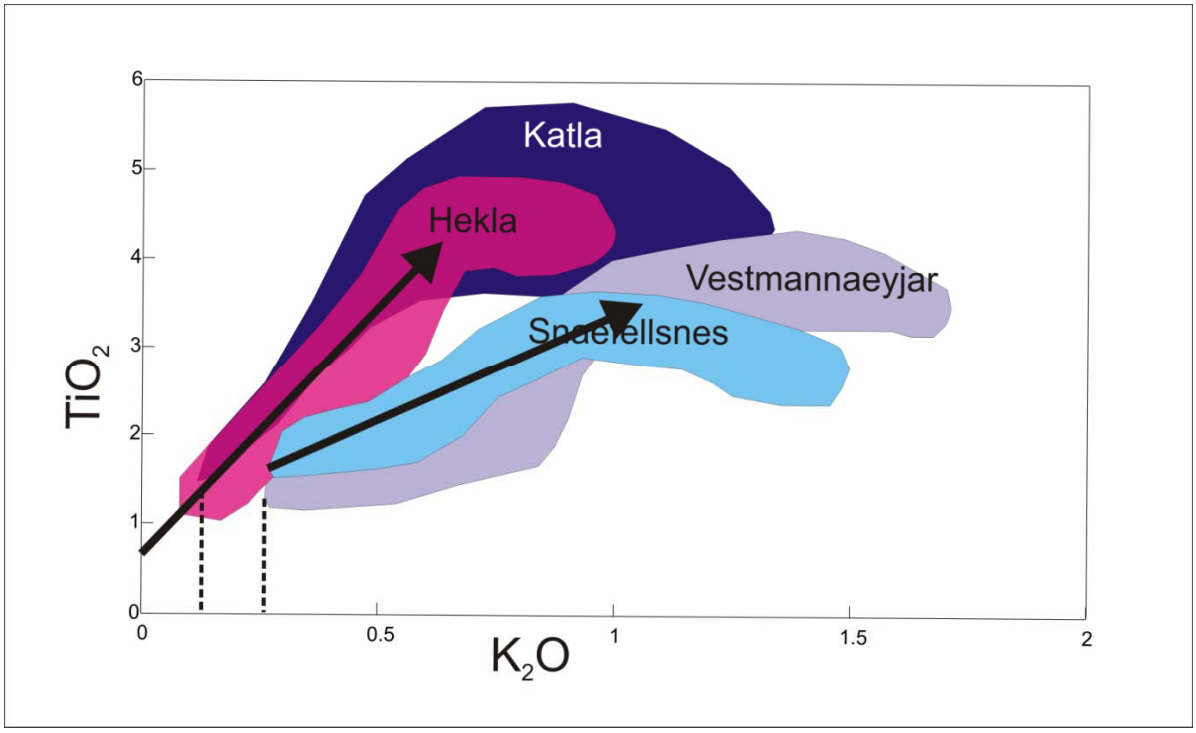

Plot 5 from figure 14 shows FeO/Na_2O and Na_2O/K_2O for Snæfellsjökull and Vestmannæyjar. As Snæfellsjökull has a lower Na_2O/K_2O range this indicates higher K_2O which would imply a smaller melt fraction as K_2O is highly incompatible.æ

Plot 6 from figure 14 shows Al_2O_3 and SiO_2/CaO and Veiðivötn, Grimsvötn, Askja, Krafla, RVZ and WVZ. RVZ is a continuation of the WVZ and therefore not suprising that it has similar composition. The smaller range of values may be solely as a result of the smaller number of volcanoes within it. The difference in Al_2O_3 between the RVZ and WVZ, and the rest of the volcanoes might imply a slightly different magma source.

Plot 11 from figure 14 shows SiO_2 and MgO/CaO and Askja and Veiðivötn. Askja has higher SiO_2 indicating its subalkaline magmas are slightly more evolved than those of Veiðivötn. Askja also has a higher range of MgO/CaO perhaps indicating variations in the amount of plagioclase crystallising.

Plots 11 and 12 from figure 14 indicate various ideas about the andesitic magmas from Askja, Veiðivötn, Katla, Hekla and Öræfajökull. FeO and MgO (plot 11) shows that fractional crystalliation may be occurring as the Veiðivötn magmas evolve with the wide range of values and fan shaped field of geochemistry. As K_2O is more incompatible than P_2O_5, a higher value of K_2O/P_2O_5 at the origin of the evolution trend indicates a smaller melt fraction. Therefore, from plot 12 of SiO_2/MgO and K_2O/P_2O_5 ,Veiðivötn has the smaller melt fraction, followed by Katla with a slightly larger melt fraction and Hekla with the largest melt fraction.

Plot 19 from figure 14 of SiO_2 and TiO_2 for Hekla, Katla, Veiðivötn, Öræfajökull, Askja and Krafla shows two distinct melt evolution trends. That of Askja and Krafla has higher TiO_2 for the equivalent SiO_2 than for the other volcanoes indicating that the NVZ containing Askja and Krafla is either richer in TiO_2 initially or magnetite ± pyroxene which limit TiO_2 in the melt are crystallising less than in the other volcanoes of the EVZ and Öræfajökull.

7.2.2 Correlation of Layers and Tephrostratigraphy

Vestra Gìsholtsvàtnand Hestvàtn

All source volcanoes are from the EVZ which is consistent with the high eruption frequency in the EVZ in recent times (e.g. Thordarson and Larsen, 2007). The record does not contain tephra layers from the West Volcanic Zone despite its proximity to the study area, emphasising that the presence of ice caps on volcanoes is important for producing sufficiently explosive basaltic eruptions for widespread tephra fallout. Tephra layers from Grimsvötn are also not seen in the record despite historical records showing 74 explosive or partly explosive eruptions from Grimsvötn. All but the 1783-84 Laki eruption took place underneath the ice-cap and it is suggested that only a fraction of the tephra is dispersed sub-aerially due to the thickness of the ice and so presumably the eruptions were not big enough to disperse tephra as far as VGHV and HST. The Laki eruption had main dispersal directions to the SW (11June and 7 September) and SE (all other eruptions) and

would probably not have gone over the lakes (Thordarson and Larsen, 2007) Grimsvötn eruptions are known to be wet which also limits dispersal area of the tephra due to premature deposition caused by flocculation of grains.
The high occurrence of basaltic tephra layers reflects the common occurrence of these subglacial phreatomagmatic eruptions in Iceland. In terms of hazard predictions, or more likely the environmental impact, the record shows that Katla is the volcano most likely to directly affect this area of Iceland.

Hvítarvàtn

Although the EVZ dominates the tephra record as in VGHV and HST, there are 2 layers from the WVZ. These are probably explained by Hvítarvàtn being closer to the WVZ and so smaller eruptions are more likely to be recorded than in VGHV and HST. Again tephra layers from Grimsvötn are not seen for the same reasons as VGHV and HST. The change from Katla being dominant in VGHV and HST to Hekla being dominant in HVT is also probably a product of their relative distances from volcano to lake. The change to a greater proportion of mixed layers is likely to be a result of the increased contribution from Hekla. In terms of hazard predictions the record shows that Hekla is the volcano most likely to directly affect this area of Iceland.

Combined Stratigraphy for South-West Iceland

Hekla and Katla are responsible for ~45% of the tephra layers each and so are equally important in terms of tephra production in this area. Veiðivötn and the WVZ produce occasional tephra layers in this region.

7.2.3 Identification of individual eruptions

It is challenging to distinguish between different eruptions from the same volcano with major element geochemistry. However, if records of major element geochemistry are produced for each tephra layer it appears that it is possible to correlate between different records based on the patterns seen in a set of tephra layers. This is not a particularly exact method but it is a first step in providing a more accurate framework of tephra layers and ages for other workers to use.

7.2.4 Trace element content of tephras

Cr_2O_3, NiO and SrO are not helpful in distinguishing between Katla and Hekla. As it is possible to distinguish between the other volcanoes that we have identified here with little problem (Katla and Hekla versus Veiðivötn or WVZ) it is not necessary to measure these elements for discrimination purposes for these four volcanoes.

7.2.5 Volatile content of tephras

As a general rule the solubility of sulphur increases with increasing iron concentration, due to it being a function of iron content, oxygen and sulphur fugacities (eg. Mathez 1976, Wallace and Carmichael, 1992). Therefore, Fe-Ti basalts (Katla and Hekla compositions) are characterised by high sulphur concentrations at depth and commonly Katla magmas contain about 2000-2500 ppm of dissolved sulphur prior to eruption (Thordarson et al. 2003).

Previous studies (Thordarson et al. 1996, 2001, 2003, Óladóttir et. al., 2005) reveal distinct differences between magmatic and phreatomagmatic concentrations of sulphur. Magmatic tephra typically contain 300-600ppm S, which is consistent with the expected sulphur solubility at one atmosphere pressure in basalts, indicating extrememly efficient degassing of the magma upon eruption. Phreatomagmatic tephras (even from the same eruption as the magmatic tephra) contain on average significantly more S, ranging from 550-1780ppm (Thordarson et al. 1996, 2001). The TiO_2/FeO versus S graph of Thordarson et al. (2003) can be used to evaluate a magmatic or phreatomagmatic origin of tephras (Figure 29). The lines A, B and C are best fit regressions through data (from Metrich et al. 1991, Thordarson et al., 1996, 2001, 2003) for melt inclusions, magmatic tephra and crystalline lava respectively for the Veiðivötn, Grimsvötn and Katla systems. These lines show typical values of S for undegassed magma (A), fully degassed magma (B) and crystalline lava (C).

Taking the highest value for Katla magmatic data as the upper sulphur value for magmatic eruptions (Thordarson et al. 2003), it is possible to distinguish between phreatomagmatic eruptions and magmatic eruptions (Figure 30). The same value was used for Hekla compositions as Hekla has very similar compositions to Katla and data is not available for Hekla. This means that the results are not of such reliable quality. Veiðivötn data was taken from Thordarson et al. (2003b). Most Hekla eruptions appear to be magmatic. Some have a phreatomagmatic component (Figure 30). Katla eruptions from 11 layers (9 (K1721), 26, 27, 28, 30, 39, 42, 43, 63,

64, 65) are phreatomagmatic, 5 layers (2 (K1955), 5, 6 (K1860), 12 (K1416), 35) are magmatic and 4 layers (10 (K1500), 20 (E934), 62 and 69) have sulphur concentrations of both magmatic and phreatomagmatic affinities. The Eldgja data fits with that of Óladóttir et al. (2005) who found also found a wide range of sulphur values for this tephra layer. They attributed this to variable degrees of degassing in measured grains as opposed to differences in the amount of degassing in different eruptions. Veiðivötn eruptions are mostly phreatomagmatic.

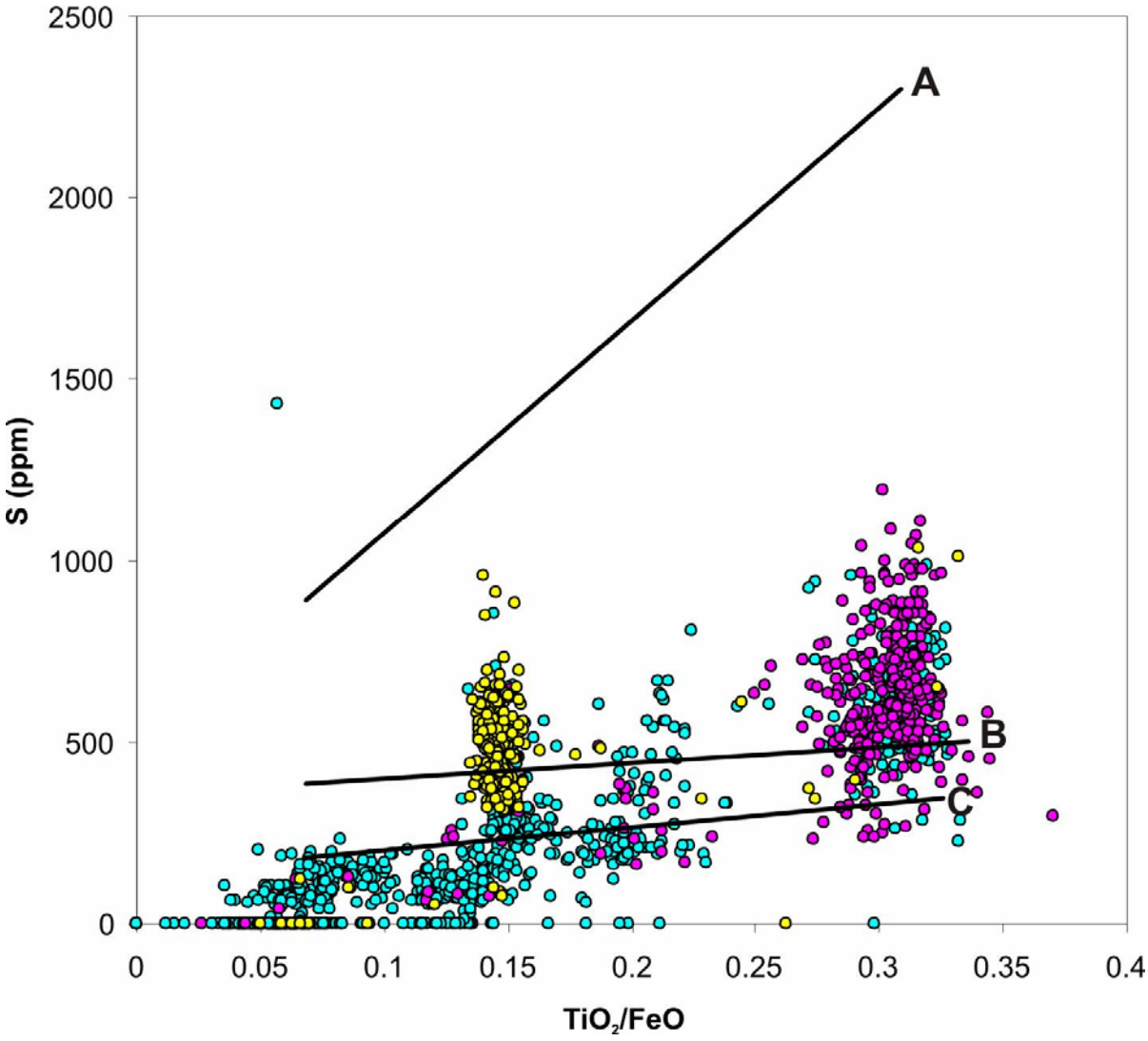

Figure 29. Graph of S versus TiO2/FeO to evaluate sulphur degassing in basaltic eruptions within the EVZ (after Thordarson et al. 2003b). Best fit regression lines for (A) inclusions, (B) magmatic tephra, and (C) crystalline lava have been calculated from samples from Grimsvötn, Veiðivötn and Katla. Data from this study is plotted as coloured circles, Hekla is turquoise, Katla is pink and Veiðivötn is yellow.

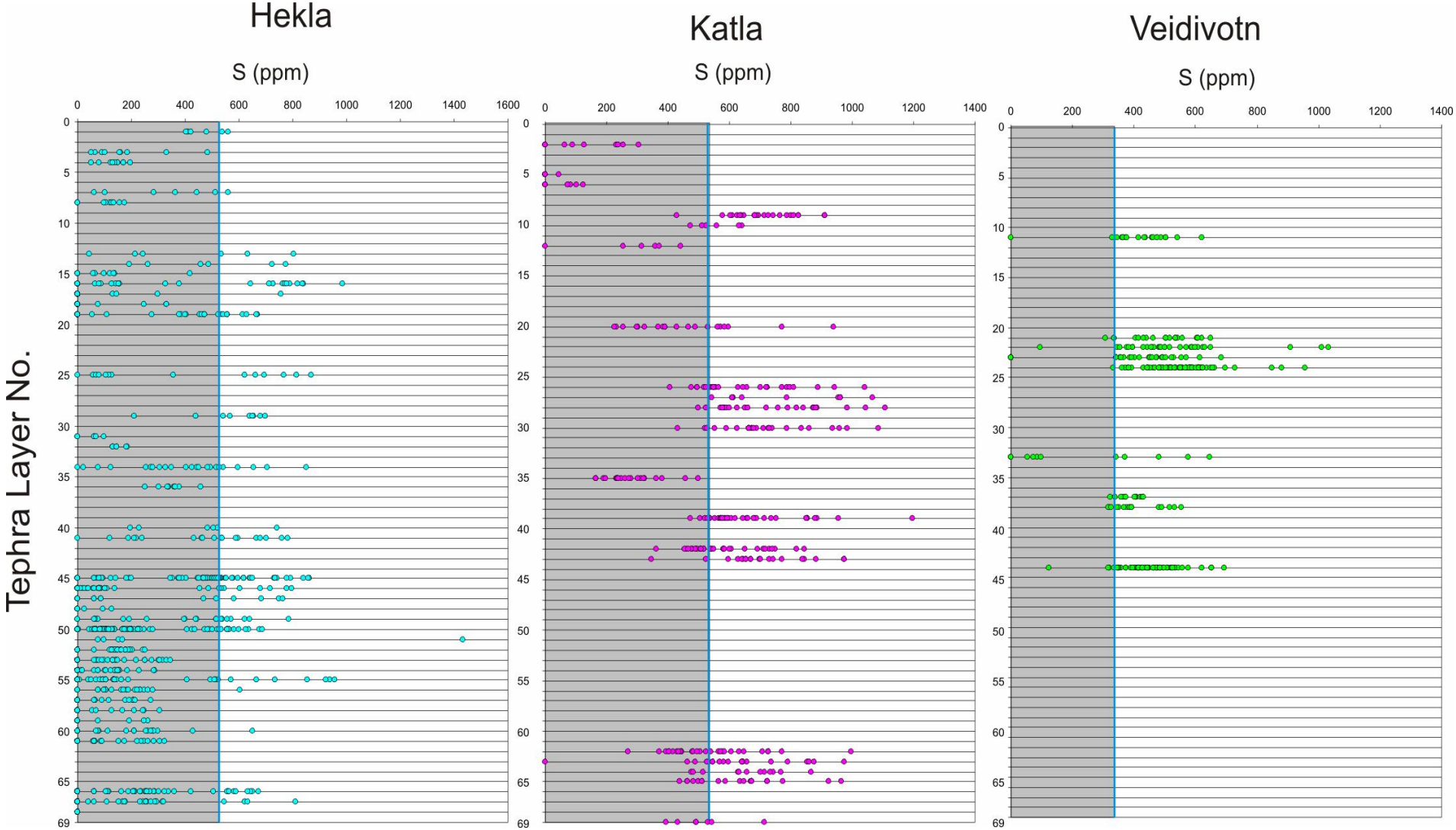
Hekla
S (ppm)
0 200 400 600 800 1000 1200 1400 1600
Katla
S (ppm)
0 200 400 600 800 1000 1200 1400
Veidivotn
S (ppm)
0 200 400 600 800 1000 1200 1400
Tephra Layer No.
0 5 10 15 20 25 30 35 40 45 50 55 60 65 69

Figure 30 (previous page). Sulphur concentration plotted with tephra layer number. The grey shaded area represents sulphur values of magmatic eruptions. The unshaded area represents phreatomagmatic eruptions.

There are layers of both magmatic and phreatomagmatic origin from Katla and the sulphur values to constrain the split between these are the most accurate. Therefore it is possible to examine the F and Cl data with respect to the type of eruption. In general F is higher in the magmatic layers than the phreatomagmatic. This could be the result of the high solubility of F in the magma meaning degassing is unlikely during eruption. However F is very soluble in water and so the presence of water during the phreatomagmatic eruption could remove some F, producing lower totals. Cl has a wider range of values (>800ppm difference) in the magmatic layers than the phreatomagmatic (~200ppm difference).This is opposite to that found by Thordarson et al. (1996) who found that the phreatomagmatic layers had a wider range than the magmatic layers.

7.3 Sediment Accumulation Rate

Many studies have noticed the increase in sedimentation rates after Settlement in lakes throughout Iceland (e.g.Thorarinsson, 1961, Hardardóttir, 2004, Dugmore and Erskine, 1994). This is generally attributed to higher soil erosion rates through the introduction of animal grazing and deforestation by the earliest settlers of Iceland. However Geirsdóttir et al. (2009) suggest that this increased erosion occurred due to a general reduction in summer solar radiation which cooled climate and caused landscape deterioration prior to human arrival by several centuries. This suggests that the dates for the tephra layers we identified for 2-300years prior to Settlement could have younger ages than those that have been assigned due to the assumption that SAR was constant between Settlement and KE. The increase in sediment accumulation after H4 could be due to increased erosion rates related to colder climates and increased precipitation. It could also be partially explained by reworking and deposition of the extra tephra into the lake which lasted for over 60 years after the eruption, and also increased erosion rates due to presence of large quantities of loose tephra (Hardardóttir et al. 2001).

Throughout the historical period there has been an increase in sediment accumulation. In particular, in Hvítarvàtn, there has been a great increase from K1721 onwards. The presence of Ice-Rafted Debris (IRD) within the cores indicates that sedimentation has been increased in this way and therefore there is the

possibility that tephra layers above K1721 have been redeposited after being deposited on the glaciers. However as all have been deposited in more than one core this does not seem likely, and the effect of the IRD is probably just to increase sediment accumulation rate.
The SAR models are shown to be useful in allowing an approximate check of new C^{14} dates as shown in the example from Vestra Gìsholtsvàtn.

7.4 Identification of historic tephra layers

Comparing identification of historical eruptions with the dates given by the SAR method gives a measure of its accuracy. Unsurprisingly there is no consistent offset and ages vary between 0 and 55 years different for Vestra Gìsholtsvàtn and Hestvàtn, which is to be expected as the SAR method assumed a constant rate for 1130 years, which is not realistic. The eruption ages tend to be older than the ages derived from the SAR method by on average 14 years, implying that SAR was over-estimated for this period in time. The SAR model could now be improved by using the dates of the known historical eruptions.
The ages from Hvítarvàtn have an additional age control. Darren Larsen has counted varves throughout the cores for a Masters Thesis for the last 2300years using the following tephra layers as age controls: K1721, H1766, H1300, H1104, Settlement. Age differences from the varve age to the actual age range between 0 and 96 years and again are not consistent. However if core 2B is ignored, then age differences are not greater than 30 years with an average deviation of 4 years. Presumably something went wrong with the varve counting in core 2B or there were some rythmites (layered sediments that did not represent a year's accumulation but usually represent much shorter periods) present leading to too many 'years' being counted. This core aside, the use of varve counting does improve the age record providing there are multiple checks on age from known tephra layers.
The main problems were with the first five layers in the combined stratigraphy. There was not rigorous enough age control to establish which eruption the tephra layers came from apart from Layer 4 (H1947). Two layers were of mixed chemistry and probably reworked. An in-depth look at the varves in cores where they appear to be counting the years accurately could improve estimates on whether H1980 or H1970 was present as Layer 1. It is difficult to know how to name Layer 2.

7.5 Frequency of Tephra Fall

Assessment of how well the record of this study represents the actual eruption frequency at an individual volcano can be conducted by comparing the number of Katla layers in this chronology to that observed in proximal sections near the volcano. Studies by Larsen (2000), Larsen et al. (2001), and Óladóttir et al. (2005), indicate that the average eruption frequency at Katla during the Holocene was as high as 40 events per 1000 years. Jóhannsdóttir (2007) found an average of 5 eruptions per 1000 years. VGHV and Hestvàtn have an average number of 2.2 Katla layers per 1000 years. This implies that only 5% of Holocene eruptions at Katla dispersed tephra this far over West Iceland, although this figure may be slightly higher due to not all the tephra layers being analyzed. From the combined stratigraphy of all three lakes there are 5.9 Katla layers per 1000 years implying that 15% of Katla layers cover the area to the W and N of Katla. Peaks in frequency of tephra fall are in agreement in age with that of Óladóttir et al. (2005) who studied Katla tephra layers in soil sections from the East of Katla.

7.6 Presence of Tephra Layers in Lakes

Vestra Gìsholtsvàtn and Hestvàtn

There are 16 more layers present at the bottom of the Hestvàtn core than the Vestra Gìsholtsvàtn core extending it for another ~1600yrs. Before 6000BP, the core from Hestvàtn commonly does not include Katla layers recorded in the Vestra Gìsholtsvàtn core whereas after 6000BP Katla layers are missing from the Vestra Gìsholtsvàtn core. This could imply a slight northward shift in general wind direction from the earlier period to that after 6000BP. Vestra Gìsholtsvàtn preserved all the Hekla layers found in the combined stratigraphy but did not include all the Veiðivötn-Bárðarbunga layers whereas Hestvàtn contained all the Veiðivötn-Bárðarbunga but did not include the Hekla layers on several occasions. Mt. Hestfjall is situated directly between Hekla and Hestvàtn and so could have affected the local winds and created a sheltered area behind the hill over VGHV.

The differences in the presence and absence of tephra layers in the two cores are important in increasing our understanding about how tephra falls and is preserved and can be applied to stratigraphies where only one log has been available. Possible reasons for missing tephra layers are that the tephra layers were not deposited in one lake and deposited in another due to being on the edge of the

dispersal area or they were deposited in both areas and not preserved in one area due to either:

- A winter-time eruption may not be recorded in the lacustrine stratigraphy if the lake is covered by ice at the time and the tephra is blown away before it can be deposited into the lake. HST is more likely to be covered in ice as it is further inland.
- Erosion of layers is a possibility but this should be obvious in the form of erosion surfaces within the cores and was not noted during sampling.
- The tephra layers being present as cryptotephra in one core which was not identified in this analysis. This could only be established by further sampling of the cores on a micro-scale.

Considering the well-documented historical record of eruptions in Iceland (Thordarson and Larsen, 2007 and references therein) in more detail, layers 1, 3, 4, 5a, 5b and 9 were missing from HST and layer 6a and 6b from VGHV. Layer 1 was produced by H1970 or H1980, which erupted in May and August respectively, and so ice on HST and not on VGHV is not likely to have been a factor in the none-deposition. In VGHV was 0.5cm thick so it seems unlikely that it would have thinned enough to be not visible in HST only 10km away. The eruption of H1693 (layer 3) had its main tephra fall on 13th February, and H1597 (layer 4) erupted on January 3rd (Thorarinsson, 1947). Therefore ice cover on Hestvàtn could have stopped deposition within HST for both layers 3 and 4. Layers 5a (K1500) and 5b (K1357) are both very thin (0.1cm) so it is conceivable that they were not visible in HST as it is further away from Katla than VGHV. There are no seasonal dates of eruptions from K1500 and older due to poorer written records. Layers 6a and 6b are deposited in HST but not VGHV. These have been attributed to the H1158 eruption which had a small volume of tephra (Thorarinsson, 1947) and therefore it is not surprising that the tephra is not found in VGHV which is further away. Layer 9 (K920) was found in VGHV and not HST. As it was a large eruption it is most likely that HST was slightly too far N of the dispersal direction.

We can also assess how well the lakes capture tephra by using the historical record. Fourteen layers might have been expected to have fallen in the study area (Table 8a). Of these 50% (7) are missing. The only one that is particularly surprising not to see is K1823. The other eruptions have dispersal directions that are not directly

overhead so tephra from a smaller eruption would not reach the lakes. It is not likely that ice on the lake was a cause of non-deposition of K1823 as it erupted on 26th June (Thordarson and Larsen, 2007). This implies that the lake is preserving as good a record as a soil section as presumably these tephras would appear in a soil section. To verify this reliably a study would need to be made of several proximal soil sections.

There are also an extra six layers deposited which would not necessarily be expected to be deposited here according to their dispersal direction (Table 8b). One of these does not have any recorded dispersal direction (K1245) and so they could very easily have dispersed to the W. The rest of the layers obviously had some dispersal of ash that was not in the main direction of dispersal, suggesting a change of wind direction throughout the eruption.

Hvítarvàtn

There are two cases where the tephra layer is not present in the core. Layer 18 is not present in core 3A. Layer 31 is not present in cores 3A and 3B. The possible explanations for not finding the tephra have been discussed above. As with VGHV and HST, in the locations concerned, erosion does not seem to have occurred. The most likely explanation is that the layers are present as cryptotephra that we did not find during analysis. For layer 31 there is the possibility, as it was not deposited in both cores in the immediate area (3A and 3B), that for some reason no tephra fell in that location or that it was blown away before having time to settle into the water column. For layer 18 this could also have happened solely for core 3A, especially as the tephra layer is composed of lighter silicic grains. The thickness of the layer ranges from 0.2 – 1.6cm in the other cores, with 3B containing 1.6cm and being the most proximal core it seems unlikely that 3A would only have received a very thin cryptotephra layer. However there are no signs of erosion and so non-deposition probably occurred.

Table 8a. Expected tephra layers in lakes Hestvàtn and Vestra Gìsholtsvàtn considering dispersal directions recorded in Larsen (2000) and Larsen et al. (2001).

Volcano	Age (years AD)	Dispersal Direction	Present
Hekla	1970	NW	No
Katla	1823	SSW	No
Hekla	1766	NNW	No
Katla	1721	NW	Yes
Hekla	1693	NW	Yes
Katla	1580	SW	Yes
Hekla	1510	SW	No
Katla	~1500	SW	No
Katla	1500	W	Yes
Katla	1440	NW	No
Hekla	1104	NNW	Yes
Katla	934	NNW+SE	No
Katla	920	WNW	Yes
Veiđivötn	870	Silicic – NW Basaltic –all directions	Yes

Table 8b. Eruptions not expected to be seen in Hestvàtn and Vestra Gìsholtsvàtn, considering dispersal directions recorded in Larsen (2000) and Larsen et al. (2001), but which were present.

Volcano	Age (years AD)	Dispersal Direction
Katla	K1625	NE
Hekla	1597	SE
Katla	1357	S
Katla	1262	NE
Katla	1245	?
Hekla	1158	NE

Table 9a. Expected tephra layers in Hvítarvàtn considering dispersal directions recorded in Larsen (2000) and Larsen et al. (2001).

Volcano	Age	Dispersal direction	Present
Hekla	2000	NNE	no
Hekla	1991	NNE	no
Hekla	1980	NNE	yes
Hekla	1970	NW	yes
Katla	1918	NE	no
Hekla	1766	NNW	yes
Katla	1721	NW	yes
Hekla	1693	NW	no
Hekla	1636	NE	no
Katla	1625	NE	no
Katla	1612	NE	no
Katla	1440	NW	no
Hekla	1300	N	yes
Katla	1262	NE	no
Hekla	1222	NE	yes
Hekla	1158	NE	no
Hekla	1104	NNW	yes
Katla	934	NW+SE	yes
Katla	920	WNW	yes

Table 9b. Eruptions not expected to be seen in but which were present considering dispersal directions recorded in Larsen (2000) and Larsen et al. (2001).

Volcano	Age (years AD)	Dispersal Direction
Hekla	1947	S
Katla	1860	S
Hekla	1845	ESE
Katla	1500	SW
Veiðivötn	1477	?
Katla	1416	E
Hekla	1389	SE
Hekla	1341	SSE
Hekla	1206	ESE
Katla	960	?
Veiðivötn	880	?
Veiðivötn	870	?

Nineteen layers might have been expected to have fallen in the Hvítarvàtn area (Table 9a). Of these 52% (10) are missing. The only ones that are suprising are H1693 and K1440. The other eruptions have dispersal directions that are not directly overhead so tephra from a smaller eruption would not reach the lakes. The tephra from H1693 has been measured at Hvitarnes (~1km east of Hvítarvàtn) as 0.5cm (Thorarinsson, 1947) and so should be deposited within the lake. However the eruption started on 13th February and due to Hvítarvàtn being in the highlands it was most likely frozen at the time. No date is known for the K1440 eruption (Thordarson and Larsen, 2007) but it was a small eruption and so might not have traveled far enough to be deposited in Hvitartvàtn. As with VGHV and HST this indicates that, on the whole, lakes are good for preserving tephra.

There are also an extra twelve layers deposited which would not necessarily be expected to be deposited here according to their dispersal direction (Table 9b). Four of these do not have any recorded dispersal direction (V1477, K960, V880, V870) and so they could very easily have dispersed to the W. The rest of the layers obviously had some dispersal of ash not in the main direction suggesting change of wind direction throughout the eruption.

Combined Stratigraphy

There are seven layers that have known source that were deposited in VGHV and HST but not in Hvítarvàtn. Of these H1597, K1580, K1245 are not suprising as the dispersal direction is either unknown or to the SW ie. not over Hvítarvàtn. However K1625, K1262 and H1158 all dispersed to the NE which is nearer to Hvítarvàtn than the other two lakes. Both of the Katla eruptions are described as large (Thordarson and Larsen, 2007) but perhaps not large enough to reach Hvítarvàtn which is further away. K1625 erupted on 3 September and so ice on Hvítarvàtn is unlikely to have been a cause of non-deposition but could have been for K1262 as the date is unknown. H1158 had a small volume of tephra and so might not have reached Hvítarvàtn. Thorarinsson (1947) concluded it was likely that it started on 19th January and so ice would have been present on Hvítarvàtn.

There are fourteen layers of known source that were deposited in Hvítarvàtn and not VGHV or Hestvàtn. All of these layers have dispersal directions that would not go over VGHV and HST.

8. Conclusions

This work, together with that of Jóhannsdóttir (2007), provides a unique tephrochronological record for Central South Iceland, because it constitutes a continuous chronology spanning the last 12ka at the resolution of decades to centuries.

1. A step by step identification scheme for source volcano from tephra data is not time consuming and discriminates between all major Icelandic volcanoes.
2. Few tephra layers from the Western Volcanic Zone are present in the record despite its proximity to the study area. This emphasises the importance of ice caps on volcanoes for producing sufficiently explosive basaltic eruptions to generate widespread tephra fallout.
3. Lack of Grímsvötn tephra layers suggests that the eruptions generally are not big enough or too wet to produce tephra layers extending this far west.
4. It is not possible to accurately distinguish different tephra layers from the same volcano using solely major element analysis. However sequences of layers from the same volcano may be recognised and distinguished within themselves.
5. 47.5% of the tephra layers from this study are basaltic, and another 41% contain a basaltic component, highlighting the importance of basaltic tephra layers in the tephrostratigraphy and their usefulness for correlation of records.
6. Cr_2O_3, NiO, SrO, SO_2, F, Cl, are not helpful in discriminating between Katla and Hekla tephra layers.
7. Most Hekla eruptions are magmatic though with a phreatomagmatic component. Veiðivötn eruptions are mostly phreatomagmatic ~50% of Katla eruptions are phreatomagmatic, 25% are magmatic and 25% are mixed.
8. Katla is the most hazardous volcano for south-western Iceland, in terms of tephra fall, even though only 5% of its eruptions have produced tephra that reaches this location.

9. The SAR method gives a reasonable age for eruptions that have not been dated by another method as during the historical period error is on average 14 years. The addition of varve counting improves ages to an average error of 4 years instead of 14 years.
10. Frequency of tephra fall is highly variable in the area, it averages at 8.4layers/500yrs.
11. The presence of tephra layers is dependent on multiple different factors which emphasizes the importance of using multiple records to get a complete stratigraphy. Lake cores appear to capture tephra layers as well as soil sections and have the advantages of larger continuous records and easier application of the tephra stratigrapy in environmental and paleoclimate studies.

Future work would be best concentrated on improving the database of known tephra layers to then check the validity of the source volcano identification scheme which is the most useful aspect of this work. Another important direction for work would be the production of a consistent methodology for the tephra community to use to establish whether the tephra was primary or reworked. The quantification of some of the parameters here would be a good starting point.

9. Acknowledgements

I would like to thank my supervisors Thorvaldur Thordarson, Godfrey Fitton and Aslaug Geirdóttir for their input to the project. Chris Hayward was helpful in setting up the analysis for the EPMA, and Mike Hall prepared a huge number of samples ready for EPMA analysis. Anthony Newton gave me a lot of invaluable assistance and support. I would also like to thank Richard Phillips and Patience Cowie for their encouragement. Amy Myrbo, Anders Noren and Kristina Brady were welcoming and easy to work with at LacCore. RANNIS funded the studentship that made this project feasible. Malcolm McMillan very nicely sorted out all the problems with the thesis work, especially my computer ones.

10. References

Axford Y., Miller G., Geirsdóttir A., Langdon P., 2005, Holocene temperature history of northern Iceland inferred from subfossil midges, Quaternary Science Reviews, 26, 3344-3358.

Bard E., Arnold M., Mangerud J., Paterne M., Labeyrie L., Duprat J., Mélières M-A., Sønstegaard E., Duplessy J-C., 1994, The North Atlantic atmosphere-sea surface ^{14}C gradient during the Younger Dryas climatic event, Earth and Planetary Science Letters, 126, 275-287

Bergman A., Wastegård S., Hammarlund D., Wohlfarth B., and Roberts S.J., 2004, Holocene tephra horizons at Klocka Bog, west-central Sweden: aspects of reproducibility in subarctic peat deposits, Journal of Quaternary Science, 19- 3, 241-249.

Birks H.H., Gulliksen S., Haflidason H., Mangerud J., Possnert G., 1996, New radiocarbon dates for the Vedde ash and the Saksunarvàtn ash from western Norway, Quaternary Research, 45, 119-127.

Björck J., and Wastegård S., 1999, Climate oscillations and tephrochronology in eastern middle Sweden during the last glacial–interglacial transition, Journal of Quaternary Science, 14, 399–410.

Björck S., Ingólfsson Ó., Haflidason H., Hallsdóttir M., Anderson N.J., 1992, Lake Torfadalsvàtn: a high resolution record of the North Atlantic ash zone I and the last glacial-interglacial environmental changes in Iceland, Boreas, 21,15-22.

Black J., Miller G., Geirsdóttir Á., Manley W.F., Björnsson H., 2004, Sediment thickness and Holocene erosion rates derived from a seismic survey of Hvítárvàtn, central Iceland, Jökull, 54, 37-56.

Bogaard van den B., Dorfler W., Sandgren P., Schmincke H.U., 1994, Correlating the Holocene records: Icelandic tephra found in Schleswig-Holstein (Northern Germany), Naturwissenschaften, 81, 554–556.

Bondevik S., Mangerud J., Gulliksen S., 2001, The marine 14C age of the Vedde Ash Bed along the west coast of Norway, Journal of Quaternary Science, 16, 3-7.

Boygle J., 1994, Tephra in lake sediments: an unambiguous geochronological marker?, PhD thesis, University of Edinburgh.

Boygle J., 1998, A little goes a long way: dicovery of a new midHolocene tephra in Sweden, Boreas, 27, 195–199.

Boygle J., 1999, Variability of tephra in lake and catchment sediments, Svínavàtn, Iceland, Global and Planetary Change, 21, 129–149.

Boygle, J., 2004, Towards a Holocene tephrochronology for Sweden: geochemistry and correlation with the North Atlantic tephrostratigraphy, Journal of Quaternary Science,19, 103-109.

Bradley R.S., 1999, Reconstructing Climates of the Quaternary, Paleoclimatology, 64.

Davies S.M., Wastegård S., Wohlfarth B., 2003, Extending the limits of the Borrobol Tephra to Scandinavia and detection of new early Holocene tephras, Quaternary Research, 59, 345–352.

Devine, J.D., Sigurdsson, H. and Davis, A.N., 1984, Estimates of sulfur and chlorine yield to the atmosphere from volcanic eruptions and potential climatic effects, Journal of Geophysical Research, 89, 6309–6325.

Dugmore A., 1989, Icelandic volcanic ash in Scotland, Scottish Geographical Magazine, 105, 168–172.

Dugmore A.J., and Newton A.J., 1998, Holocene tephra layers in the Færoe Islands, Frodskaparrit, 46, 191–204.

Dugmore A.J., Newton A.J., Sugden D.E., Larsen G., 1992, Geochemical stability of fine-grained silicic Holocene tephra in Iceland and Scotland, Journal of Quaternary Science, 7, 173–183.

Dugmore A.J., Larsen G., Newton A.J., 1995a, Seven tephra isochrones in Scotland, The Holocene, 5, 257–266.

Dugmore A.J., Cook G.T., Shore J.S., Newton A.J., Edwards K.J., Larsen G., 1995b, Radiocarbon dating tephra layers in Britain and Iceland, Proceedings of the 15th International 14C conference, edited by Cook G., Harkness D., Miller B.F., Scott E., Radiocarbon, 37-2, 379-388.

Dugmore A. J., Newton, A. J., Larsen, G. and Cook, G. T., 2000, Tephrochronology, environmental change and the Norse settlement of Iceland, Environmental Archaeology, 5, 21-34.

Dugmore A.J., Church, M.J., Mairs K.A., McGovern T.H., Perdikaris S. and Vésteinsson O., 2007, Abandoned farms, volcanic impacts and woodland management: Revisiting Þjórsárdalur, the 'Pompeii of Iceland'. Arctic Anthropology, 44-1, 1-11.

Einarsson, Th., 1982, The history of Hvitárglijúfur and Gullfoss in the light of tephrochronology, In Eldur er í nordri, Editors: Thórarinsdóttir H., Óskarsson O.H., Steinthórsson S., Einarsson Th., Reykjavik: Sögufélag, 443-51.

Eiríksson J., Knudsen K.L., Haflidason H., Heinemeier J., 2000, Chronology of late Holocene climatic events in the northern North Atlantic based on AMS C-14 dates and tephra markers from the volcano Hekla, Iceland, Journal of Quaternary Science, 15, 573-580.

Eiríksson J., Larsen G., Knudsen K.L., Heinemeier J. and Símonarson L.A., 2004, Marine reservoir age variability and water mass distribution in the Iceland Sea. Quaternary Science Reviews, 23, 2247-2268.

Ewart A., and Fieldes M., 1962, Low temperature thermal effects in natural volcanic glass due to strain, Mineralogical Magasine, 33, 237-246.

Fisher R.V., 1961, Proposed classification of volcanoclastic sediments and rocks, Geological Society of America Bulletin, 72, 1409–1414.

Fraser, D.G., 1995, The nuclear microprobe - PIXE, PIGE, RBS, NRA and ERDA, *In* P.J. Potts, J.F.W. Bowles, S.J.B. Reed and M.R. Cave (eds) Microprobe techniques in the earth sciences, Mineralogical Society Series 6, Chapman and Hall, London, 141–162.

Froggatt P.C., 1992, Standardization of the chemical analysis of tephra deposits, Report of the ICCT working group, Quaternary International 13/14, 93–96.

Gee M.A.M., Thirwall M., Taylor R., Lowry D., Murton B., 1998, Crustal Processes: Major Controls on Reykjanes Peninsula Lava Chemistry, SW Iceland, Journal of Petrology, 39 (5), 819-839.

Geirsdóttir A., Miller G., Thordarson Th., Olafsdóttir K., 2009, A 2000yr record of climate variations reconstructed from Haukadalsvàtn, West Iceland. Journal of Paleolimnology, 41, 95-115.

Gilbert J., and R.S.J. Sparks, (eds), 1998, The physics of explosive volcanic eruptions, Geol Soc London Spec Publ 145, 186pp.

Grönvold K, 1984, Myvàtn fires 1724-1729, chemical composition of the lava, Nordic Volcanological Institute University of Iceland, 8401, 24pp.

Grönvold K, and Johannesson H., 1984, Eruption in Grimsvötn 1983; course of events and chemical studies of the tephra, Jökull, 34, 1-11.

Grönvold K., Oskarsson N., Johsen S., Clausen H., Hammer C., Bond G., Bard E., 1995, Ash layers from Iceland in the Greenland GRIP ice core correlated with oceanic and land sediments. Earth and Planetary Science Letters, 164, 1-5.

Gudmundsdóttir E.R., Eirikisson J., Larsen G., 2008, Tephrochronological framework for the North Icelandic Shelf during the Late Glacial and Holocene, Poster, IAVCEI General Assembly, Reykjavik, Iceland.

Gudmundsson A., 2000, Dynamics of volcanic systems in Iceland. Annual Reviews of Earth And Planetary Sciences, 28, 107–140.

Haflidason H., 1983, The marine geology of Eyjafjordur, North Iceland: Sedimentological, Petrographical and Stratigraphical studies. MPhil Thesis, University of Edinburgh, Edinburgh; 281 pp.

Haflidason, H., Larsen., G. and Olafsson, G., 1992, The recent sedimentation history of Thingvallavàtn, Iceland, Oikos, 64, 80–95.

Haflidason H., King E.L., Sejrup H.P., 1998a, Late Weichselian and Holocene sediment fluxes of the northern North Sea Margin, Marine Geology, 152, 189–215.

Haflidason H., Sejrup H.P., Kristensen D.K., Eiríksson J., Knudsen K.L., Heinemeier J., 1998b, Reservoir age estimate for the Norwegian-Greenland Sea for the Late glacial and the Holocene time period. 6th International Conference on Palaeoceanography, Lisboa, 22– 28 August.

Haflidason H., Eiríksson J., van Kreveld S., 2000, The tephrochronology of Iceland and the North Atlantic region during the Middle and Late Quaternary: a review, Journal of Quaternary Science,15, 3-22.

Hall, V. A., Plicher, J. R. and McCormac, F. G., 1994, Icelandic volcanic ash and the mid-Holocene Scots pine (Pinus sylvestris) decline in the north of Ireland: no correlation, The Holocene, 4-1, 79-83.

Hall V.A., and Pilcher J.R., 2002, Late-Quaternary Icelandic tephras in Ireland and Great Britain: detection, characterization and usefulness, The Holocene, 12, 223-230.

Hannesdóttir H., 2006, Reconstructing environmental change in South Iceland during the last 12,000 years- based on sedimentological and seismostratigraphical studies in lake Hestvàtn. M.Sc. thesis.

Hannon G.E., Hermanns-Auðardáttir M., and Wastegård S., 1998, Human impact at Tjørnuvik in the Faeroe Islands, Froðskaparrit, 46, 215-228.

Harðardóttir J., Geirsdóttir Á., Thórdarson T., 2001, Tephra layers in a sediment core from Lake Hestvàtn, southern Iceland: implications for evaluating sedimentation processes and environmental impacts on a lacustrine system caused by tephra fall deposits in the surrounding watershed. In: White J, Riggs N (eds) Lacustrine Volcaniclastic Sedimentation. Association of Sedimentologists (IAS) Special Publication, Blackwell, Oxford, p 225-246.

Hardarson B.S., 1993, Alkalic rocks in Iceland with special reference to the Snæfellsjökull volcanic system. PhD thesis, University of Edinburgh.

Hemond C., N.T. Arndt, U. Lichtenstein, A.W. Hofmann, N. Oskarsson and S. Steinthorsson, The heterogeneous Iceland plume: Nd-Sr-O isotope and trace element constraints, Journal of Geophysical Research, 98, 15833–15850.

Hinton R.W., Harte B. and Witt-Eichschen G., 1995, Ion probe measurements of National Institute of Standards and Technology standard reference material lSRM 610 glass, trace elements, Analyst, 120, 1315-1319.

Holmes, J., Hall, V. A. and Wilson, P., 1999, Volcanoes and peat bogs, Geology Today, 60-63.

Hunt JB. and Hill PG., 1993, Tephra geochemistry: a discussion of some persistent analytical problems, The Holocene, 3, 271–278.

Hunt JB, and Hill PG., 1996, An inter-laboratory comparison of the electron probe microanalysis of glass geochemistry, Quaternary International, 34–36, 229–241.

Hunt JB, and Hill PG., 2001, Tephrological implications of beam-size and sample-size effects in electron microprobe analysis of glass shards, Journal of Quaternary Science, 16, 105–117.

Ingolfsson O., 1988, Glacial history of the lower Borgarfjördur area, western Iceland, Geologiska Foreningens i Stockholm Forhanddlingar, 110, 293–309.

Ingolfsson O., 1991, A review of the Late Weichselian and early Holocene glacial and environment history of Iceland, *In* Environmental Change in Iceland: Past and Present, Editors: Maizels JK, Caseldine C., Kluwer Academic Publishers, Dordrecht, 13–29.

Ingolfsson O., Norddahl H., Haflidason H., 1995, Rapid isostatic rebound in south-western Iceland at the end of the last glaciation, Boreas, 24, 245–259.

Jakobsson S.P., 1968, The geology and petrography of the Vestmann Islands: A preliminary report, Surtsey Research Progress Report IV, 113-129.

Jakobsson S.P., 1979a, Outline of the petrology of Iceland, Jökull, 29, 57-73

Jakobsson S.P., 1979b, Petrology of recent basalts of the Eastern Volcanic Zone, Iceland, Acta Naturalia Islandica, 26,103.

Jakobsson S.P., Jonsson J., Shido F., 1978, Petrology of the Western-Reykjanes-Peninsula, Iceland, Journal of Petrology, 19, 669-705.

Jakobsson S.P., Jonasson K., Sigurdson I., 2008, The three igneous rock series of Iceland, Jökull, 58, 117-138.

Jennings A.E., Grönvold K., Hilberman R., Smith M., Hald M., 2002, High-resolution study of Icelandic tephras in the Kangerlussuaq Trough, southeast Greenland, during the last deglaciation. Journal of Quaternary Science 17, 747-757.

Jezek P.A. and Noble D.C., 1978, Natural Hydration and ion exchange of obsidian; and electron microprobe study, American Minerologist, 63, 266-273.

Johannesson H., Flores R.M., Jonsson J., 1981, A short account of the Holocene tephrochronology of the Snæfellsjökull central volcano, Western Iceland, Jökull, 31, 23–30.

Jóhannesson H., 1982, Quaternary volcanism in Western Iceland, *In*, Eldur er i Norðri, Editors: H. Thorarinsdóttir, O.H. Oskarsson, S. Steinthorsson and T. Einarsson, Reykjavik, Sögufélagið.

Jóhannsdóttir G., 2007, Mid Holocene to late glacial tephrochronology in West Iceland as revealed in three lacustrine environments, Masters Thesis, University of Iceland.

Jónasson K., 1994, Rhyolite volcanism in the Krafla central volcano, north-east Iceland, Bulletin of Volcanology, 56, 516-528.

Jónsson, J., 1978a, Jarðfræðikort af Reykjanesskaga. I. Skýringar við jardfræðikort. (Geological map of the Reykjanes Peninsula), National Energy Authority Research Report OS-JHD 7831, Orkustofnun, Reykjavík.

Jónsson J., 1978b, Eldstöðvar og hraun í Skaftafellsþingi (Volcanic vents and lava flows in V-Skaftafellssysla county), Náttúrufræðingurinn, 48, 3-4, 196-232.

Jónsson, J., 1983, Eldgos á sögulegum tíma á Reykjanesskaga (Volcanic eruptions in historical time on the Reykjanes peninsula, SW Iceland), Náttúrufrædingurinn, 52, 127-139.

Kirkbride M. and Dugmore A., 2005, Permafrost and Frozen Ground
Late Holocene solifluction history reconstructed using tephrochronology, Geological Society, London, Special Publications; 2005; 242, 145-155;

Kjartansson, 1943, Arnesinger Saga, Naturulysing Arnnesyslu, fyrri hluti. Yfirlit og Jardsaga. Reykjavik, Arnesingafelgid i Reykjavik.

Koç Karpuz N., and Jansen, E., 1992, A high resolution diatom record of the last deglaciation from the SE Norwegian Sea: Documentation of rapid climatic changes, Palaeoceanography, 7, 499-520.

Kristjánsdóttir G.B., Stoner J.S., Jennings A., Andrews J., Grönvold K., 2007, Geochemistry of Holocene cryptotephras from the North Iceland Shelf (MD99-2269): Intercalibration with radiocarbon and paleomagnetic chronostratigraphies, The Holocene, 17, 155-176.

Kvamme T., Mangerud J., Furnes H., Ruddiman W.F., 1989, Geochemistry of Pleistocene ash zones in cores from the North Atlantic, Norsk Geologisk Tidsskrift, 69, 251–272.

Lacasse C., Sigurdsson H., Johannesson H., Paterne M., Carey S., 1995, Source of Ash Zone 1 in the North Atlantic, Bulletin of Volcanology, 57, 18–32.

Landgon P. G. and Barber K. E., 2001, Rapid Communication: New Holocene tephras and a proxy climate record from a blanket mire in northern Skye, Scotland, Journal of Quaternary Science, 16, 8, 753 – 759.

Larsen G., 1978, Gjoskulog i nagrenni kotlu, Masters Thesis, University of Iceland.

Larsen, G., 1979, Um aldur Eldgjárhrauna (Tephrochronological dating of the Eldgjá lavas in S-Iceland), Náttúrufrædingurinn, 49, 1-25.

Larsen G., 1982. Gjoskutímatal Jokuldals og na´grennis. In Eldur er i Nordri, Thorarinsdóttir H., Oskarsson O.H., Steinthorsson S., and Einarsson Th. (eds). Souflas: Reykjavik; 51–65.

Larsen G., 1984a, Recent volcanic history of the Veiðivötn fissure swarm, southern Iceland—an approach to volcanic risk assessment. In Volcano Monitoring, Oskarsson N. (eds), Journal of Volcanological and Geothermal Research, 22, 33–58.

Larsen G., 1984b, Gjoskurannsoknir vegna fornleifauppgraftar i Herjolfsdal, Vestmannaeyjum, Nordic Volcanological Institute Report, 8402; Reykjavik, 23 pp.

Larsen G., 1993, Nokkur ord um Kotlugos og Kotlugjosku. Kotlustefna - 27-29, Mars 1993 Rannsoknir a eldvirkni undir Mrydalsjökull, 6–7. Raunvisindastofnun Haskolans Report Series, RH-3-93.

Larsen G., 2000, Holocene eruptions within the Katla volcanic system, south Iceland: Characteristics and environmental impact, Jökull, 49,1-28.

Larsen G., 2006, Tephra layers as part of Holocene volcanic history, Natural Science Symposium, Reykjavik, Abstracts: Earth Sciences and Geography, BE2.

Larsen G., and Eiríksson J., 2007, Late Quaternary terrestrial tephrochronology of Iceland—frequency of explosive eruptions, type and volume of tephra deposits, Jounral of Quaternary Science, 23, 2, 109-120.

Larsen, G., and J. Eiríksson., 2008a, Holocene tephra archives and tephrochronology in Iceland: A brief overview, Jökull, 58, 229–250.

Larsen, G., and J. Eiríksson, 2008b, Late Quaternary terrestrial tephrochronology of Iceland: Frequency of explosive eruptions, type and volume of tephra deposits, Journal of Quaternary Science, 23, 109–120.

Larsen G. and Thorarinsson S.,1977, H4 and other acid tephra layers, Jökull, 27, 28–46.

Larsen G., Gudmundsson M.T., Bjornsson H., 1998, Eight centuries of periodic volcanism at the centre of the Iceland hotspot revealed by glacier tephrostratigraphy, Geology 26: 943–946.

Larsen G., Dugmore A.J., Newton A.J., 1999, Geochemistry of historical-age silicic tephras in Iceland, The Holocene, 9, 463-471.

Larsen G., Newton A.J., Dugmore A.J., Vilmundardóttir E.G., 2001, Geochemistry, dispersal, volumes and chronology of Holocene silicic tephra layers from the Katla volcanic system, Iceland, Journal of Quaternary Science, 16, 119-132.

Larsen G., Eiríksson J., Knudsen K.L., Heinemeier J., 2002, Correlation of late Holocene terrestrial and marine tephra markers, north Iceland: implications for reservoir age changes, Polar Research 21, 283-290.

Lowe J.J., and Turney C.S.M., 1997, Vedde Ash layer discovered in small lake basin on Scottish mainland, Journal of the Geological Society of London, 154, 605–612.

Lowe J.J., and Walker M.J.C., 2000, Radiocarbon dating the last glacial interglacial transition (ca. 14–9 14C ka BP) in terrestrial and marine records: the need for new quality assurance protocols, Radiocarbon, 42, 53–68.

Lowe D.J., Newnham R.M. and McCraw J.D., 2002, Volcanism and early Maori society in New Zealand, In: Natural Disasters and Cultural Change, Editors: Torrence R. And Grattan J., Routledge, 126-161.

Mangerud J., Lie S.E., Furnes H., Kristiansen I.L., Lømo L., 1984, A Younger Dryas ash bed in Western Norway, and its possible correlations with tephra in cores from the Norwegian Sea and the North Atlantic, Quaternary Research, 21, 85–104.

Mangerud J., Furnes H., Johansen J., 1986, A 9000-year-old ash bed on the Faroe Islands, Quaternary Research, 26, 262–265.

Mathez E.A., 1976, Sulphur solubility and magmatic sulfides in submarine basaltic glass, Journal of Geophysical Research, 81, B23, 4269-4276.

Mattson H., and Höskuldson A., 2003, Geology of the Heimaey volcanic centre, south Iceland: early evolution of a central volcano in a propagating rift?, Journal of Volcanology Geothermal Research, 127, 55-71.

Merkt J., Muller H., Knabe W., Muller P., Weiser T., 1993, The early Holocene Saksunarvàtn tephra found in lake sediments in NW Germany, Boreas, 22, 93–100.

Metrich N., Sigurdsson H., Meyers P., and Devine J., 1991, The 1783 Lakagigar eruption in Iceland, geochemistry, CO2 and sulphur degassing, Contributions to Mineralogy and Petrology, 107, 435-447.

Meyer P.S., Sigurdsson H., and J.-G. Schilling, 1985, Petrological and geochemical variations along Iceland's neovolcanic zones, Journal of Geophysical Research, 90, B12, 10043–10072.

Morrissey M., Zimanowski B., Wohletz K.H., Büttner R., 2000. Phreatomagmatic Fragmentation. In: Sigurdsson, H. (Ed.), Encyclopedia of Volcanoes. Academic Press, San Diego, pp. 431–446.

Nielsen C., and Sigurdsson H., 1981, Quantitative methods for electron microprobe analysis of sodium in natural and synthetic glasses, American Mineralogist, 66, 547-552.

Norddahl H., 1991, A review of the glaciation maximum concept and the deglaciation of Eyjafjordur, North Iceland, *In* Environmental Change in Iceland: Past and Present, Maizels J.K. Caseldine C (eds). Kluwer Academic Publishers: Dordrecht; 31–47.

Norddahl H., and Haflidason H., 1992, The Skogar Tephra, a Younger Dryas marker in North Iceland, Boreas, 21, 23–41.

Óladóttir B., 2004, Masters Thesis, University of Iceland.

Óladóttir B., Larsen G., Thordarson T., Sigmarsson O., 2005, The Katla Volcano S-Iceland: Holocene tephra stratigraphy and eruption frequency, Jökull, 55, 53-74.

Óladóttir B. A., 2009, Holocene eruption history and magmatic evolution of the subglacial Vàtnajökull volcanoes, Grímsvötn, Bárdarbunga and Kverkfjöll, Iceland, PhD thesis, 395pp, U.F.R. de recherche Scientifique et Technique, Université Blaise Pascal.

Parfitt E., and Wilson L., 2008, Fundamentals of Physcial Volcanology, Chapter 10, Eruption Styles, Scales and Frequencies, 144-164, Blackwell Publishing, Oxford, 232pp.

Pearce N., J.A. Westgate, W.T. Perkins, W.J. Eastwood and P. Shane, 1999, The application of laser ablation ICP-MS to the analysis of volcanic glass shards from tephra deposits: bulk glass and single shard analysis, Global Planetary Change, 21,151–171.

Pearce N.J.G., Alloway B.V., Westgate J.A., 2008, Mid-Pleistocene silicic tephra beds in the Auckland region, New Zealand: Their correlation and origins based on the trace element analyses of single glass shards, Quaternary International, 178, 1, 16-43.

Persson C., 1996a, Forsok til tefrokronologisk datering av nagra svenska torvmossar, Geologiska Foreningens Stockholm Forhandlinger, 88, 361–394.

Persson C., 1966b, Undersokning av tre sura asklager pa Island, Geologiska Foreningens Stockholm Forhandlinger, 88, 500–519.

Pouchou L., and Pichoir F., 1984, A new model for quantitative X-ray microanalysis. Reserche Aerospatiale, 3, 167-192.

Pilcher J.R., and Hall V.A., 1996, Tephrochronological studies in northern England, The Holocene, 6, 100–105.

Pilcher J.R., Hall V.A., McCormac F.G., 1995, Dates of Holocene Icelandic volcanic eruptions from tephra layers in Irish peats, The Holocene, 5, 103–110.

Pyne-O'Donnell S.D.F., 2006, Three new distal tephras in sediments spanning the Last Glacial-Interglacial Transistion in Scotland, Journal of Quaternary Science, 22, 6, 559-570.

Ranner P. H., Allen J. R. M. and Huntley B., 2005, A new early Holocene cryptotephra from northwest Scotland, Journal of Quaternary Science, 20, 3, 201 – 208.

Rasmussen S.O., Andersen K.K., Svenson A.M., Steffensen J.P., Vinther B.M., Clausen H.B., Siggaard-Andersen M.L., Johnsen S.J., Larsen L.B., Dahl-Jensen D., Bigler M., Röthlisberger R., Fischer H., Goto-Azuma K., Hansson M.E., Ruth U., 2006, A new Greenland ice core chronology for the last glacial termination, Journal of Geophysical Research, 111, D06102, doi:10.1029/2005JD006079.

Róbertsdóttir B.G., 1992a, Thrlu forsoguleg gjoskulog fra Hekla, HA, HB og HC. In Geoscience Society of Iceland. Spring Meeting. Conference Proceedings, p6-7, Reykjavik, The Geoscience Society of Iceland.

Róbertsdóttir B.G., 1992b, Forsoguleg gjoskulog fra Kotlu, adur nefnd 'Katla 5000'. In Geoscience Society of Iceland. Spring Meeting. Conference Proceedings, p8-9, Reykjavik: The Geoscience Society of Iceland.

Róbertsdóttir B.G., Larsen G. and Eiríksson J., 2002, A new detailed stratigraphical and geochemical record of 30 tephra layers from the Hekla volcanic

system, Iceland, 2980-850 cal. BP, The 25th Nordic Geological Winter Meeting, Abstracts volume, 178, Reykjavík.

Ross K., and Fisher R., 1986, Biogenic grooving on glass shards, Geology, 14, 571-573.

Sarna-Wojcicki, A.M., H.W. Bowman and P.C. Russell, 1979, Chemical correlation of some late Cenozoic tuffs of northern and central California by neutron activation analysis of glass and comparison with X-ray fluorescence analysis, US Geological Survey Professional Paper, 1147.

Sæmundsson K., 1991, Jarðfræði Kröflukerfisins (Geology of the Krafla volcanic system), *In* Gardarson, A. & Einarsson, Á. (eds.) Náttúra Mývàtns, 25-95, Hið íslenska náttúrufræðifélag, Reykjavík.

Sæmundsson K., 1992, Geology of the Thingvallavàtn area, In: Jonasson, P.M., (Ed.), Ecology of Oligothropic, Subarctic Thingvallavàtn, Oikos,64, 40–68.

Sæmundsson K., 1995, Hengill Geological Map (Bedrock), 1:50,000. Orkustofnun, Hitaveita Reykavikur and Landmælingar Íslands, Reykjavik.

Sæmundsson K., and Fridleifsson G. K., 2001, Jarðfræði- og jarðhitakort af Torfajökulssvæðinu Geological and geothermal map of the Törfajökulll area, Orkustofnun, OS-2001/036.

Shane P., 2000, Tephrochronology: a New Zealand case study, Earth Science Reviews, 49, 223–259.

Siani G., Paterne M., Arnold M., Bard E., Metivier B., Tisnert N., Bassinot F., 2000, Radiocarbon reservoir ages in the Mediterranean Sea and Black Sea, Radiocarbon, 42, 271–280.

Sigmarsson O., Steinþórsson S., 2007, Origin of Icelandic basalts: A review of their petrology and geochemistry, Journal of Geodynamics, 43, 87-100.

Sigurdsson H., 1970, The petrology and chemistry of the Setberg volcanic Region and of the intermediate and acidic rocks of Iceland, Unpublished Phd thesis, University of Durham, 321 pp.

Sigurdsson H., and Sparks R.S.J., 1981, Petrology of rhyolitic and mixed magma ejecta from the 1875 eruption of Askja, Iceland, Journal of Petrology, 22, 41–84.

Sigurgeirsson M.A,´1992, Tephra studies on the Reykjanes peninsula, Masters thesis, (in Icelandic) University of Iceland, 114 pp.

Sigurgeirsson M.A., Leosson M.A., 1993, Two early Holocene tephra layers in the Sogamyri peat depoit, Reykjavik, Natturufraedingurinn, 62, 129–137.

Sigvaldason G.E., 1974, The petrology of Hekla and origin of silicic rocks in Iceland, In: The eruption of Hekla 1947–1948, V, 1–44.

Sigvaldason G.E., Annertz K., Nilsson M., 1992, Effect of glacier loading/deloading on volcanism: postglacial volcanic production rate of the Dyngjufjöll area, central Iceland, Bulletin of Volcanology, 54, 385-392.

Sinton J., Grönvold K., Sæmundsson K., 2005, Post-glacial eruptive history of the Western Volcanic Zone, Iceland, Geochemistry, Geophysics, Geosystems, 6, Q12009, doi:12010.11029/12005GC001021

Sjøholm J., Sejrup H.P., Furnes H., 1991, Quaternary volcanic ash zones on the Iceland Plateau, southern Norwegian Sea, Journal of Quaternary Science, 6, 159–173.

Slater L., Jull M., McKenzie D., Grönvold K., 1998, Deglaciation effects on mantle melting under Iceland: results from the northern volcanic zone, Earth and Planetary Science Letters, 164, 151-164.

Smith and Westgate, 1969, Electron probe technique for characterising pyroclastic deposits, Earth and Planetary Science Letters, 5, 313-319.

Steinthórsson S., 1978, Tephra layers in a drill core from the Vàtnajökull Ice Cap, Jökull, 27, 2–27.

Sveinbjörnsdóttir Á.E., Heinemeier J., Kristensen P., Rud N., Geirsdóttir Á., Harðardóttir J., 1998, C-14 AMS dating of Icelandic lake sediments. Radiocarbon, 40, 865-872.

Sverrisdóttir G., 2007, Hybrid magma generation preceding Plinian silicic eruptions at Hekla, Iceland: Evidence from mineralogy and chemistry of two zoned deposits, Geological Magazine, 144, 4, 643-659.

Telford R.J., Heegaard, E., Birks, H.J.B., 2004, All age–depth models are wrong: But how badly?, Quaternary Science Reviews, 23, 1–5.

Thorarinsson S., 1944, Tefrokronologiska studier pa Island, Geografiska Annaler, 26, 1–217.

Thorarinsson S., 1947, The eruption of Hekla in Historical Times: A tephrochronological study, Visindafelag Islendinga (Societas Scientiarum Islandica).

Thorarinsson S., 1951, Laxárgljúfur and Laxárhraun: A tephrochronological study, Geografika Annaler, 33, (1-2), 1-89.

Thorarinsson S., 1954. The tephra-fall from Hekla on March 29th 1947. In The Eruption of Hekla 1947–1948, vol. II, Einarsson T., Kjartansson G., Thorarinsson S (eds). Societas Scientiarum Islandica: Reykjavik; 1–68.

Thorarinsson S., 1958, The Öræfajökull eruption of 1362, Acta Naturalia Islandica II, 2, 1-100.

Thorarinsson S., 1965, Nedansjávargos vid Ísland (Submarine eruptions of the coast of Iceland), Náttúrufrædingurinn 35, 49-74.

Thorarinsson S., 1967, The eruptions of Hekla in historical times. In: Einarsson, T., Kjartansson G., and Thorarinsson S., (Eds.), The eruption of Hekla 1947-48 I. Society Scientific Islandica, Reykjavík, pp. 1-177.

Thorarinsson, S., 1968, Sídustu thættir Eyjaelda (The last phases of the Surtsey eruption), Náttúrufrædingurinn, 38, 113-135.

Thorarinsson S., 1974, Vötnin stríd. Saga Skeidarárhlaupa og Grímsvàtnagosa (The Swift Flowing Rivers—The History of Grimsvötn Eruptions and Jökulhlaups in Skeidara), Menningarsjodur Publishing, Reykjavik, 254 pp.

Thorarinsson S., 1975, Katla and its annual of eruptions, Icelandic Travel Club Yearbook 1975, 124–149.

Thorarinsson S., 1979, Tephrochronology and its application in Iceland, Jökull, 29, 33–36.

Thorarinsson S., 1980, Distant transport of tephra in three Katla eruptions and one Grimsvötn(?) eruption, Jökull, 30, 65–73.

Thorarinsson S, 1981, The application of tephrochronolgy in Iceland, In: Self S., and Sparks R.S.J., (eds) Tephra Studies: proceedings of the NATO Advanced Study Institute "Tephra studies as a tool in Quaternary research", 75, D, Reidel Publishing Company, 109-134

Thorarinsson S., and Saemundsson K., 1979, Volcanic activity in historical time, Jökull, 29, 29–32.

Thordarson T., and Larsen G., 2007, Volcanism in Iceland in historical time: Volcano types, eruption styles and eruptive history. Journal of Geodynamics, 43,118-152.

Thordarson, T., and S. Self, 1993, The Laki (Skaftár Fires) and Grímsvötn eruptions in 1783–1785, Bulletin of Volcanology, 55, 233–263.

Thordarson T., and S. Self, 1998, The Roza Member, Columbia River Basalt Group: A gigantic pahoehoe lava flow field formed by endogenous processes?, Journal of Geophysical Research, 103, 27,411–27,445.

Thordarson T., S. Self, N. Oskarsson and T. Hulsebosch, 1996, Sulfur, chlorine, and fluorine degassing and atmospheric loading by the 1783–1784 A.D. Laki (Skaftár Fires) eruption in Iceland, Bulletin of Volcanology, 58, 205–225.

Thordarson T., D.J. Miller and G. Larsen, 1998, New data on the age and origin of the Leidólfsfell cone group in south Iceland, Jökull, 46, 1998, 3–15.

Thordarson T., D. J. Miller, G. Larsen, S. Self and H. Sigurdsson, 2001, New estimates of sulfur degassing and atmospheric mass-loading by the A.D. 934 Eldgjá eruption, Iceland, Journal of Volcanology and Geothermal Research, 108, 33–54.

Thordarson T., Self S., Miller D.J., Larsen G., and Vilmundardóttir E.G., 2003b, Sulphur release from flood lava eruptions in the Veiðivötn, Grímsvötn and Katla volcanic systems, Iceland. In: Oppenheimer C., Pyle D.M. and Barclay J. (Eds.), Volcanic Degassing. Geological Society of London Special Publications, 213, 103-121.

Thordarson T., and Höskuldson A., 2008, Postglacial Volcanism in Iceland, Jökull, 58, 197.

Thorseth I., Furnes H., Tumyr O., 1991, A textural and chemical study of Icelandic palagonite of varied composition and its bearing on the mechanism of the glass-palagonite transformation, Geochimica et Cosmochimica Acta, 55, 731-749.

Thorseth I., Furnes H., Heldal M., 1992, The importance of microbiological activity in the alteration of natural basaltic glass, Geochimica et Cosmochimica Acta, 56, 845-850.

Tomassen H., 1961, Hestvàtn Hydroelectric Project. The State Electricity Authority. 22pp. and figures.

Trønnes R. G., 1990, Low-Al, high-K amphiboles in subducted lithosphere from 200–400 km depth: experimental evidence, EOS Transactions, American Geophysical Union, 71, 1587.

Turney C.S.M., 1998, Extraction of rhyolitic component of Vedde microtephra from microgenic lake sediments, Journal of Palaeolimnology, 19, 199-206.

Turney C.S.M., Harkness D.D., Lowe J.J., 1997, The use of microtephra horizons to correlate Late-glacial lake sediment successions in Scotland, Journal of Quaternary Science,12, 525-531.

Turney C.S.M., Coope G.R., Harkness D.D., Lowe J.J., Walker M.J.C., 2000, Implications for the dating of Wisconsinan (Weichselian) Lateglacial events of systematic radiocarbon age differences between terrestrial plant macrofossils from a site in SW Ireland, Quaternary Research, 53, 114–121.

Vilmundardóttir E.G., Á. Gudmundsson, and S.P. Snorrason, 1983, Geological map, Búrfell-Langalda, 3540 B, National Energy Authority and National Power Company, Reykjavík.

Vilmundardóttir E.G., S.P. Snorrason, G. Larsen, and Á. Gudmundsson, 1988, Geological map, Sigalda-Veiðivötn, 3340 B, National Energy Authority and National Power Company, Reykjavík.

Vilmundardóttir E.G., Á. Gudmundsson, S.P. Snorrason., and G. Larsen, 1990, Geological map Botnafjöll, 1913 IV, 1:50.000, Iceland Geodetic Survey, National Energy Authority and National Power Company: Reykjavík.

Vilmundardóttir E.G., G. Larsen and S.P. Snorrason, 1999a, Geological map Nyrdri Háganga 1914 II, 1:50.000. Iceland Geodetic Survey, National Energy Authority and National Power Company, Reykjavík.

Vilmundardóttir E.G., S.P. Snorrason, G. Larsen and B. Adalsteinsson, 1999b, Geological map, Tungnaárjökull 1913 I, 1:50.000, Iceland Geodetic Survey, National Energy Authority and National Power Company, Reykjavík.

Waagstein R., and Johansen J., 1968, Tre vulkanske askelag fra Faeroerne, Meddelelser Dansk Geologisk Forening, 34, 257–264.

Waelbroeck C., Duplessy J-C., Michel E., Labeyrie L., Paillard D., Duprat J., 2001, The timing of the last deglaciation in the North Atlantic climate records, Nature, 412, 724–727.

Wallace P., and Carmichael I.S.E., 1992a, Sulfur in basaltic magmas, Geochimica et Cosmochimica Acta, 56, 1863-1 874.

Wastegård S., 2002, Early to middle Holocene silicic tephra horizons from the Katla volcanic system, Iceland: new results from the Faroe Islands. Journal of Quaternary Science, 17, 723–730.

Wastegård S., 2005, Late Quaternary tephrochronology of Sweden: a review, Quaternary International, 130, 49-62.

Wastegård S., Björck S., Possnert G., Wohlfarth B., 1998, Evidence for the occurrence of Vedde Ash in Sweden: radiocarbon and calendar age Estimates, Journal of Quaternary Science, 13, 271–274.

Wastegård S., Wohlfarth B., Subetto D.A., Sapelko T.V., 2000, Extending the known distribution of the Younger Dryas Vedde Ash into north-western Russia, Journal of Quaternary Science, 15, 581–586.

Wastegård S., 2001, The Mjáuvøtn tephra and other Holocene tephra horizons from the Faroe Islansa: a link between Icelandic source region, the Nordic Seas and the European continent, The Holocene, 11, 1, 101 – 109.

Westgate J.A., and Gorton M.P., 1981, Correlation techniques in tephra studies, *In* Tephra Studies, Self S., Sparks R.S.J. (eds). Dordrecht: Reidel, 73–94.

Wohlfarth B., Björck S., Possnert G., Lemdahl G., Brunnberg L., Ising J., Olsson S., Svensson N.O., 1993, AMS dating Swedish varved clays of the last glacial/interglacial transition and the potential difficulties of calibrating Late Weichselian 'absolute' chronologies, Boreas, 22, 113–128.

Wolfe C.J., Bjarnason I.T., Van Decar J.C., Solomon S.C., 1997, Seismic structure of the Iceland mantle plume, Nature, 385, 245–47.

Zielinski G.A., Germani M. S., Larsen G., Baille M.G.L., Whitlow S., Twickler M. S. and Taylor K. C., 1997, Volcanic aerosol records and tephrochronology of the Summit, Greenland, ice cores, Journal of Geophysical Research, 102, 26625 – 26640.